# UNDERSTANDING THE BIOLOGICAL EFFECTS OF ISOPRENE-DERIVED SECONDARY ORGANIC AEROSOL

Maiko Arashiro

A dissertation submitted to the faculty of the University of North Carolina at Chapel Hill in partial fulfillment of the requirements for the degree of Doctor of Philosophy in the Department of Environmental Sciences and Engineering in the Gillings School of Global Public Health.

Chapel Hill
2017

Approved by:

Jason Surratt

Daniel Costa

Rebecca Fry

Ilona Jaspers

David Leith

**ABSTRACT**

Maiko Arashiro: Understanding the Biological Effects of Isoprene-Derived Secondary Organic Aerosol
(Under the direction of Jason Surratt)

Isoprene (2-methyl-1,3-butadiene), a volatile organic compound released primarily by terrestrial vegetation, is an important precursor to the formation of secondary organic aerosol (SOA). Isoprene-derived SOA, which comprises a large mass fraction of global fine particulate matter ($PM_{2.5}$), results from the atmospheric chemical transformations of isoprene with controllable anthropogenic emissions such as oxides of nitrogen ($NO_x$) and sulfur dioxide. Because $PM_{2.5}$ from isoprene is a relatively new discovery, little is known about its toxicity. Through a series of *in vitro* exposure studies, we explored the effects of isoprene-derived SOA on oxidative stress-related gene expression levels in human bronchial epithelial cells (BEAS-2B). We generated atmospherically-relevant compositions of isoprene-derived SOA in an outdoor smog chamber, starting from isoprene as a precursor in the presence of $NO_x$ and acidic sulfate aerosol, to expose BEAS-2B cells to the total isoprene SOA mixture. We then systematically explored the effects of three known composition types of isoprene-derived SOA by generating SOA through dark reactive uptake experiments by starting with key gaseous intermediates, including *trans*-β-isoprene epoxydiol (*trans*-β-IEPOX), methacrylic acid epoxide (MAE), or isoprene hydroxyhydroperoxides (ISOPOOH).

Chemical characterization coupled with biological analyses show that atmospherically-relevant compositions of isoprene-derived SOA alter the levels of 41 oxidative stress-related genes. Of the different composition types of isoprene-derived SOA, MAE-derived SOA altered the greatest number of genes. Taken together, the different composition types accounted for 34 of the genes altered by the

total isoprene SOA mixture while 7 remained unique to the total mixture exposures indicating that there is either a synergistic effect of the different isoprene-derived SOA components or an unaccounted component in the mixture.

Importantly, this work reveals an enrichment for altered expression of genes transcriptionally controlled by Nuclear factor (erythroid-derived 2)-like 2 (Nrf2) in cells exposed to all types of isoprene-derived SOA. The enrichment of the Nrf2 pathway may indicate a response to inflammation initiated by isoprene SOA exposure. The findings from this initial exploration emphasize the importance of future *in-vitro* and *in-vivo* work to inform policy not only because of the atmospheric abundance of isoprene-derived SOA, but also because the anthropogenic contribution is the only component amenable to control.

**ACKNOWLEDGEMENTS**

This dissertation would not have been possible without the help of many people who have been vital to my academic and personal wellbeing. First, I would like to express my gratitude to my advisor Dr. Jason Surratt for taking me on as his PhD student and guiding me throughout the whole process. I am also thankful to Dr. Rebecca Fry, Dr. Ilona Jaspers, Dr. Daniel Costa, and Dr. David Leith for serving on my committee.

My PhD journey would not have been enjoyable or productive without having amazing lab mates. I would like to thank all the former and current members of the Surratt lab group who have been there to support me academically and personally. I am grateful to Dr. Matthieu Riva and Yuzhi Chen for helping with chamber experiments, Hilary Green and Dr. Weruka Rattanavaraha for helping with chemical analysis, and Dr. Sari Budisulistiorini for keeping my spirits up throughout all the experiments. I am especially grateful to Dr. Ying-Hsuan Lin for being an amazing mentor who was always willing to help and being the best research companion as we navigated through many hurdles.

I would also like to thank many members of the Fry lab including Dr. Julia Rager, Lisa Smeester, Dr. Emily Bailey, Dr. Samira Brooks, and Martha Scott, who have helped me with laboratory training that was indispensable to my research.

I have been blessed with the support of so many people I have met during my time in North Carolina. To Dave and Maryanne, I am forever grateful that you brought me to this wonderful place and will never forget how quickly you two made it feel like home for me.

To my family, I am thankful for all the love and support especially from my mom who has witnessed both the highs and lows of the process. To all my friends, thank you for keeping me sane

throughout this whole crazy process and providing me with endless love and support. I truly could not have done this myself. I would like to especially thank Kristen Downs and Brandon Smith for helping me through the final and most difficult part of writing and completing my dissertation.

This work was supported by the Health Effects Institute (HEI), an organization jointly funded by the United States Environmental Protection Agency (EPA) (Assistance Award No. R-82811201), and certain motor vehicle and engine manufacturers. Other funding and financial support came from National Science Foundation (DGE-0646083), the Center for Faculty Excellence, University of North Carolina at Chapel Hill, and in part by a grant from the National Institute of Environmental Health Sciences (T32-ES007018).

**TABLE OF CONTENTS**

**LIST OF TABLES**

**LIST OF FIGURES**

## LIST OF ABBREVIATIONS

| | |
|---|---|
| BEAS-2B | human bronchial epithelial cells |
| DMA | differential mobility analyzer |
| DTT | dithiothreitol |
| EAVES | Electrostatic Aerosol *in vitro* Exposure |
| EDTA | Ethylenediaminetetraacetic acid |
| EIC | extracted ion chromatogram |
| GC/MS | gas chromatography interfaced with an electron ionization quadrupole mass spectrometer |
| $H_2SO_4$ | sulfuric acid |
| HMML | hydroxymethyl-methyl-α-lactone |
| *HMOX1* | heme oxygenase 1 |
| IEPOX | isoprene epoxydiols |
| *IL-8* | interleukin 8 |
| ISOPOOH | isoprene hydroxyhydroperoxides |
| ISOPTHP | isoprene trihydroxyhydroperoxide |
| $ISOP(OOH)_2$ | isoprene dihydroxydihydroperoxide |
| KBM | keratinocyte basal medium |
| KGM | keratinocyte growth medium |
| MACR | methacrolein |
| MAE | methacrylic acid epoxide |
| MCPC | mixing condensation particle counter |
| $MgSO_4$ | magnesium sulfate |
| MVK | methylvinyl ketone |
| NIOG | normalized index of oxidant generation |

| | |
|---|---|
| *NQO1* | NAD(P)H dehydrogenase, quinone 1 |
| $NO_x$ | oxides of nitrogen |
| $O_3$ | ozone |
| PBS | phosphate buffer solution |
| PM | particulate matter |
| $PM_{2.5}$ | particulate matter less than 2.5 microns diameter |
| ppm | parts per million |
| *PTGS2* | prostaglandin-endoperoxide synthase 2 |
| qRT-PCR | quantitative real-time reverse transcription polymerase chain reaction |
| RH | relative humidity |
| RNA | ribonucleic acid |
| ROS | reactive oxygen species |
| SEM | standard error of the mean |
| SOA | secondary organic aerosol |
| $SO_2$ | sulfur dioxide |
| TIC | total ion chromatogram |
| TME | tetramethylethylene |
| UPLC/ESI-HR-QTOFMS | ultra-performance liquid-chromatography coupled to electrospray ionization quadrupole time-of flight mass spectrometry |
| VOC | volatile organic compound |

## CHAPTER I: INTRODUCTION AND OBJECTIVES

Recent work has shown that isoprene (2-methyl-1,3-butadiene) is an important precursor of secondary organic aerosol (SOA), which has potential impacts on climate change and public health (Y-H Lin et al. 2013; Lin et al. 2016; Rohr 2013). Current understanding of isoprene SOA formation is based on laboratory studies showing that gas-phase photooxidation (or hydroxyl radical (OH)-initiated oxidation) of isoprene generates key SOA precursors, including isomeric isoprene epoxydiols (IEPOX) (Lin et al. 2012; Lin et al. 2014; Nguyen et al. 2014; Paulot et al. 2009; Surratt et al. 2010), methacrylic acid epoxide (MAE) (Y-H Lin et al. 2013), hydroxymethyl-methyl-α-lactone (HMML) (Nguyen et al. 2015), and isoprene hydroxyhydroperoxides (ISOPOOH) (Krechmer et al. 2015; Liu et al. 2016; Riva et al. 2016a). As shown in Figure 1, these highly reactive gaseous intermediates (shown in red) resulting from OH-initiated oxidation of isoprene, can subsequently react with OH radicals and lead to SOA formation through acid-catalyzed multiphase chemistry (Kjaergaard et al. 2012; Kramer et al. 2016; Lin et al. 2012; Y-H Lin et al. 2013; Nguyen et al. 2015; Riva et al. 2016a; Surratt et al. 2010). Recent work has shown that isoprene-derived multifunctional hydroperoxides can undergo multiphase chemistry (Riva et al. 2016b); however, as shown in Figure 1, more work is needed to understand these processes.

SOA formation from the precursors shown in Figure 1 is highly influenced by controllable anthropogenic emissions such as oxides of nitrogen ($NO_x$) and sulfur dioxide ($SO_2$). Atmospheric oxidation of $SO_2$ contributes to particle acidity, which enhances isoprene SOA formation through acid-catalyzed reactive uptake and multiphase chemistry of IEPOX and MAE (Gaston et al. 2014; Lin et al. 2012; Riedel et al. 2015; Surratt et al. 2007; Surratt et al. 2010), while $NO_x$ determines whether the oxidation pathway leading to IEPOX or MAE/HMML predominates (Y-H Lin et al. 2013; Nguyen et al. 2015; Surratt et al. 2010), which ultimately alters the resultant SOA composition and yield (Edney et al.

2005; Surratt et al. 2006). Isoprene SOA comprises a large portion of global atmospheric fine particles ($PM_{2.5}$, aerosol with aerodynamic diameters ≤ 2.5 μm) (Carlton et al. 2009; Hallquist et al. 2009; Henze et al. 2008; Hu et al. 2015), but few studies have focused on its health implications prior to the work presented in this dissertation. Evaluating the health effects of SOA from isoprene oxidation is important from a public health perspective, not only because of its atmospheric abundance, but also because the anthropogenic contribution is the only component amenable to control (Gaston et al. 2014; Pye et al. 2013; Riedel et al. 2015; Xu et al. 2015).

Many studies have shown that $PM_{2.5}$ is closely linked to health effects ranging from exacerbation of asthma symptoms to mortality associated with lung cancer and cardiopulmonary disease (Dockery et al. 1993; Samet et al. 2000; Schwartz et al. 1993). $PM_{2.5}$, in particular, has been linked to negative health outcomes with an estimated contribution of 3.2 million premature deaths worldwide as reported in the Global Burden of Disease Study 2010 (Lim et al. 2012). Despite evidence that particle composition affects toxicity, fewer studies focus on the link between chemical composition and health/biological outcomes (Kelly and Fussell 2012). Prior work on complex air mixtures has shown that gaseous volatile organic compounds (VOCs) alter the composition and ultimately the toxicity of particles (Ebersviller et al. 2012a, b). SOA resulting from natural and anthropogenic gaseous precursors, such as α-pinene and 1,3,5-trimethylbenzene, have been shown to affect cellular function (Gaschen et al. 2010; Jang et al. 2006). A few studies have investigated the biological effects associated with isoprene oxidation products. Wilkins et al. (2001), showed significant upper airway irritation in mice exposed to mixtures of isoprene and oxidants ($O_3$ and $NO_2$). However, the residual reactants and some identified reaction products, including formaldehyde, formic acid, acetic acid, methacrolein (MACR), and methylvinyl ketone (MVK) could only partially explain the sensory irritation. Similarly, Doyle et al. (2004) showed enhanced expression of proinflammatory cytokines in a human lung cell model (A549) after an exposure to a mixture of gaseous products from OH-initiated isoprene oxidation, but $O_3$ alone or with

the addition of a few known first-generation gas-phase products (e.g., MACR and formaldehyde) only accounted for part of the inflammatory response. Both of these studies suggested that a reactive product may have been formed that was responsible for the airway irritation and inflammatory response observed. The recently discovered precursors (IEPOX, MAE, HMML, and ISOPOOH) formed from gas-phase photooxidation of isoprene could potentially explain the observed differences. Our laboratory has recently demonstrated through a chemical assay that isoprene-derived SOA formed from the various precursors has the potential for inducing reactive oxygen species (ROS) (Kramer et al. 2016). ROS are oxygen-containing species including superoxide anion ($O_2^-$), hydrogen peroxide ($H_2O_2$), and hydroxyl radicals (OH) which can act as powerful oxidants and are linked to oxidative stress and inflammation (Li et al. 2003a; Reuter et al. 2010). Oxidative stress is associated with chronic pulmonary inflammation, and contributes to respiratory and cardiovascular health outcomes (Donaldson et al. 2001; Kirkham and Barnes 2013; Rahman and Adcock 2006).

The overall objective of this dissertation was to investigate the early biological effects of isoprene SOA, based on the current understanding of their formation through key precursors, on human bronchial epithelial cells (BEAS-2B) with a particular focus on the alteration of oxidative stress-related genes. To achieve this objective, we began exploring the overall isoprene SOA system using a direct deposition exposure device in Chapter 2 to determine the effects of isoprene-derived SOA, generated through isoprene photooxidation experiment, on *PTGS2* and *IL-8* gene expression. In Chapter 3, we explore the effect of isoprene-derived SOA exposure on a greater number of oxidative stress-related gene expression using pathway-focused gene expression profiling. We then move on to systematically explore the effects of different types of isoprene SOA derived from MAE, IEPOX, and ISOPOOH on oxidative stress-related genes in Chapters 4 and 5. In Chapter 6, we provide our conclusions from this work and suggest future avenues of research based on the findings presented from this dissertation.

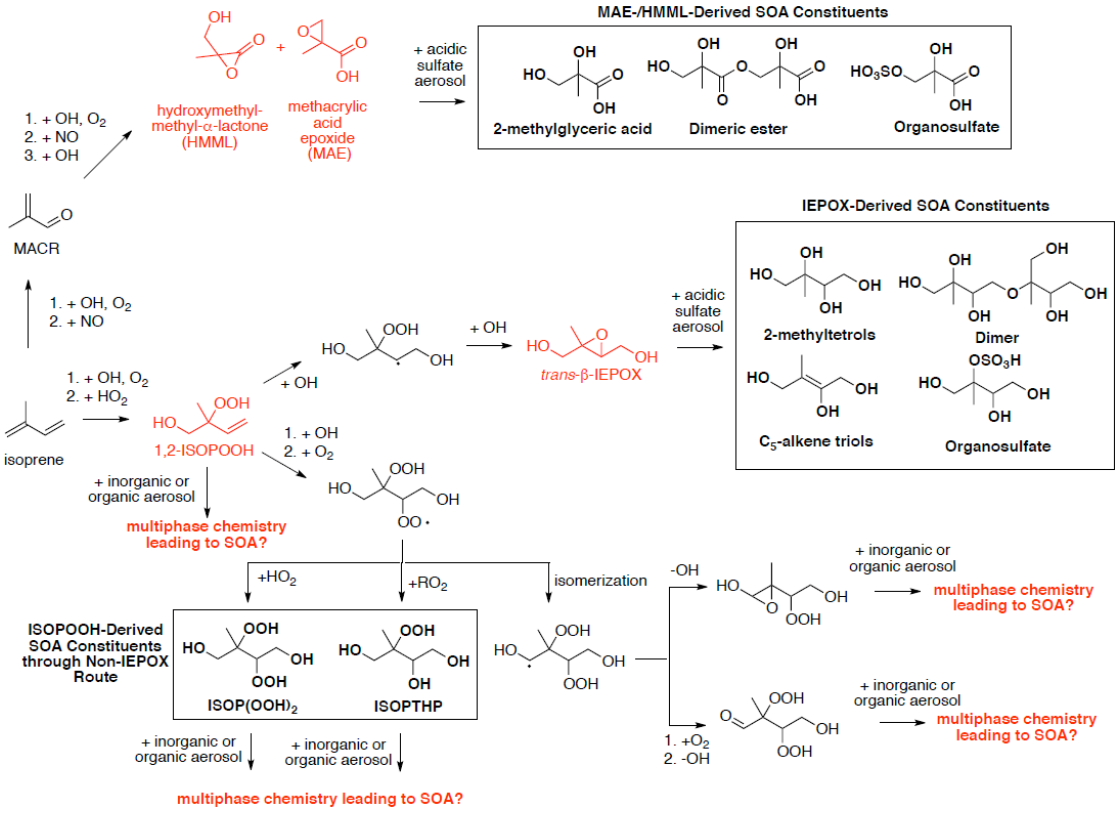


**Figure 1.1.** Current understanding of isoprene SOA formation mechanism.

## CHAPTER II: EFFECT OF ISOPRENE-DERIVED SECONDARY ORGANIC AEROSOL ON *PTGS2* AND *IL-8*[1]

### *2.1 Overview*

The objective of this study was to generate atmospherically relevant compositions of isoprene-derived SOA and to examine its toxicity through *in vitro* exposures using a direct deposition device. Compared to exposure of cells in culture media to resuspended particles, direct particle deposition likely provides a more biologically relevant exposure model and enhances sensitivity of cells to air pollution particle exposures (Hawley and Volckens 2013; Hawley et al. 2014a; Hawley et al. 2014b; Lichtveld et al. 2012; Volckens et al. 2009; Zavala et al. 2014). The Electrostatic Aerosol *in vitro* Exposure System (EAVES) used in this study deposits particles generated in our outdoor photochemical chamber directly onto lung cells by electrostatic precipitation (de Bruijne et al. 2009). Similar techniques and devices have been used to expose cells to diesel exhaust particles (Hawley et al. 2014b; Lichtveld et al. 2012), but this study is the first to utilize the EAVES to explore the potential adverse effects of isoprene SOA on human lung cells. Additionally, for a more atmospherically relevant exposure, isoprene SOA was photochemically generated in an outdoor chamber to mimic its formation in the atmosphere. In this study we chose to examine the gene expression levels of interleukin-8 (*IL-8*) and prostaglandin-endoperoxide synthase 2 (*PTGS2*), not only for their links to inflammation and oxidative stress (Kunkel et al. 1991; Uchida 2008), but because both have been examined in previous studies using the EAVES for fresh and aged diesel exhaust (Lichtveld et al. 2012). We compared the gene expression levels in cells exposed to SOA generated in an outdoor chamber from photochemical oxidation of isoprene in the

[1] This chapter has been adapted from an article in Atmospheric Chemistry and Physics. The original citation is as follows: Arashiro, Maiko, Ying-Hsuan Lin, Kenneth G. Sexton, Zhenfa Zhang, Ilona Jaspers, Rebecca C. Fry, William G. Vizuete, Avram Gold, and Jason D. Surratt. "In vitro exposure to isoprene-derived secondary organic aerosol by direct deposition and its effects on COX-2 and *IL-8* gene expression." Atmospheric Chemistry and Physics 16, no. 22 (2016): 14079-14090.

presence of NO and acidified sulfate seed aerosol to cells exposed to a dark control mixture of isoprene, NO, and acidified sulfate seed aerosol to isolate the effects of the isoprene-derived SOA on the cells using the EAVES. In addition, we collected SOA onto filters for subsequent resuspension exposure to ensure that effects observed from EAVES were attributable to particle-phase organic products.

### *2.2 Experimental Section*

#### *2.2.1 Generation of SOA in the Outdoor Chamber Facility*

SOA were generated by photochemically oxidizing a mixture of acidified sulfate seed aerosol, isoprene, and NO injected into an outdoor smog chamber facility. The outdoor chamber is a 120-$m^3$ triangular cross-section Teflon chamber located on the roof of the Gillings School of Global Public Health, University of North Carolina at Chapel Hill. The chamber facility has been described in detail elsewhere by Lichtveld et al. (2012). The outdoor chamber facility is equipped with sampling lines that allow direct deposition exposure of cells, online chemical measurements, and filter collection for offline chemical analysis. Sampling lines run from the underside of the chamber directly to the chemistry lab below where online measurement instruments and the direct deposition exposure device are located. Injection ports are also located on the underside of the chamber.

To generate isoprene-derived SOA, the chamber was operated on sunny days, under high relative humidity, to allow natural sunlight to trigger photochemical reactions. Acidified sulfate seed aerosols were generated by nebulizing an aqueous solution containing 0.06 M $MgSO_4$ + 0.06 M $H_2SO_4$ into the chamber to a particle concentration of approximately 170 μg $m^{-3}$, which was allowed to stabilize for 30 min to ensure a well-mixed condition. After stabilization, 3.5 ppmv isoprene (Sigma-Aldrich, 99%) and 200 ppbv NO (AirGas, 1.00%) were injected into the chamber. Photochemical aging was allowed for approximately one hour to reach the desired exposure conditions of 30-40 μg $m^{-3}$ growth of isoprene-derived SOA on the pre-existing 170 μg $m^{-3}$ of acidified sulfate aerosol. This chamber experiment was

replicated on three separate sunny days with temperatures ranging from 24.9°C to 26.8°C with a relative humidity of approximately 70% in the chamber.

### *2.2.2 Control Chamber Experiments*

As a dark chamber negative control, to isolate the effect of SOA on exposed cells, mixtures of isoprene, NO, and 170 μg $m^{-3}$ of acidified sulfate seed aerosol were injected into the chamber in the dark (after sunset). Conducting the chamber experiments in the dark ensured no photochemical oxidation of isoprene. The dark control was replicated on three different nights. Except for the absence of solar radiation (no SOA), all chamber operations and exposure conditions were similarly maintained.

As an added control to ensure that the device itself and the cell handling had no significant effect on cell cytotoxicity, cells were exposed in the EAVES to a clean chamber and compared to unexposed cells kept in an incubator for the same duration as the exposure. The cytotoxicity results ensured that there is no effect of chamber conditions and device operation on the cells.

### *2.2.3 Cell Culture*

Human bronchial epithelial (BEAS-2B) cells were maintained in keratinocyte growth medium (KGM BulletKit; Lonza), a serum-free keratinocyte basal medium (KBM) supplemented with 0.004% of bovine pituitary extract and 0.001% of human epidermal growth factor, insulin, hydrocortisone, and GA-1000 (gentamicin, amphotericin B), and passaged weekly. Passage number for photochemical exposures and dark control exposures varied between 52 and 60. Because BEAS-2B are an immortalized line of human bronchial epithelium, there are limitations with its use such as it being genetically homogeneous, being a single cell type, and being SV-40 transformed (Reddel et al. 1988). However, BEAS-2B is a stable, proliferative cell line shown to be useful in airway inflammation studies such as ours (Devlin et al. 1994).

### *2.2.4 Direct Deposition Exposure*

In preparation for air-liquid interface exposures, cells were seeded onto collagen-coated Millicell cell culture inserts (30 mm diameter, 0.4 μm pore size, 4.2 $cm^2$ filter area; Millipore, Cambridge, MA) at

a density of 200,000 cells/well 24 hours prior to exposure. At the time of exposure, cells reached ~80% confluence, confirmed through microscopy. Immediately before exposure, cell medium was removed from the apical and basolateral sides of 2 seeded Millicell cell culture inserts. One insert was transferred to a titanium dish containing 1.5 mL of keratinocyte basal medium (KBM; Lonza), supplying cells with nutrients from the basolateral side and constant moisture while allowing exposure to be performed at an air-liquid interface. The other insert was transferred into a 6 well plate with 2 mL of KBM and placed in the incubator as an unexposed control.

Cells were exposed to chamber-generated isoprene SOA using the EAVES located in the laboratory directly beneath the outdoor chamber (de Bruijne et al. 2009; Lichtveld et al. 2012). The EAVES, located in an incubator at 37°C, sampled chamber air at 1 L $min^{-1}$. The target relative humidity (RH) in the chamber during EAVES exposures was approximately 70%. Exposure time was one hour commencing when target exposure conditions were achieved in the outdoor chamber for both photochemical and dark control experiments. Detailed description of the EAVES can be found in de Bruijne et al. (2009).

Following exposure, the cell culture insert was transferred to a 6-well tissue culture plate containing 2 mL of fresh KBM. The control Millicell was also transferred to 2 mL of fresh KBM. Nine hours post-exposure, extracellular medium was collected and total RNA was isolated using Trizol (Life Technologies), consistent with past studies (de Bruijne et al. 2009). Isolated RNA samples were further purified using the spin column-based Direct-zol RNA MiniPrep (Zymo Research). Extracellular medium and the extracted RNA samples were stored at -20°C and -80°C, respectively, until further analysis. The quality and quantity of RNA were assessed with Agilent 2100 Bioanalyzer (Agilent Technologies) and the NanoDrop 2000c spectrophotometer (Thermo Scientific). The RNA integrity number equivalents (RINe) ranged from 9.1 to 10, indicating good integrity of the RNA samples maintained during storage.

### *2.2.5 Filter Resuspension Exposure*

Chamber particles were collected, concurrently with EAVES sampling, onto Teflon membrane filters (47 mm diameter, 1.0 µm pore size; Pall Life Science) for photochemical (light) and dark chamber experiments to be used for chemical analysis and resuspension exposures. The resuspension experiments served as a control for possible effects of gaseous components such as ozone ($O_3$) and $NO_x$ present in the direct deposition experiments; however, prior studies have shown that gaseous components do not yield cellular responses within the EAVES device (de Bruijne et al. 2009; Ebersviller et al. 2012a, b). Mass loadings of SOA collected on the filters were calculated from sampling volumes and average aerosol mass concentrations in the chamber during the sampling period. A density correction of 1.6 g $cm^{-3}$ (Riedel et al. 2016) and 1.25 g $cm^{-3}$ (Kroll et al. 2006) was applied to convert the measured volume concentrations to mass concentrations for the acidified sulfate seed and SOA growth, respectively. The particles collected on Teflon filter membranes for resuspension cell exposure were extracted by sonication in high-purity methanol (LC/MS CHROMASOLV, Sigma-Aldrich). Filter samples from multiple experiments were combined and the combined filter extract was dried under a gentle stream of nitrogen ($N_2$). KBM medium was then added into the extraction vials to re-dissolve SOA constituents.

In preparation for filter resuspension exposures, cells were seeded in 24-well plates at a density of $2.5\times10^4$ cells/well in 250 µL of KGM 2 days prior to exposure. At the time of exposure when cells reached ~80% confluence, cells were washed twice with phosphate buffered saline (PBS) buffer, and then exposed to KBM containing 0.01 and 0.1 mg $mL^{-1}$ isoprene SOA extract from photochemical experiment and seed particles from dark control experiments.

Following a 9-hour exposure, extracellular medium was collected and total RNA was isolated using Trizol (Life Technologies) and stored alongside samples from direct deposition exposures until further analysis.

### *2.2.6 Chemical and Physical Characterization of Exposures*

Online and offline techniques were used to characterize the SOA generated in the chamber. The online techniques measured the gas-phase species NO, $NO_x$ and $O_3$ and the physical properties of the aerosol continuously throughout the chamber experiments. Offline techniques measured aerosol-phase species collected onto Teflon membrane filters (47 mm diameter, 1.0 μm pore size; Pall Life Science) from photochemical and dark chamber experiments. Filter samples were stored in 20 mL scintillation vials protected from light at -20°C until analyses.

Real-time aerosol size distributions were measured using a Differential Mobility Analyzer (DMA, Brechtel Manufacturing Inc.) coupled to a Mixing Condensation Particle Counter (MCPC, Model 1710, Brechtel Manufacturing Inc.) located in the laboratory directly underneath the chamber. $O_3$ and $NO_x$ were measured with a ML 9811 series Ozone Photometer (Teledyne Monitor Labs, Englewood, CO) and ML 9841 series $NO_x$ Analyzer (American Ecotech, Warren RI), respectively. Data were collected at one-minute intervals using a data acquisition system (ChartScan/1400) interfaced to a computer. The presence of isoprene in the chamber was confirmed and quantified using a Varian 3800 gas chromatograph (GC) equipped with a flame ionization detector (FID).

Chemical characterization of SOA constituents was conducted offline from extracts of filters collected from chamber experiments by gas chromatography interfaced with an electron ionization quadrupole mass spectrometer (GC/EI-MS) or by ultra performance liquid chromatography interfaced with a high-resolution quadrupole time-of-flight mass spectrometer equipped with electrospray ionization (UPLC/ESI-HR-QTOFMS). Detailed operating conditions for the GC/EI-MS and UPLC/ESI-HR-QTOFMS analyses as well as detailed filter extraction protocols have been described previously by Lin et al. (2012). For GC/EI-MS analysis, filter extracts were dried under a gentle stream of $N_2$ and trimethylsilylated by the addition of 100 μL of BSTFA + TMCS (99:1 v/v, Supelco) and 50 μL of pyridine (anhydrous, 99.8%, Sigma-Aldrich) and heated at 70 ºC for 1 h. For UPLC/ESI-HR-QTOFMS analysis,

residues of filter extracts were reconstituted with 150 µL of a 50:50 (v/v) solvent mixture of high-purity water and methanol.

The isoprene-derived SOA markers: 2-methyltetrols, isomeric 3-methyltetrahydrofurans-3,4-diols (3-MeTHF-3,4-diols), and 2-methylglyceric acid, synthesized according to the published procedures (Y-H Lin et al. 2013; Zhang et al. 2012), were available in-house as authentic standards to quantify the major components of isoprene SOA. 2-Methyltetrol organosulfates, synthesized as a mixture of tetrabutylammonium salts, were also available as a standard. Purity was determined to be >99% by $^{1}$H NMR and UPLC/ESI-QTOFMS analysis (Budisulistiorini et al. 2015). The $C_5$-alkene triols and IEPOX dimer were quantified using the response factor obtained for the synthetic 2-methyltetrols.

A representative ambient $PM_{2.5}$ sample collected from the rural southeastern U.S. (Yorkville, GA) (YH Lin et al. 2013) during the summer of 2010 was analyzed in an identical manner to confirm atmospheric relevance of the chamber-generated SOA constituents.

***2.2.7 Cytotoxicity Assay***

Cytotoxicity was assessed through measurement of lactate dehydrogenase (LDH) released into the extracellular medium from damaged cells using the LDH cytotoxicity detection kit (Takara). To ensure that the EAVES device itself and operation procedure had no effect on cytotoxicity, the LDH release from cells exposed to clean chamber air was measured. LDH release by cells exposed via the EAVES to the photochemically aged (light) and non-photochemically aged (dark) particles was compared to release from unexposed cells maintained in the incubator for the same duration. For the resuspension exposures, LDH release by cells exposed to SOA through resuspended extract of photochemically aged and non-photochemically aged particles was compared to release by cells maintained in KBM only. Additionally, LDH release from the light exposures, dark control, and resuspension exposures was compared to release by positive control cells exposed to 1% Triton X-100 to ensure that cell death would not affect gene expression results.

### *2.2.8 Gene Expression Analysis*

We chose to measure the levels of the inflammation-related mRNA in the BEAS-2B cells exposed to isoprene-derived SOA generated in our outdoor chamber because various particle types are capable of sequestering cytokines (Seagrave 2008). Other direct deposition studies have also used mRNA transcripts as a proxy for cytokine production (Hawley and Volckens 2013; Hawley et al. 2014a; Hawley et al. 2014b; Lichtveld et al. 2012; Volckens et al. 2009). Changes in *IL-8* and *PTGS2* mRNA levels were measured using QuantiTect SYBR Green RT-PCR Kit (Qiagen) and QuantiTect Primer Assays for Hs_ACTB_1_SG (Catalog #QT00095431), Hs_*PTGS2*_1_SG (Catalog #QT00040586), and Hs_CXCL8_1_SG (Catalog #QT00000322) for one-step RT-PCR analysis. All mRNA levels were normalized against β-actin mRNA, which was used as a housekeeping gene. The relative expression levels (i.e., fold change) of *IL-8* and *PTGS2* were calculated using the comparative cycle threshold ($2^{-\Delta\Delta CT}$) method (Livak and Schmittgen 2001). For EAVES exposures, changes in *IL-8* and *PTGS2* from isoprene-derived SOA exposed cells were compared to cells exposed to the dark controls. Similarly, for resuspension exposures changes in *IL-8* and *PTGS2* from isoprene-derived SOA exposed cells were compared to cells exposed to particles collected under dark conditions.

### *2.2.9 Statistical Analysis*

The software package GraphPad Prism 4 (GraphPad) was used for all statistical analyses. All data were expressed as mean ± SEM (standard error of means). Comparisons between data sets for cytotoxicity and gene expression analysis were made using unpaired *t*-test with Welch's correction. Significance was defined as $p < 0.05$.

### *2.3 Results and Discussion*

#### *2.3.1 Physical and Chemical Characterization of Exposure*

Figure 2.1 shows the change in particle mass concentration and gas ($O_3$, NO, $NO_x$) concentration over time during typical photochemical and dark control experiments. Under dark control conditions (Fig. 2.1a) there is no increase in aerosol mass concentration following isoprene injection. Average total aerosol mass concentration was 155.0±2.69 μg $m^{-3}$ (1 standard deviation) with no particle mass attributable to organic material.

In contrast, Fig. 2.1 b shows an increase in aerosol mass concentration after 1-hr post isoprene injection, which can be attributed to the photochemical oxidation of isoprene and subsequent production and reactive uptake of its oxidation products. The average increase in aerosol mass concentration attributable to SOA formation for three daylight chamber experiments conducted on separate days was 44.5±5.7 μg $m^{-3}$. Average total aerosol mass concentration during particle exposure was 173.1± 4.2 μg $m^{-3}$.

$O_3$ and $NO_x$ concentrations measured during EAVES exposure were approximately 270 ppb and 120 ppb for photochemical experiments. For dark control experiments (e.g., Fig. 2.1a), the $O_3$ and $NO_x$ concentrations were approximately 15 ppb and 180 ppb. Previous studies characterizing the EAVES device show definitively that gas-phase products do not induce cell response (de Bruijne et al. 2009). However, resuspension exposures were conducted in addition to EAVES exposure to ensure that biological effects were attributable to only particle-phase constituents and not gas-phase products such as $O_3$ and $NO_x$.

The chemical composition of aerosol, collected onto filters concurrently with cell exposure and characterized by GC/EI-MS and UPLC/ESI-HR-QTOFMS, are shown in Fig. 2.2. No isoprene-derived SOA tracers were observed in the filters collected from dark control experiments. The dominant particle-phase products of the isoprene-derived SOA collected from photochemical experiments are derived

from the low-NO channel, where IEPOX reactive uptake onto acidic sulfate aerosol dominates, including 2-methyltetrols, $C_5$-alkene triols, isomeric 3-MeTHF-3,4-diols, IEPOX-derived dimers, and IEPOX-derived organosulfates. Figure 2.3 shows that the IEPOX-derived organosulfate (*m/z* 215.0231, $C_5H_{11}O_7S^-$), have been detected with high abundance. MAE/HMML-SOA tracers (i.e., high-$NO_x$ channel), including 2-methylglyceric acid and its organosulfate derivative (*m/z* 198.9918, $C_4H_7O_7S^-$), and the ISOPOOH-derived SOA tracer (*m/z* 231.01801, $C_5H_{11}O_8S^-$) (i.e., low-$NO_x$ channel, non-IEPOX route) have also been observed, but contribute to a much smaller fraction of the overall SOA formation. The sum of the IEPOX-derived SOA constituents quantified by the available standards accounted for ~80% of the observed SOA mass.

As demonstrated in Figure 2.2, all the same particle-phase products are measured in the $PM_{2.5}$ sample collected in Yorkville, GA (a typical low-NO region), demonstrating that the composition of the chamber-generated SOA is atmospherically relevant. Recent SOA tracer measurements from the Southern Oxidant and Aerosol Study (SOAS) campaign at Look Rock, TN, Centerville, AL, and Birmingham, AL, also support the atmospheric relevance of IEPOX-derived SOA constituents that dominate the isoprene SOA mass in summer in the southeastern U.S. (Budisulistiorini et al. 2016; Rattanavaraha et al. 2016).

### *2.3.2 Cytotoxicity*

LDH release for cells exposed using the EAVES device is expressed as a fold-change relative to the unexposed incubator control. For resuspension exposures, LDH release is expressed as fold-change relative to cells exposed to KBM only. Results shown in Fig. 2.4a confirm that there is no effect of chamber conditions and device operation on the cells when comparing LDH release from cells exposed to a clean air chamber and cells unexposed in an incubator. Additionally, LDH release from all exposure conditions in EAVES exposed cells (Fig. 2.4b) and resuspension exposed cells (Fig. 2.4c) is negligible relative to positive controls exposed to 1% Triton X-100, confirming that the exposure concentration of

isoprene-derived SOA utilized in this study was not cytotoxic. All cytotoxicity results ensured that exposure conditions were not adversely affecting the cells nor their gene expression.

### *2.3.3 Pro-inflammatory Gene Expression*

Changes in the mRNA levels of *IL-8* and *PTGS2* from cells exposed to isoprene-derived SOA using the EAVES are shown as fold-changes relative to dark controls in Fig. 2.5. This comparison, as well as the results of the resuspension experiment discussed below, ensures that all effects seen in the cells are attributable to the isoprene-derived SOA and no other factors. A 1-hr exposure to a mass concentration of approximately 45 μg $m^{-3}$ of organic material was sufficient to significantly alter gene expression of the inflammatory biomarkers in bronchial epithelial cells. Based on deposition efficiency characterized by de Bruijne et al. (2009), the estimated dose was 0.29 μg $cm^{-2}$ of total particle mass with 23% attributable to organic material formed from isoprene photooxidation (0.067 μg $cm^{-2}$ of SOA).

Changes in the mRNA levels of *IL-8* and *PTGS2* from cells exposed to resuspended isoprene-derived SOA collected from photochemical experiments are shown as fold-changes relative to cells exposed to resuspended particles from dark control experiments in Fig. 2.6. At a low dose of 0.01 mg $mL^{-1}$ of isoprene SOA extract there is no significant increase in *IL-8* and *PTGS2* mRNA expression. The isoprene SOA extract, however, induces a response at a dose of 0.1 mg $mL^{-1}$. The statistically significant increase in mRNA expression from the resuspension exposure at 0.1 mg $mL^{-1}$ confirms that similar fold changes observed for both *IL-8* and *PTGS2* from the EAVES exposures are not attributable to gaseous photooxidation products, such as $O_3$, and support the characterization of the EAVES as a particle exposure device (de Bruijne et al. 2009).

The similar fold change observed in both the EAVES exposure and resuspension exposure, in addition to confirming that the biological effects can be attributed to the particle-phase photochemical products (isoprene-derived SOA), suggests that exposure by resuspension may be appropriate for isoprene-derived SOA and may yield results similar to direct deposition exposures. Unlike diesel

particulate extracts, which agglomerate during resuspension exposures, isoprene-derived SOA constituents are water-soluble based on reverse-phase LC separations (Lin et al. 2012; Surratt et al. 2006) and remain well mixed in the cell medium used for exposure. Therefore, resuspension exposures do not appear to be a limitation for toxicological assessments of isoprene SOA.

### *2.3.4 Biological Implications*

The goal of this study was to initially identify potential biological response associated with exposure to isoprene-derived SOA by using a direct exposure device as a model that has both atmospheric and physiological relevance. With this model, a dose of 0.067 μg $cm^{-2}$ of isoprene SOA, induced statistically significant increases in *IL-8* and *PTGS2* mRNA levels in exposed BEAS-2B cells. There are many ways to classify *in vitro* particle dosimetry based on the various properties of particles (Paur et al. 2011). For this direct deposition study, we chose to classify dose as SOA mass deposition per surface area of the exposed cells to mimic lung deposition. Gangwal et al. (2011) used a multiple-path particle dosimetry (MPPD) model to estimate that the lung deposition of ultrafine particles ranges from 0.006 to 0.02 μg $cm^{-2}$ for a 24-hr exposure to a particle concentration of 0.1 mg $m^{-3}$. Based on this estimate, a dose of 0.067 μg $cm^{-2}$ of isoprene SOA in our study can be considered a prolonged exposure over the course of a week. In fact, most other in vitro studies require dosing cells at a high concentration sometimes close to a lifetime exposure to obtain a cellular response. Despite this limitation, *in vitro* exposures serve as a necessary screening tool for toxicity (Paur et al. 2011).

Our findings are consistent with other studies showing that photochemical oxidation of similar chemical mixtures increases toxicity in cell culture models and elevates expression of inflammatory biomarker genes (Lichtveld et al. 2012; Rager et al. 2011). Previous *in vitro* studies using a gas-phase only exposure system have shown that gas-phase products of isoprene photooxidation significantly enhance cytotoxicity and *IL-8* expression (Doyle et al. 2004; Doyle et al. 2007).

By choosing *IL-8* and *PTGS2* as our genes of interest, we were able to compare our results to other studies of known harmful particle exposures. In a similar study using the EAVES, normal human bronchial epithelial (NHBE) cells exposed to 1.10 μg $cm^{-2}$ diesel particulate matter showed less than a 2-fold change over controls in both *IL-8* and *PTGS2* mRNA expression (Hawley et al. 2014b). In another study, A549 human lung epithelial cells were exposed by direct deposition for 1 hour to photochemically-aged diesel exhaust particulates at a dose of 2.65 μg $cm^{-2}$ from a 1980 Mercedes or a 2006 Volkswagen (Lichtveld et al. 2012). Exposure to aged Mercedes particulates induced a 4-fold change in *IL-8* and ~2-fold change in *PTGS2* mRNA expression, while exposure to aged Volkswagen particulates induced a change of ~1.5-fold in *IL-8* and 2-fold in *PTGS2* mRNA expression (Lichtveld et al. 2012). Although the differences in cell types preclude direct comparisons, the finding of significant increases in *PTGS2* and *IL-8* expression at doses much lower than reported for comparable increases in gene expression levels induced by photochemically-aged diesel particulates is notable.

*IL-8* and *PTGS2* are both linked to inflammation and oxidative stress (Kunkel et al. 1991; Uchida 2008). *IL-8* is a potent neutrophil chemotactic factor in the lung and its expression by various cells plays a crucial role in neutrophil recruitment leading to lung inflammation (Kunkel et al. 1991). *PTGS2* is the inducible form of the cyclooxygenase enzyme, regulated by cytokines and mitogens, and is responsible for prostaglandin synthesis associated with inflammation (FitzGerald 2003). Consistent with the reports that *IL-8* and *PTGS2* play important roles in lung inflammation (Li et al. 2013; Nocker et al. 1996), *in vivo* studies have shown that isoprene oxidation products cause airflow limitation and sensory irritation in mice (Rohr et al. 2003). In humans, the role of *IL-8* and *PTGS2* in lung inflammation can be associated with diseases such as chronic obstructive pulmonary disease and asthma (Fong et al. 2000; Nocker et al. 1996; Peng et al. 2008).

The mechanism by which isoprene SOA causes elevation of the inflammatory markers *IL-8* and *PTGS2* is not yet fully understood. However, recent work from our laboratory using the acellular

dithiothreitol (DTT) assay demonstrated that isoprene-derived SOA has significant ROS generation potential (Kramer et al. 2016). High levels of ROS in cells can overwhelm the antioxidant defense and lead to cellular oxidative stress (Bowler and Crapo 2002; Li et al. 2003a; Sies 1991). Oxidative stress caused by ROS plays a major role in lung inflammation and the induction of oxidative stress can lead to *IL-8* expression (Tao et al. 2003; Yan et al. 2015). Specifically, oxidants can activate the transcription factor NF-κB, which regulates a wide range of inflammatory genes including *IL-8* and *PTGS2* (Barnes and Adcock 1997; Schreck et al. 1992). Therefore, isoprene SOA may cause increases in both *IL-8* and *PTGS2* primarily through an oxidative stress response. Additionally, the relationship between *IL-8* and *PTGS2* can also explain the observed increase in *IL-8* gene expression as the production of *IL-8* can be stimulated through a *PTGS2* dependent mechanism in airway epithelial cells (Peng et al. 2008).

*In vitro* studies such as this one using a direct deposition model cannot fully elucidate mechanisms of lung inflammation and potential pathogenesis but serve as a necessary part of hazard characterization, particularly for a complex air mixture that has not been fully studied (Hayashi 2005; Paur et al. 2011). Ozone exposure studies have shown that comparable dose and effect measurements for *IL-8* and *PTGS2* can be found between *in vivo* and *in vitro* exposures which add promise to extrapolating effects seen *in vitro* to effects *in vivo* (Hatch et al. 2014).

### *2.4 Conclusions*

The results of this study indicates that an atmospherically relevant composition of isoprene-derived SOA is capable of increasing the expression of *IL-8* and *PTGS2* in human bronchial epithelial cells. The SOA were generated as NO levels approached zero, which represents conditions characteristic of urban locales downwind of rural isoprene sources. As shown in Fig. 2.2, the aerosol generated for exposures in this study are chemically similar to fine aerosol samples collected from the Southeastern U.S., which indicates that the chamber exposures are representative of exposures that may be encountered by populations in regions where isoprene emissions interact with anthropogenic

pollutants. The same particle-phase products found in our photochemical experiments have been measured in significant quantities (accounting on average for 40% of fine organic aerosol mass) in ambient fine organic particles collected in the Southeastern U.S. (Budisulistiorini et al. 2013; Budisulistiorini et al. 2016; Y-H Lin et al. 2013; Rattanavaraha et al. 2016) and in other isoprene-rich environments (Hu et al. 2015). The results of this study show that, because of its abundance, isoprene SOA may be a public health concern warranting further toxicological investigation. Additionally, based on the result of this study, resuspension exposure techniques may be an adequate method to study isoprene SOA.

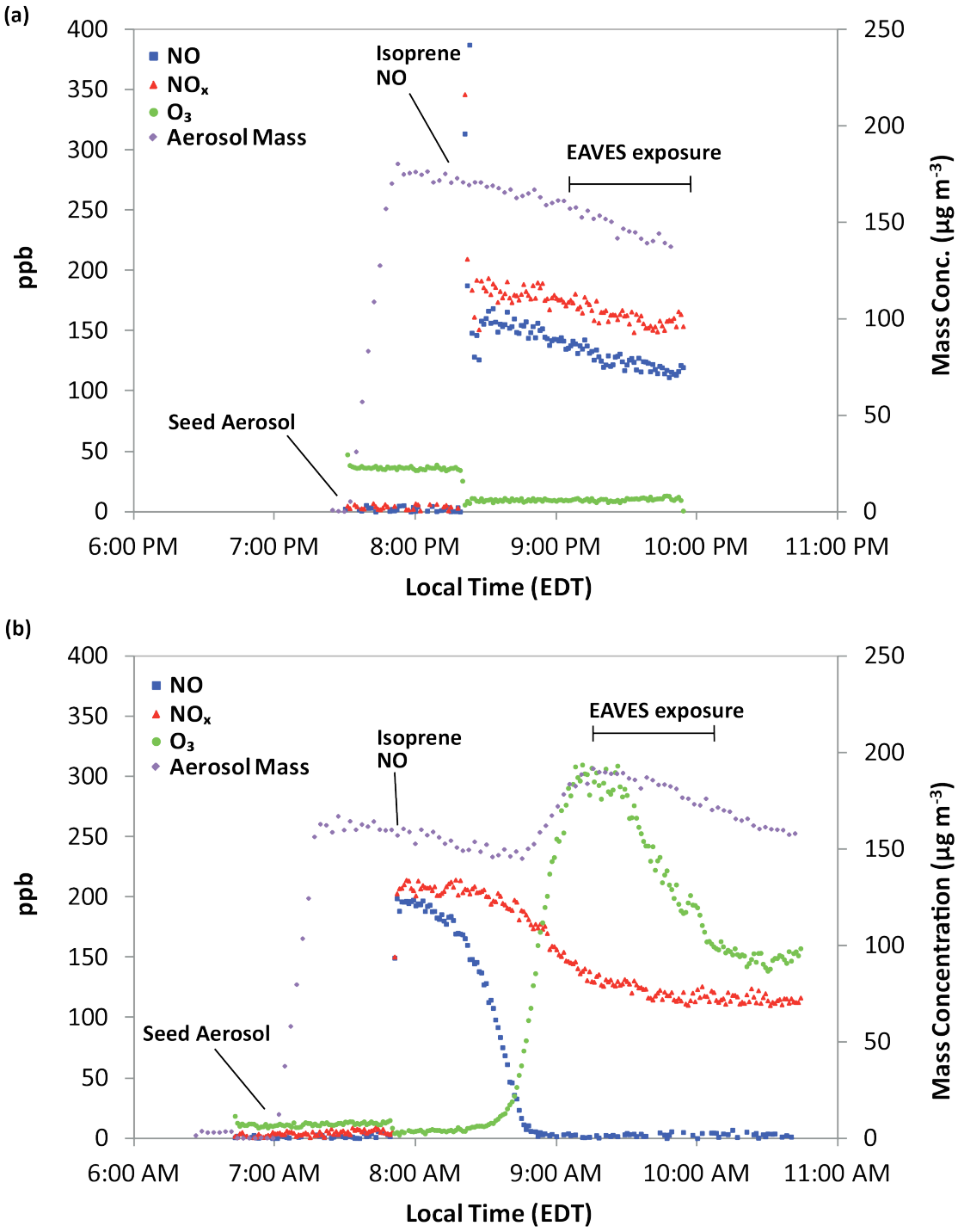


**Figure 2.1.** Aerosol mass concentration and gas-phase product concentrations over time for (a) dark control chamber experiment and (b) photochemically produced isoprene-derived SOA exposure chamber experiment.

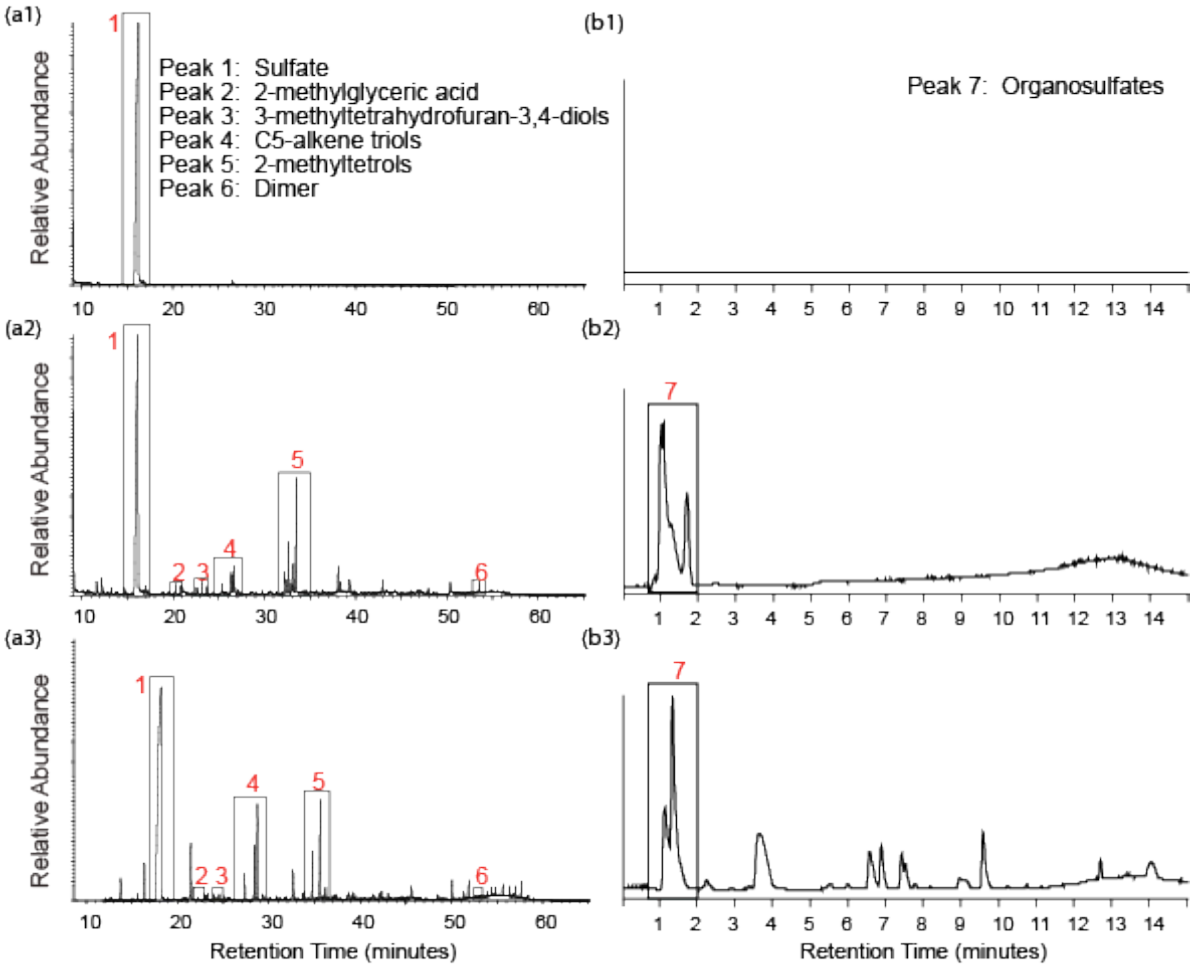


**Figure 2.2.** (a) GC/EI-MS total ion chromatograms (TICs) and (b) UPLC/ESI-HR-QTOFMS base peak chromatograms (BPCs) from a (1) dark control chamber experiment, (2) isoprene-derived SOA exposure chamber experiment, and (3) $PM_{2.5}$ sample collected from Yorkville, GA during summer 2010.

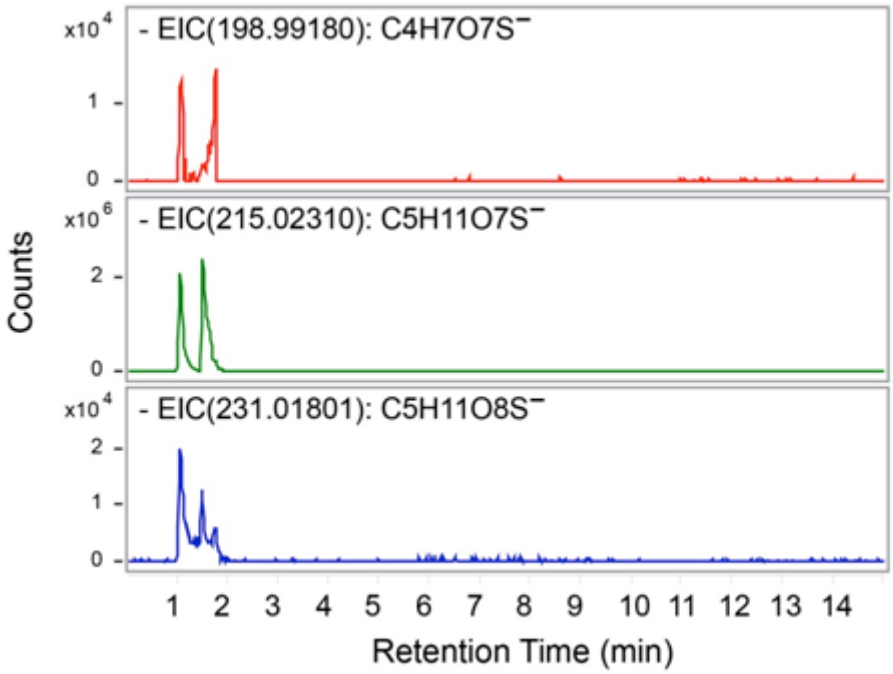


**Figure 2.3.** UPLC/(–)ESI-HR-QTOFMS extracted ion chromatograms (EICs) at *m/z* 198.99180, 215.02310, and 231.01801 corresponding to the MAE-, IEPOX-, and ISOPOOH-derived organosulfates, respectively.

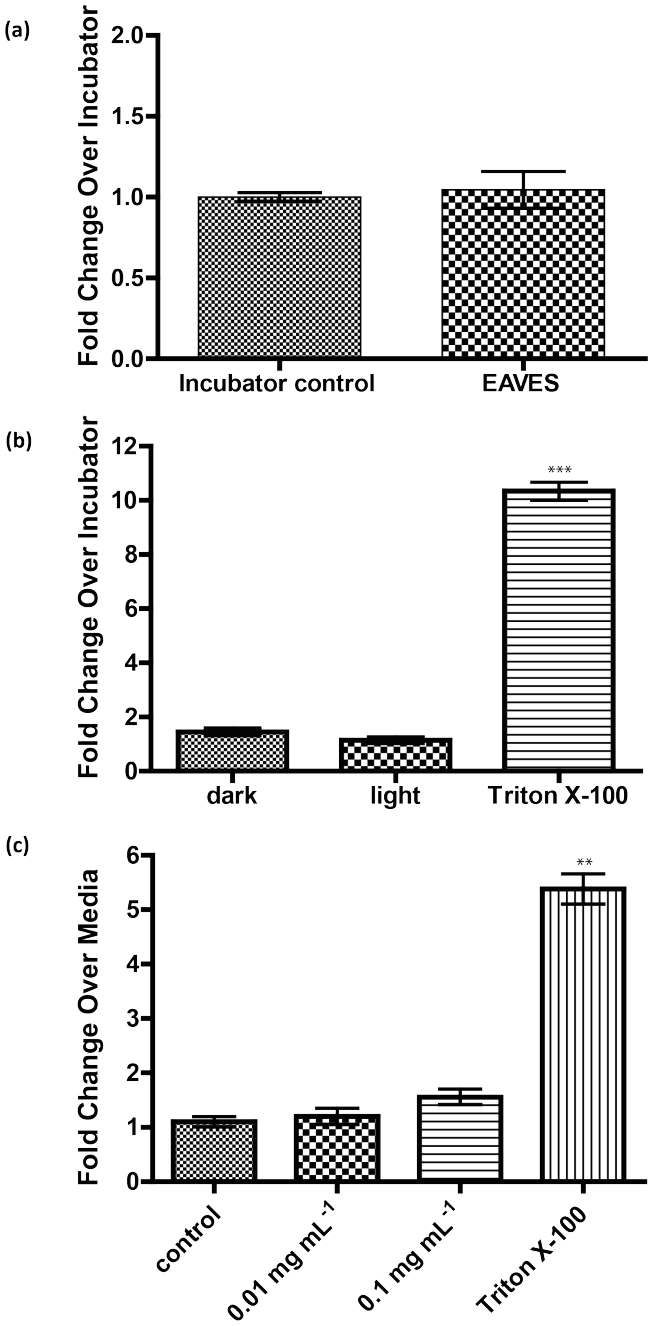


**Figure 2.4.** LDH release for (a) clean air controls, (b) EAVES exposures, normalized to incubator control, and (c) resuspension exposures, normalized to KBM only control. **p<0.005 and ***p<0.0005.

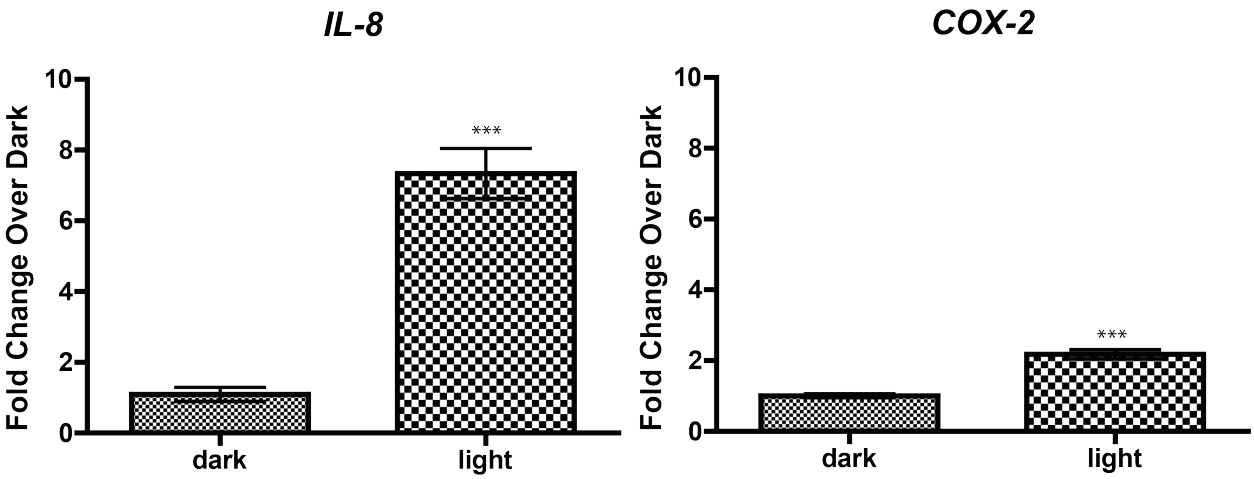


**Figure 2.5.** *IL-8* and *PTGS2* mRNA expression induced by exposure to isoprene-derived SOA using EAVES device all normalized to dark control experiments and against housekeeping gene, β-actin. All experiments conducted in triplicate. ***p<0.0005.

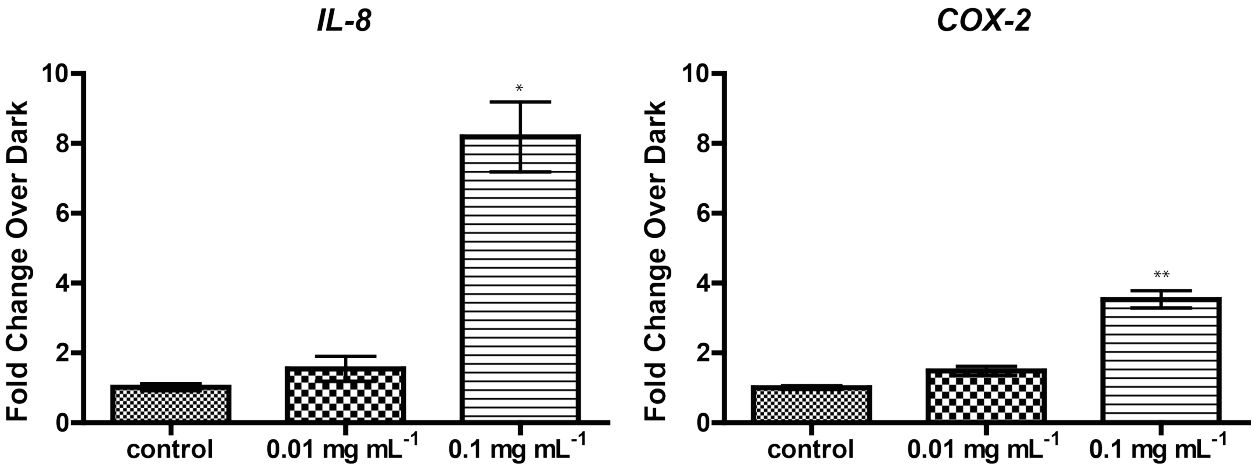


**Figure 2.6.** *IL-8* and *PTGS2* expression induced by exposure to isoprene-derived SOA using resuspension method all normalized to dark control experiments and against housekeeping gene, β-actin. All experiments conducted in triplicate. *p<0.05 and **p<0.005.

## CHAPTER III: EFFECT OF ISOPRENE-DERIVED SOA ON OXIDATIVE STRESS-ASSOCIATED GENES

### *3.1 Overview*

The objective of this study was to expand on the study presented in Chapter 2 by investigating the effect of isoprene SOA generated in the outdoor chamber on a greater number of genes though pathway-focused gene expression profiling using Qiagen Human Oxidative Stress Plus RT² Profiler PCR Array, which includes 84 oxidative stress-related genes. We chose to explore oxidative stress-related genes not only because of the elevated expression of *IL-8* and *PTGS2* found in Chapter 2, but also due to the ROS generation potential of isoprene-derived SOA demonstrated by Kramer et al. (2016).

Following the direct deposition study presented in Chapter 2, we concluded that resuspension exposures could be used for isoprene-derived SOA exposure studies. By utilizing resuspension exposure techniques, we ensured greater control in exposure conditions and were also able to incorporate an additional exposure time which was difficult with the direct deposition device. Therefore, this study examines the altered gene expression of 84 oxidative stress-related genes in BEAS-2B exposed to 0.1 mg $mL^{-1}$ of isoprene-derived SOA extract, collected from outdoor photooxidation chamber experiment in Chapter 2, for a 9-hr and 24-hr exposure time.

### *3.2 Experimental Section*

#### *3.2.1 Resuspension Exposures*

In this study we utilized cellular material from the 9-hr resuspension exposures at 0.1 mg $mL^{-1}$ of isoprene-derived SOA described in Chapter 2. Additionally, we conducted a 24-hr resuspension exposure at 0.1 mg $mL^{-1}$ of isoprene-derived SOA collected from the outdoor chamber experiments described previously. In preparation for filter resuspension exposures, cells were seeded in 24-well plates at a density of $2.5\times10^4$ cells/well in 250 µL of KGM 2 days prior to exposure. At the time of exposure, cells

were washed twice with phosphate buffered saline (PBS) buffer, and then exposed to KBM containing 0.1 mg $mL^{-1}$ isoprene SOA extract from photochemical experiment and seed particles from dark negative control experiments. Following a 24-hr exposure, extracellular medium was collected and total RNA was isolated using Trizol (Life Technologies).

### *3.2.2 Oxidative Stress-Associated Gene Expression Analysis*

Isolated RNA samples were further purified using the spin column-based Direct-zol RNA MiniPrep (Zymo Research). RNA quality and concentrations were determined using a NanoDrop 2000 spectrophotometer (Thermo Fisher Scientific). The absorbance ratios 260/280 nm of all samples were determined to be > 1.8. An aliquot of RNA (100 ng) was copied into cDNA using a $RT^2$ First Strand Kit (Qiagen). Gene expression analysis was performed using the pathway-focused Human Oxidative Stress Plus $RT^2$ Profiler PCR Array (Qiagen, 96-well format, catalog #: PAHS-065Y) with 84 oxidative stress-associated genes with a Stratagene Mx3005P real time qPCR System (Agilent Technologies). A list of all 84 oxidative stress-associated gens and housekeeping genes included in the array can be found in Table 3.1. Additionally, qRT-PCR assays (QuantiTect SYBR® Green RT-PCR Kit, Qiagen) of selected individual genes, including prostaglandin-endoperoxide synthase 2 (*PTGS2*) and beta-actin (*ACTB*, housekeeping gene), were also carried out for quality control

### *3.2.3 Data Analysis*

Relative levels of gene expression for exposure and control groups, given as fold changes, were calculated using the comparative cycle threshold ($2^{-\Delta\Delta CT}$) method (Livak and Schmittgen 2001). Transcriptional changes in cells exposed to isoprene-derived SOA extract from photochemical experiment were compared to changes in cells exposed to the extracts from dark control experiments for each time exposure (9-hr or 24-hr) to assess the effects induced solely by the extracted SOA constituents. Differentially expressed genes were identified using the Qiagen $RT^2$ Profiler Data Analysis Software v3.5. Results with arbitrary fold change (FC) cutoffs $\geq 1.5$ and $p < 0.05$ were considered

significant. The p-value adjusted for false discovery rate (FDR) was estimated to be 0.0005 (α/n; α=0.05, and n=84 genes). Network-based analysis to identify canonical pathways and transcription factors was carried out using Ingenuity Pathway Analysis (IPA) software (Ingenuity Systems, Inc., Redwood City, CA).

### *3.3 Results and Discusssion*

#### *3.3.1 Altered Expression of Genes from Exposure to Isoprene-derived SOA*

Volcano plots of differential gene expression in BEAS-2B cells upon exposure to isoprene-derived SOA are shown in Figure 3.1. More genes are differentially expressed after a 24-hr exposure than a 9-hr exposure. A complete list of significantly altered genes and p-values for the 9-hr exposure and 24-hr exposure is provided in Tables 3.2 and 3.3, respectively. With a fold change cut off of 1.5, 34 genes are differentially expressed in the 9-hr exposure group and 41 genes are differentially expressed in the 24-hr exposure. When adjusting for the FDR, fold changes in 17 genes for a 9-hr exposure and 23 genes for a 24-hr exposure remain significant. *HMOX1* has the highest fold change in both exposure time groups; its expression decreases over time but still remains significant after 24-hrs.

#### *3.3.2 Pathway Enrichment Analysis*

The 41 and 34 differentially expressed gene for the 9-hr and 24-hr exposure group were analyzed for enrichment within biological pathways. The top canonical pathway for both time points was the nuclear factor erythroid 2-like 2 (Nrf2)-mediated oxidative stress response with 15 genes from the 9-hr exposure ($p= 6.98x10^{-22}$) and 16 genes from the 24-hr exposure ($p=4.17x10^{-22}$) associated with the pathway. When adjusted for the FDR, 8 genes in the 9-hr exposure group and 9 genes in the 24-hr exposure group are still present.

Nrf2-related gene expression has been linked with exposures to other ambient PM (Huang et al. 2011) including diesel exhaust (Baulig et al. 2003; Wittkopp et al. 2016). For diesel exhaust, Nrf2 serves as a key transcription factor protecting against proinflammatory effects of particulate pollutants through its regulation of antioxidant defense (Li et al. 2004). Nrf2-mediated oxidative stress response may have

similar antioxidant defense capabilities against isoprene SOA exposure. Of all the genes associated with the Nrf2-pathway from our exposure, *HMOX1* is the most significantly altered gene. *HMOX1*, the inducible isoform of heme oxygenase, has been associated with exposure to diesel exhaust using *in vitro* (Gong et al. 2007) and *in vivo* (Peretz et al. 2007) models and may serve as a biomarker of oxidative-stress related defense when taken together with protein expression levels (Delfino et al. 2011). *HMOX1* plays a crucial role in preventing inflammation and oxidant-induced damage in the lung and is highly upregulated by oxidative stress (Choi and Alam 1996). Overexpression of *HMOX1* can actually play a protective role in many disease states (Morse and Choi 2002). Therefore, even though, *HMOX1* promoter polymorphisms are rare they leave certain populations at risk of respiratory diseases due to decreased defenses against oxidative stress (Fredenburgh et al. 2007; Yamada et al. 2000).

### *3.4 Conclusion*

The results of this study show that isoprene-derived SOA alters the expression of oxidative stress-related genes with a greater number oxidative stress related genes being altered after a 24-hour exposure when compared to a 9-hour exposure. Oxidative stress is known to be associated with chronic pulmonary inflammation, and contributes to respiratory and cardiovascular health outcomes (Donaldson et al. 2001; Kirkham and Barnes 2013; Rahman and Adcock 2006). However, our analysis showed that Nrf2-mediated stress response, which has antioxidant defense properties, was the top canonical pathway triggered by our exposure. More studies are needed to understand the role of the Nrf2 pathway in isoprene SOA exposure and its potential interconnection with other pathways and downstream effects.

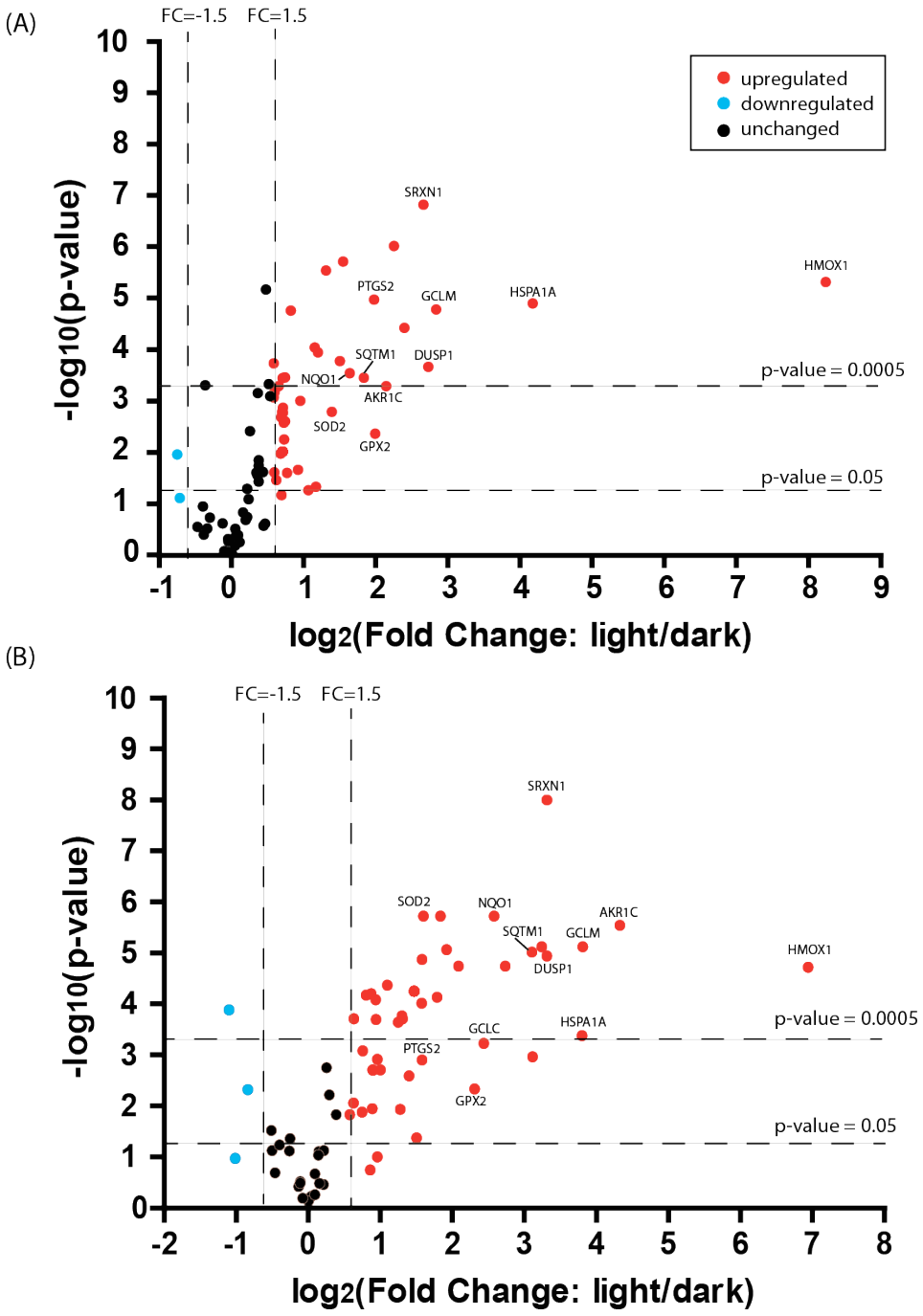


**Figure 3.1.** Volcano plot of differentially expressed genes in BEAS-2B cells upon exposure to isoprene-derived SOA for (A) 9 hours and (B) 24 hours. A full list of differentially expressed genes can be found in Table 3.2.

**Table 3.1** Gene symbols and full names of 84 oxidative stress-associated genes and housekeeping genes included in RT² Profiler™ PCR Array Human Oxidative Stress Pathway Plus (PAHS-065Y).

| # | Gene Symbol | Full Name |
|---|---|---|
| 1 | *ALB* | Albumin |
| 2 | *ALOX12* | Arachidonate 12-lipoxygenase |
| 3 | *AOX1* | Aldehyde oxidase 1 |
| 4 | *APOE* | Apolipoprotein E |
| 5 | *ATOX1* | ATX1 antioxidant protein 1 homolog (yeast) |
| 6 | *BNIP3* | BCL2/adenovirus E1B 19kDa interacting protein 3 |
| 7 | *CAT* | Catalase |
| 8 | *CCL5* | Chemokine (C-C motif) ligand 5 |
| 9 | *CCS* | Copper chaperone for superoxide dismutase |
| 10 | *CYBB* | Cytochrome b-245, beta polypeptide |
| 11 | *CYGB* | Cytoglobin |
| 12 | *DHCR24* | 24-dehydrocholesterol reductase |
| 13 | *DUOX1* | Dual oxidase 1 |
| 14 | *DUOX2* | Dual oxidase 2 |
| 15 | *DUSP1* | Dual specificity phosphatase 1 |
| 16 | *EPHX2* | Epoxide hydrolase 2, cytoplasmic |
| 17 | *EPX* | Eosinophil peroxidase |
| 18 | *FOXM1* | Forkhead box M1 |
| 19 | *FTH1* | Ferritin, heavy polypeptide 1 |
| 20 | *GCLC* | Glutamate-cysteine ligase, catalytic subunit |
| 21 | *GPX1* | Glutathione peroxidase 1 |
| 22 | *GPX2* | Glutathione peroxidase 2 (gastrointestinal) |
| 23 | *GPX3* | Glutathione peroxidase 3 (plasma) |
| 24 | *GPX4* | Glutathione peroxidase 4 (phospholipid hydroperoxidase) |
| 25 | *GPX5* | Glutathione peroxidase 5 (epididymal androgen-related protein) |
| 26 | *GSR* | Glutathione reductase |
| 27 | *GSS* | Glutathione synthetase |
| 28 | *GSTP1* | Glutathione S-transferase pi 1 |
| 29 | *GSTZ1* | Glutathione transferase zeta 1 |
| 30 | *HSPA1A* | Heat shock 70kDa protein 1A |
| 31 | *KRT1* | Keratin 1 |
| 32 | *LPO* | Lactoperoxidase |
| 33 | *MB* | Myoglobin |
| 34 | *MBL2* | Mannose-binding lectin (protein C) 2, soluble |
| 35 | *MPO* | Myeloperoxidase |
| 36 | *MPV17* | MpV17 mitochondrial inner membrane protein |
| 37 | *MSRA* | Methionine sulfoxide reductase A |
| 38 | *MT3* | Metallothionein 3 |
| 39 | *NCF1* | Neutrophil cytosolic factor 1 |
| 40 | *NCF2* | Neutrophil cytosolic factor 2 |
| 41 | *NOS2* | Nitric oxide synthase 2, inducible |
| 42 | *NOX4* | NADPH oxidase 4 |
| 43 | *NOX5* | NADPH oxidase, EF-hand calcium binding domain 5 |
| 44 | *NUDT1* | Nudix (nucleoside diphosphate linked moiety X)-type motif 1 |
| 45 | *PDLIM1* | PDZ and LIM domain 1 |

| | | |
|---|---|---|
| 46 | *PRDX1* | Peroxiredoxin 1 |
| 47 | *PRDX2* | Peroxiredoxin 2 |
| 48 | *PRDX3* | Peroxiredoxin 3 |
| 49 | *PRDX4* | Peroxiredoxin 4 |
| 50 | *PRDX5* | Peroxiredoxin 5 |
| 51 | *PRDX6* | Peroxiredoxin 6 |
| 52 | *PRNP* | Prion protein |
| 53 | *PTGS1* | Prostaglandin-endoperoxide synthase 1 (prostaglandin G/H synthase and cyclooxygenase) |
| 54 | *PTGS2* | Prostaglandin-endoperoxide synthase 2 (prostaglandin G/H synthase and cyclooxygenase) |
| 55 | *RNF7* | Ring finger protein 7 |
| 56 | *VIMP* | Selenoprotein S |
| 57 | *SEPP1* | Selenoprotein P, plasma, 1 |
| 58 | *SFTPD* | Surfactant protein D |
| 59 | *SIRT2* | Sirtuin 2 |
| 60 | *SOD1* | Superoxide dismutase 1, soluble |
| 61 | *SOD2* | Superoxide dismutase 2, mitochondrial |
| 62 | *SOD3* | Superoxide dismutase 3, extracellular |
| 63 | *SQSTM1* | Sequestosome 1 |
| 64 | *SRXN1* | Sulfiredoxin 1 |
| 65 | *TPO* | Thyroid peroxidase |
| 66 | *TTN* | Titin |
| 67 | *TXNRD2* | Thioredoxin reductase 2 |
| 68 | *UCP2* | Uncoupling protein 2 (mitochondrial, proton carrier) |
| 69 | *AKR1C2* | Aldo-keto reductase family 1, member C2 (dihydrodiol dehydrogenase 2; bile acid binding protein; 3-alpha hydroxysteroid dehydrogenase, type III) |
| 70 | *BAG2* | BCL2-associated athanogene 2 |
| 71 | *FHL2* | Four and a half LIM domains 2 |
| 72 | *GCLM* | Glutamate-cysteine ligase, modifier subunit |
| 73 | *GLA* | Galactosidase, alpha |
| 74 | *HMOX1* | Heme oxygenase (decycling) 1 |
| 75 | *HSP90AA1* | Heat shock protein 90kDa alpha (cytosolic), class A member 1 |
| 76 | *LHPP* | Phospholysine phosphohistidine inorganic pyrophosphate phosphatase |
| 77 | *NCOA7* | Nuclear receptor coactivator 7 |
| 78 | *NQO1* | NAD(P)H dehydrogenase, quinone 1 |
| 79 | *PTGR1* | Prostaglandin reductase 1 |
| 80 | *SLC7A11* | Solute carrier family 7 (anionic amino acid transporter light chain, xc- system), member 11 |
| 81 | *SPINK1* | Serine peptidase inhibitor, Kazal type 1 |
| 82 | *TRAPPC6A* | Trafficking protein particle complex 6A |
| 83 | *TXN* | Thioredoxin |
| 84 | *TXNRD1* | Thioredoxin reductase 1 |
| Housekeeping Genes | *ACTB* | Actin, beta |
| | *B2M* | Beta-2-microglobulin |
| | *GAPDH* | Glyceraldehyde-3-phosphate dehydrogenase |
| | *HPRT1* | Hypoxanthine phosphoribosyltransferase 1 |
| | *RPLP0* | Ribosomal protein, large, P0 |

**Table 3.2** List of genes identified with significant expression fold-changes (p<0.05) upon exposure to Isoprene SOA for a 9 hour exposure. False Discovery Rate (FDR) adjusted p-value: 0.05/84=0.0005. Full names of gene symbols can be found in Table 3.1.

| Exposure Time | Gene Symbol | Fold Regulation | p-value | NRF2-associated Genes | <FDR |
|---|---|---|---|---|---|
| 9 hour | *AKR1C2* | 4.45 | 0.000535 | | |
| | *ALOX12* | 2.27 | 0.048148 | | |
| | *AOX1* | 1.62 | 0.002151 | + | |
| | *CCL5* | 1.52 | 0.025327 | | |
| | *DUSP1* | 6.68 | 0.000223 | | * |
| | *FHL2* | 2.31 | 0.000117 | | * |
| | *FTH1* | 2.85 | 0.000172 | + | * |
| | *GCLC* | 2.95 | 0.000002 | + | * |
| | *GCLM* | 7.21 | 0.000017 | + | * |
| | *GLA* | 2.24 | 0.000094 | | * |
| | *GPX2* | 4.01 | 0.004499 | + | |
| | *GPX3* | 1.59 | 0.00053 | | |
| | *GSR* | 1.69 | 0.00258 | + | |
| | *HMOX1* | 304.44 | 0.000005 | + | * |
| | *HSP90AA1* | 2.50 | 0.000003 | | * |
| | *HSPA1A* | 18.21 | 0.000013 | | * |
| | *LPO* | 1.67 | 0.005768 | | |
| | *MPO* | 1.72 | 0.026056 | | |
| | *NCOA7* | 1.52 | 0.0007 | | |
| | *NQO1* | 3.14 | 0.000297 | + | * |
| | *PRDX1* | 1.78 | 0.000018 | + | * |
| | *PRNP* | 1.51 | 0.000884 | | |
| | *PTGS2* | 3.96 | 0.000011 | | * |
| | *SLC7A11* | 4.80 | 0.000001 | | * |
| | *SOD1* | 1.67 | 0.002737 | + | |
| | *SOD2* | 2.64 | 0.001677 | + | |
| | *SOD3* | 1.91 | 0.022473 | + | |
| | *SQSTM1* | 3.60 | 0.000366 | + | * |
| | *SRXN1* | 6.09 | 0 | | * |
| | *TXN* | 1.95 | 0.001029 | + | |
| | *TXNRD1* | 5.30 | 0.000039 | + | * |
| | *UCP2* | 1.55 | 0.035816 | | |
| | *VIMP* | 1.65 | 0.000368 | | * |
| | *CCS* | -1.67 | 0.011423 | | |

**Table 3.3** List of genes identified with significant expression fold-changes (p<0.05) upon exposure to Isoprene SOA for a 24 hour exposure. False Discovery Rate (FDR) adjusted p-value: 0.05/84=0.0005. Full names of gene symbols can be found in Table 3.1.

| Exposure Time | Gene Symbol | Fold Regulation | p-value | NRF2-associated Genes | <FDR |
|---|---|---|---|---|---|
| 24 hour | *AKR1C2* | 20.21 | 0.000003 | | * |
| | *ALOX12* | 1.83 | 0.189227 | | |
| | *ATOX1* | 1.57 | 0.000203 | | * |
| | *BAG2* | 2.48 | 0.000181 | | * |
| | *BNIP3* | 1.50 | 0.015483 | | |
| | *DUOX2* | 1.69 | 0.013911 | | |
| | *DUSP1* | 10.01 | 0.000012 | | * |
| | *EPX* | 2.02 | 0.002065 | | |
| | *FHL2* | 1.93 | 0.000212 | | * |
| | *FTH1* | 6.71 | 0.000019 | + | * |
| | *GCLC* | 5.45 | 0.000627 | + | |
| | *GCLM* | 14.12 | 0.000008 | + | * |
| | *GLA* | 4.28 | 0.000019 | | * |
| | *GPX2* | 4.99 | 0.004839 | + | |
| | *GPX3* | 1.88 | 0.002074 | | |
| | *GSR* | 2.66 | 0.002702 | + | |
| | *GSTP1* | 1.70 | 0.000867 | + | |
| | *HMOX1* | 123.64 | 0.00002 | + | * |
| | *HSP90AA1* | 3.01 | 0.000014 | | * |
| | *HSPA1A* | 14.03 | 0.000441 | | * |
| | *NCF1* | 2.85 | 0.04451 | | |
| | *NQO1* | 6.02 | 0.000002 | + | * |
| | *PRDX1* | 3.82 | 0.000009 | + | * |
| | *PRDX4* | 1.56 | 0.009166 | | |
| | *PRDX6* | 2.15 | 0.000045 | | * |
| | *PRNP* | 1.85 | 0.000066 | | * |
| | *PTGS1* | 1.87 | 0.011846 | | |
| | *PTGS2* | 3.02 | 0.001327 | | |
| | *RNF7* | 1.87 | 0.002062 | | |
| | *SLC7A11* | 9.54 | 0.000008 | | * |
| | *SOD1* | 2.50 | 0.000203 | + | * |
| | *SOD2* | 3.05 | 0.000002 | + | * |
| | *SOD3* | 1.96 | 0.001269 | + | |
| | *SQSTM1* | 8.67 | 0.00001 | + | * |
| | *SRXN1* | 8.52 | 0 | | * |
| | *TXN* | 3.48 | 0.000078 | + | * |
| | *TXNRD1* | 8.71 | 0.001145 | + | |

| | | | | |
|---|---|---|---|---|
| *UCP2* | 2.44 | 0.01224 | | |
| *VIMP* | 3.60 | 0.000002 | | * |
| *CAT* | -1.78 | 0.005005 | + | |
| *MSRA* | -2.13 | 0.000138 | | * |

## CHAPTER IV: EFFECT OF MAE- AND IEPOX-DERIVED SOA ON THE EXPRESSION OF OXIDATIVE STRESS-RELATED GENES[2]

### *4.1 Overview*

Because isoprene-derived SOA, as described in Chapter 2, was generated through photochemical oxidation in the outdoor chamber facility as a mixture, biological effects cannot be attributed to specific components that comprise the isoprene SOA system (Figure 1 of Chapter 1). Therefore, the objective of this study is to evaluate the potential contributions to gene expression induction from SOA derived from the reactive uptake of *trans*-β-IEPOX or MAE. Although, the IEPOX-derived SOA constituents were the major contributor to the mass of the isoprene-derived SOA generated in Chapter 2, Kramer et al. (2016) has shown that MAE-derived SOA has a greater oxidizing potential than IEPOX-derived SOA which may mean greater contribution to the changes in oxidative stress-related genes observed in the total isoprene SOA exposure.

Based on Chapter 3, more oxidative stress-related genes were upregulated after a 24-hr exposure than a 9-hr exposure, so we chose a 24-hr exposure time for IEPOX- and MAE-derived SOA exposures. Additionally, we continue with resuspension exposures of 0.1 mg $mL^{-1}$ to be comparable to the PCR array data already presented.

[2] This chapter has been adapted from an article in Environmental Science & Technology Letters. The original citation is as follows: Lin, Y.-H., Arashiro, M., Martin, E., Chen, Y., Zhang, Z., Sexton, K. G., Gold, A., Jaspers, I., Fry, R. C., and Surratt, J. D.: Isoprene-Derived Secondary Organic Aerosol Induces the Expression of Oxidative Stress Response Genes in Human Lung Cells, Environmental Science & Technology Letters, 3, 250-254, 10.1021/acs.estlett.6b00151, 2016.

### *4.2 Experimental Section*

#### *4.2.1 Synthesis of SOA Precursors*

*Trans*-β-IEPOX and MAE were synthesized according to published synthetic procedures (Y-H Lin et al. 2013; Zhang et al. 2012). Identity and purity (>99%) were confirmed by $^{1}H$ and $^{13}C$ NMR, gas chromatography/electron ionization-mass spectrometry (GC/EI-MS) analysis with prior trimethylsilylation (TMS), or ultra-performance liquid-chromatography coupled to electrospray ionization quadrupole time-of flight mass spectrometry (UPLC/ESI-QTOFMS).

#### *4.2.2 Generation and Chemical Characterization of IEPOX- and MAE-derived SOA*

Reactive uptake experiments were performed in a 10-$m^3$ flexible Teflon indoor chamber at the University of North Carolina. The operation of chamber facility has been described in detail previously (Lin et al. 2012). Prior to each experiment, the chamber was flushed for at least 24-hr to replace at least five volumes of chamber air to ensure particle-free conditions. Particle size distributions were measured continuously using a differential mobility analyzer (DMA; BMI model 2002) coupled to a mixing condensation particle counter (MCPC; BMI model 1710), or a scanning mobility particle sizer (SMPS; TSI) consisting of a differential mobility analyzer (DMA; TSI model 3081) coupled to a condensation particle counter (CPC; TSI model 3776). Acidified sulfate seed aerosol solutions containing 0.06 M magnesium sulfate ($MgSO_4$) and 0.06 M sulfuric acid ($H_2SO_4$) were nebulized into the chamber to provide a preexisting aerosol surface for reactive uptake of epoxides. Seed aerosols were atomized into the chamber until total aerosol mass concentrations of 78-92 μg $m^{-3}$ and 61-300 μg $m^{-3}$ were attained for experiments with IEPOX and MAE, respectively. Experiments were conducted under dry conditions (<10% RH) to minimize loss of gas-phase epoxides to chamber walls. Temperature and RH inside the chamber were continuously monitored using an OM-62 temperature RH data logger (OMEGA Engineering, Inc.). A summary of the experimental conditions is given in Table 4.1. Multiple experiments

were performed to collect ~900 μg SOA for each SOA source. Acidified sulfate seed aerosol-only experiments served as controls. For reactive uptake experiments, 600-1200 ppbv of gas phase *trans*-β-IEPOX or MAE was introduced into the indoor chamber by passing high-purity $N_2$ gas at 2 L $min^{-1}$ through a manifold heated to ~70 °C for 2-hr. The concentrations were chosen to ensure formation of sufficient SOA mass for subsequent chemical and toxicological analyses. Following 2-hr of reaction to allow maximum SOA growth and stabilization, aerosol samples were collected onto Teflon membrane filters (47 mm diameter, 1.0 μm pore size; Pall Life Science) at a flow rate of 25 L $min^{-1}$ for 3 h. Exact mass loadings on the filters were calculated from total air volume sampled and average mass concentrations of aerosol during the sampling period. A density of 1.25 g $cm^{-3}$ for IEPOX-derived SOA and 1.35 g $cm^{-3}$ for MAE-derived-SOA was applied to convert the measured volume concentrations to mass concentrations after SOA growth (Kroll et al. 2006). Following aerosol sample collection, filter samples were stored in 20 mL scintillation vials at -20°C until analysis. Filter samples were chemically characterized by GC/EI-MS and UPLC/ESI-HR-QTOFMS. Detailed filter extraction procedures have been previously described by Lin et al.(Lin et al. 2012) The removal efficiency of isoprene epoxide-derived SOA constituents from filters was estimated above 90%. Detailed sample preparation, column conditions, operating parameters for GC/EI-MS and UPLC/ESI-HR-QTOFMS have been published elsewhere (Zhang et al. 2011).

#### *4.2.3 Cell Culture*

BEAS-2B cells were cultured in keratinocyte growth medium (KGM™ BulletKit™) (Lonza), which is serum-free keratinocyte basal medium (KBM) supplemented with bovine pituitary extract, human epidermal growth factor, insulin, hydrocortisone, and GA-1000 (gentamicin, amphotericin B). The cells were grown at 37°C and 5% $CO_2$ in a humidified incubator.

### *4.2.4 Extraction of SOA Constituents for Cell Exposure*

The Teflon filter membranes were extracted by sonication in high-purity methanol (LC/MS CHROMASOLV, Sigma-Aldrich) in the same manner as for chemical analysis. Multiple filter samples were combined to achieve the desired dose levels for both IEPOX- and MAE-derived SOA, and the combined filter extracts were dried under a gentle stream of nitrogen. Growth factor-deprived KBM medium was then added to the extraction vials to re-dissolve IEPOX- and MAE-derived SOA constituents for cell exposure. Control filters collected from acidified sulfate aerosol-only experiments were extracted and reconstituted in the same manner.

### *4.2.5 Cell Exposure*

Cells were seeded in 24-well plates at a density of $2.5\times10^4$ cells/well in 250 µL of KGM 2 days prior to exposure. At the time of exposure, cells were washed twice with the phosphate buffered saline (PBS) buffer, and then exposed to KBM medium containing 1, 0.1, or 0.01 mg $mL^{-1}$ SOA extract of chamber-generated aerosol samples for 24 hours. Cells representing the negative control group were exposed to KBM media containing 1, 0.1, or 0.01 mg $mL^{-1}$ acidified sulfate aerosol only. Experiments were conducted in triplicate per treatment group.

### *4.2.6 Assessment of Cytotoxicity*

Cytotoxicity was assessed with the lactate dehydrogenase (LDH) cytotoxicity detection kit (Takara) according to the manufacturer's protocol to ensure toxicity of exposure levels would not interfere with gene expression analysis. After 24-hr exposure, the supernatants were collected to assess LDH levels. Cells exposed to filter extracts from acidified sulfate aerosol-only experiments and cells maintained in KBM alone were treated as control groups.

### *4.2.7 Oxidative Stress-Associated Gene Expression Analysis*

Cells were lysed with 350 µL of Trizol Reagent (Life Technologies) at the end of exposure for total RNA isolation. Isolated RNA samples were further purified using the spin column-based Direct-zol RNA MiniPrep (Zymo Research). RNA quality and concentrations were determined using a NanoDrop 2000 spectrophotometer (Thermo Fisher Scientific). The absorbance ratios 260/280 nm of all samples were determined to be > 1.8. An aliquot of RNA (100 ng) was copied into cDNA using a $RT^2$ First Strand Kit (Qiagen). The pathway-focused Human Oxidative Stress Plus $RT^2$ Profiler PCR Array (Qiagen, 96-well format, catalog #: PAHS-065Y) with 84 oxidative stress-associated genes was used to assess the exposure-induced differential gene expression with a Stratagene Mx3005P real time qPCR System (Agilent Technologies). Additionally, qRT-PCR assays (QuantiTect SYBR® Green RT-PCR Kit, Qiagen) of selected individual genes, including prostaglandin-endoperoxide synthase 2 (*PTGS2*) and beta-actin (*ACTB*, housekeeping gene), were also carried out for quality control.

### *4.2.8 Data Analysis*

Relative levels of gene expression for exposure and control groups, given as fold changes, were calculated using the comparative cycle threshold ($2^{-\Delta\Delta CT}$) method (Livak and Schmittgen 2001). Transcriptional changes in cells exposed to SOA constituents were compared to changes in cells exposed to the extracts from acidic sulfate aerosol controls to assess the effects induced solely by the extracted SOA constituents. Differentially expressed genes were identified using the Qiagen $RT^2$ Profiler Data Analysis Software v3.5, with significance defined as $p < 0.05$. The p-value adjusted for false discovery rate (FDR) was estimated to be 0.0005 ($\alpha/n$; $\alpha=0.05$, and n=84 genes). Network-based analysis to identify canonical pathways and transcription factors was carried out using Ingenuity Pathway Analysis (IPA) software (Ingenuity Systems, Inc., Redwood City, CA). Gene networks representing enriched

perturbed pathways were identified through enrichment analysis carried out using the Fisher's Exact test as detailed previously (Rager et al. 2013).

### *4.3 Results and Discussion*

#### *4.3.1 Generation of SOA Constituents from Reactive Uptake of Epoxides*

Time profiles of aerosol mass concentrations measured during the reactive uptake experiments are shown in Figure 4.1. SOA mass yields from reactive uptake of *trans*-β-IEPOX onto acidified sulfate aerosol are substantially larger than from reactive uptake of MAE under the same experimental conditions (<10% RH) and time scale (2 hr reaction time). These observations are consistent with recent flow tube studies of uptake kinetics that reported a higher reaction probability (γ) for *trans*-β-IEPOX than for MAE, (Gaston et al. 2014; Riedel et al. 2015) as well as with ambient measurements in the Southeastern U.S. which found the sum of IEPOX-derived SOA tracers (642-1225 ng $m^{-3}$) to be substantially larger than that of MAE-derived SOA tracers (~20 ng $m^{-3}$) (YH Lin et al. 2013).

#### *4.3.2 Aerosol Chemical Composition*

In Figure 4.2, the GC/MS total ion current (TIC) chromatograms of TMS-derivatized particle-phase reaction products from reactive uptake of *trans*-β-IEPOX (Fig. 4.2A) and MAE (Fig. 4.2B) in the chamber experiments are compared to that of an ambient $PM_{2.5}$ sample (Fig. 4.2C) collected at a rural site in Yorkville, GA, downwind of a coal-burning power plant and experiencing high isoprene emissions during summer. The most abundant ion (Peak 1) is the bis(trimethylsilyl) sulfate derivative of extractable inorganic particle sulfate (YH Lin et al. 2013). The isoprene SOA tracers in chamber samples are identical to those in field samples. In Figure 4.3, TICs from UPLC/ESI-QTOFMS analysis of the same samples are compared. The most abundant peaks in extracts of chamber samples represent the isomeric sulfate esters of 2-methyltetrol (*m/z* 215; $C_5H_{11}O_7S^-$) (Fig. 4.3A), and the sulfate ester of 2-methylglyceric acid (*m/z* 199; $C_4H_7O_7S^-$) (Fig. 4.3B).(Y-H Lin et al. 2013; Surratt et al. 2010) Both ions are present in the

extract of a typical ambient $PM_{2.5}$ sample (Fig. 4.2C). Consistent with previous studies, (YH Lin et al. 2013) the epoxide-derived SOA products represent the major OA constituents of the ambient $PM_{2.5}$ samples collected from the Southeastern U.S. during summertime, and support the validity of the chamber experiments as representative of ambient SOA composition.

### *4.3.3 Cytotoxicity Measurements*

We observed significant cell death in acidified sulfate aerosol-only controls at a concentration of 1 mg/mL (cell death ~27%, $p$=0.02), while acidified sulfate aerosol-only concentrations ≤ 0.1 mg/mL were not cytotoxic (cell death ≤10%, $p$>0.05). Therefore, cells exposed to the dose level of 0.1 mg/mL were selected for gene expression analysis.

### *4.3.4 Altered Expression of Genes from Exposure to Isoprene-derived SOA*

Volcano plots of differential gene expression in BEAS-2B cells upon exposures to IEPOX-derived SOA and MAE-derived SOA are shown in Figure 4.4. A complete list of genes and p values is provided in Table 4.2. With a fold change cutoff value of 1.5, six oxidative stress-associated genes with significant fold changes were induced by exposure to IEPOX-derived SOA extract and 36 oxidative stress-associated genes by exposure to MAE-derived SOA extract. When FDR is considered, fold changes in two genes from exposure to IEPOX-derived SOA extract and in 13 genes from exposure MAE-derived SOA extract remain significant.

Of the 41 genes ($p<0.05$) altered due to isoprene-derived SOA exposure in Chapter 3, 26 gene can be found in common with genes altered by exposure to IEPOX- and MAE-derived SOA

### *4.3.5 Quality Check of Expression Changes through qRT-PCR*

Expression of *PTGS2* was selected as a quality control check for qRT-PCR analysis because exposure to both IEPOX- and MAE-derived SOA induced significant fold changes in expression. The comparison of fold change values between RT² Profiler PCR Arrays and qRT-PCR is shown in Figure 4.5.

Expression levels of *PTGS2* induced by exposure to IEPOX- or MAE-derived SOA extracts are normalized to the housekeeping gene (*ACTB*) and acidified sulfate aerosol exposure controls. At 0.1 mg/mL, MAE-derived SOA induces significantly a higher level of *PTGS2* gene expression (7.09-fold; $p$=0.01), than IEPOX-derived SOA (3.29-fold; $p$=0.20), consistent with RT² Profiler PCR array results (Table 4.2). At low exposure concentrations (0.01 mg/mL), induction of *PTGS2* gene expression was not significant for either IEPOX- or MAE-derived SOA ($p$>0.05).

### *4.3.6 Pathway Enrichment Analysis*

The 38 differentially expressed genes in the gene sets exposed to IEPOX- and MAE-derived SOA extracts were analyzed for enrichment within biological pathways. Similar to the isoprene SOA exposures, the canonical pathway for nuclear factor erythroid 2-like 2 (NRF2)-mediated oxidative stress response ($p=10^{-16}$) was enriched in both sets, with 1 of 6 genes (16%) represented in the IEPOX-SOA set and 13 of 36 genes (36%) represented in the MAE set (Table 4.2), NADPH dehydrogenase, quinone 1 (*NQO1*) being represented in both sets at $p<0.05$ (while it didn't pass the stringent FDR, it does show differential expression via RT-PCR). *HMOX1* was represented in the MAE set but did not pass the stringent FDR and was absent from the IEPOX set.

### *4.3.7 Cellular Oxidative Stress Response and Oxidative Potential of PM*

Our gene expression analysis indicates that the constituents of isoprene–derived SOA generated from MAE (high-$NO_x$ SOA precursor) are more potent inducers of oxidative stress than those of SOA generated from IEPOX (low-$NO_x$ SOA precursor). The difference in toxicity may be attributed to the distinct chemical composition of the SOA from the two epoxide precursors, which may determine bioavailability and chemical reactivity (Kelly and Fussell 2012). The oxidative potency of isoprene – derived SOA extracts has been assessed by the dithiothreitol (DTT) assay (Kramer et al. 2016). MAE-derived SOA extracts were more strongly oxidizing ($2.74\pm0.27 \times 10^{-3}$ nmol DTT consumed/min/μg

sample) than IEPOX-derived SOA extracts (1.58±0.13 $\times 10^{-3}$ nmol DTT consumed/min/µg sample). This result is in accord with the oxidative stress responses of BEAS-2B cells observed in this study. Induction of *HMOX1* gene expression in BEAS-2B cells by MAE-derived SOA exposure (Table 4.2) is consistent with reports of strong correlation between DTT activity of PM samples and exposure-induced *HMOX1* gene expression (Cho et al. 2005; Li et al. 2003b).

### *4.4 Conclusion*

IEPOX- and MAE-derived SOA both altered the expression of oxidative stress-related genes and the canonical pathway for Nrf2-mediated oxidative stress response was enriched in both sets of exposures similar to the isoprene-derived SOA exposure presented in Chapter 3. MAE-derived SOA had a greater effect than IEPOX-derived SOA on gene expression. However, the genes altered following exposure to IEPOX- and MAE-derived SOA taken together did not account for all the genes altered following an exposure to isoprene-derived SOA as discussed in Chapter 3. Additionally, we were unable to explain the high fold change in the *HMOX1* gene expression seen following 24-hr exposure to isoprene-derived SOA.

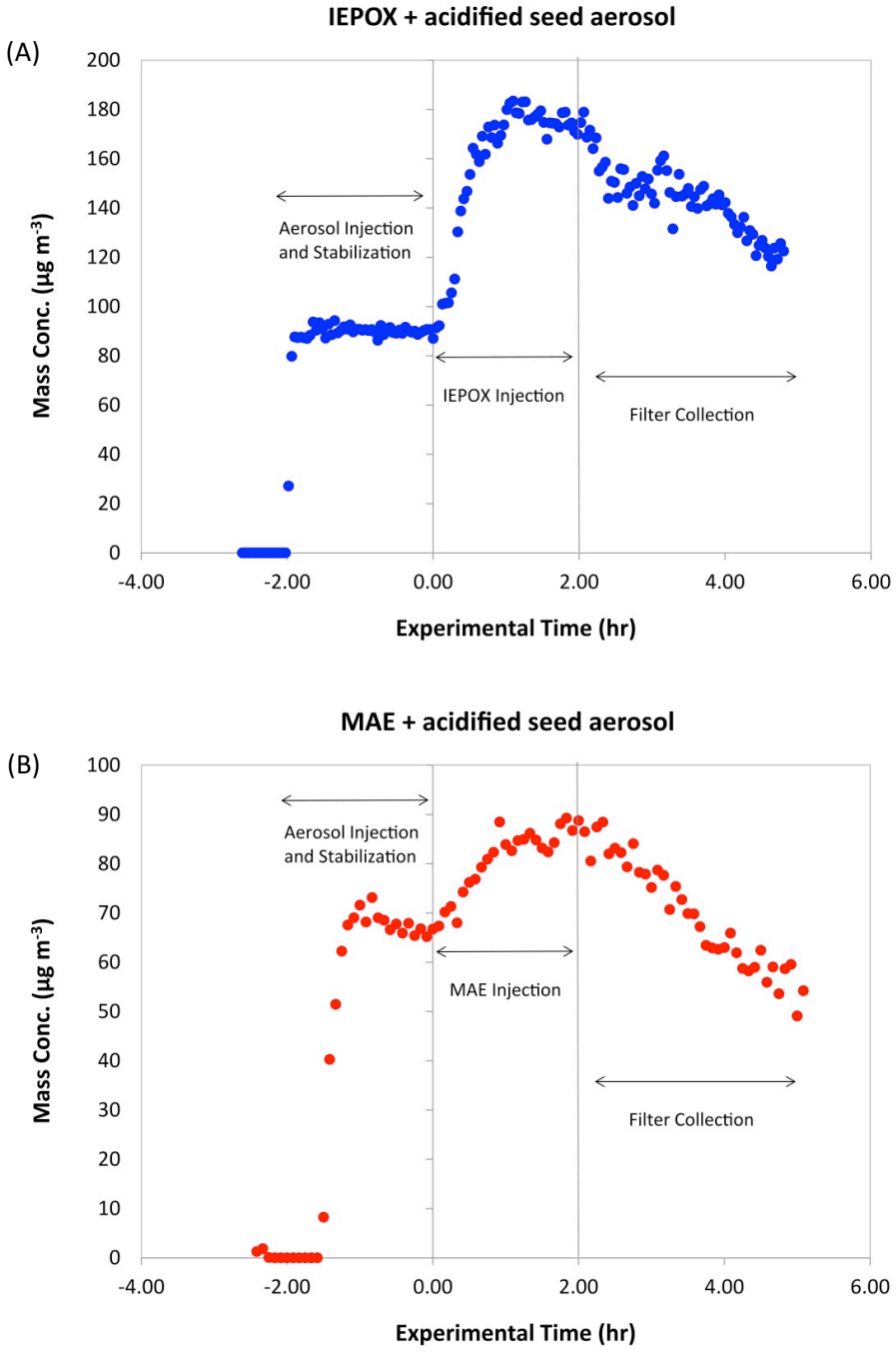


**Figure 4.1.** Time profiles of measured aerosol mass concentrations during the reactive uptake of (A) *trans*-β-IEPOX, and (B) MAE by acidified sulfate aerosols in chamber experiments.

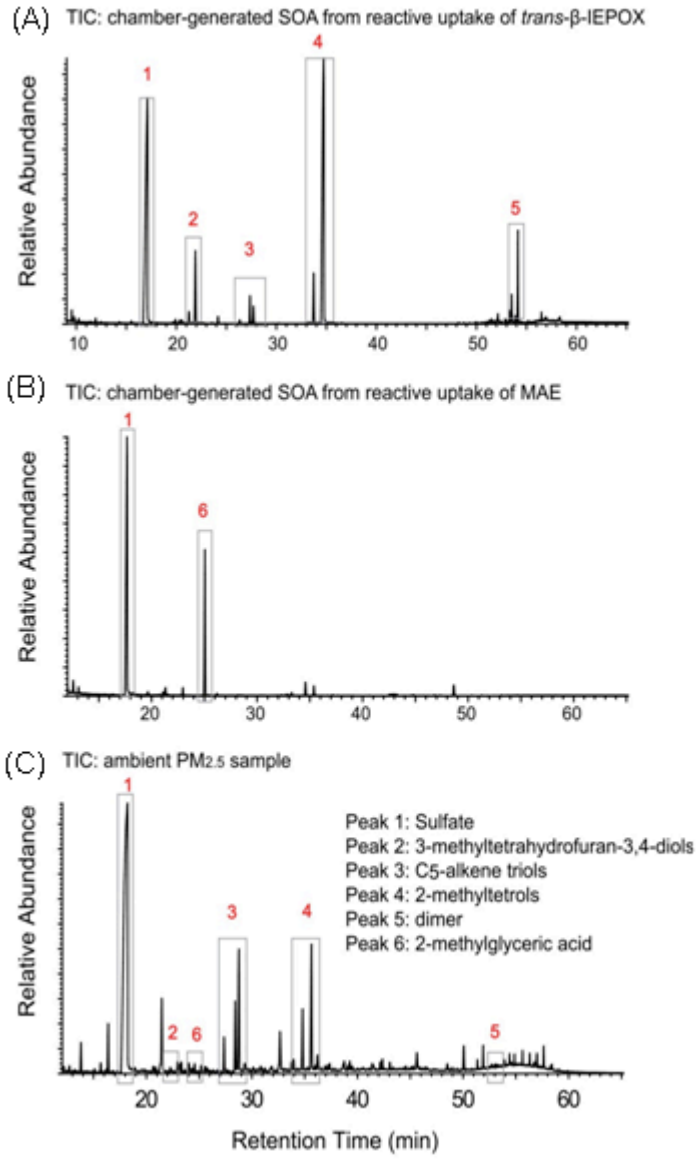


**Figure 4.2.** GC/MS total ion current chromatograms (TICs) of TMS-derivatized particle-phase reaction products from reactive uptake of (A) *trans*-β-IEPOX and (B) MAE onto acidified sulfate seed aerosol in chamber experiments, and (C) $PM_{2.5}$ field sample from Yorkville, GA. Mixtures of isomeric SOA products are grouped as one peak.

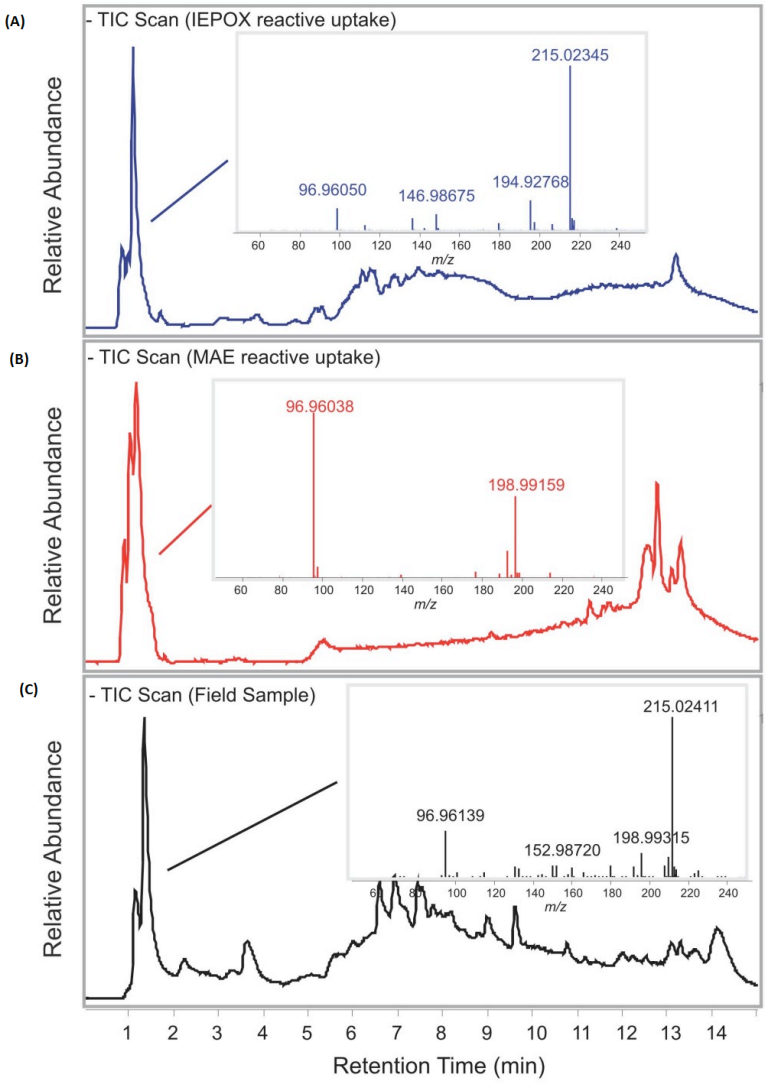


**Figure 4.3.** UPLC/(–)ESI-HR-QTOFMS total ion current chromatograms (TICs) of particle-phase reaction products from reactive uptake of (A) *trans*-β-IEPOX and (B) MAE onto acidified sulfate seed aerosol in chamber experiments, and (C) a $PM_{2.5}$ field sample from Yorkville, GA.

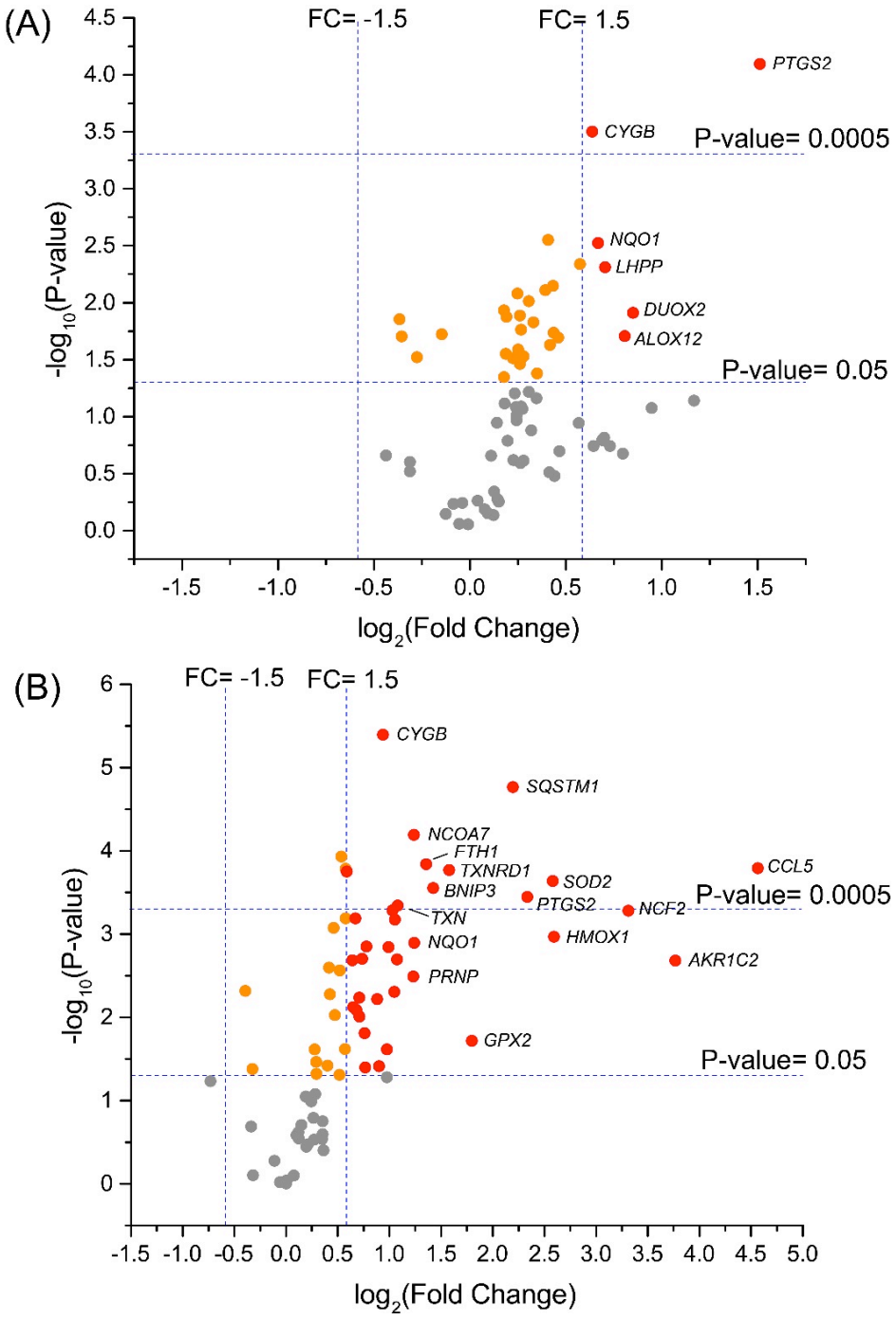


**Figure 4.4.** Volcano plots of differential gene expression in BEAS-2B cells upon exposures to (A) IEPOX-SOA and (B) MAE-SOA, respectively. A complete list of altered genes and p values is provided in Table 4.2.

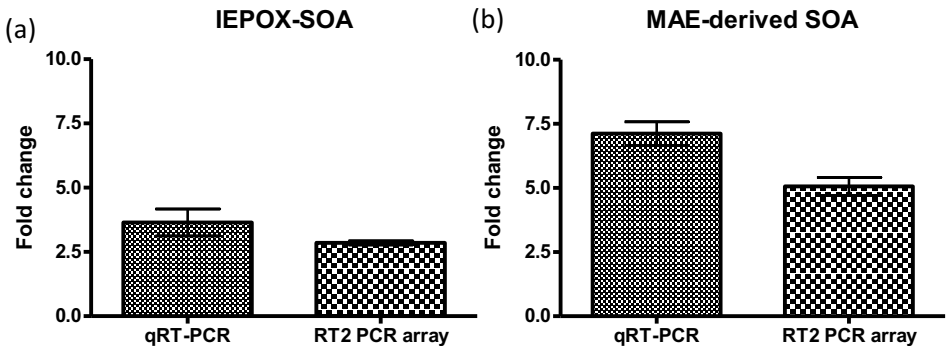


**Figure 4.5.** Quality check of *PTGS2* gene expression changes induced by (a) IEPOX- and (b) MAE-derived SOA through qRT-PCR.

**Table 4.1.** Summary of experimental conditions for reactive uptake and control experiments.

| # | Experiment | Epoxide Precursor (ppbv) | | Initial Seed (μg $m^{-3}$) | SOA Growth (μg $m^{-3}$) | Sampling Volume ($m^3$) | Mass Collected (μg) |
|---|---|---|---|---|---|---|---|
| 1 | reactive uptake | IEPOX | 600 | 92 | 114.0 | 3.06 | 348.8 |
| 2 | reactive uptake | IEPOX | 600 | 84 | 45.3 | 3.06 | 138.5 |
| 3 | reactive uptake | IEPOX | 600 | 78 | 147.1 | 3.06 | 450.2 |
| 4 | reactive uptake | MAE | 600 | 61 | 21.6 | 3.06 | 66.1 |
| 5 | reactive uptake | MAE | 600 | 62 | 36.5 | 3.06 | 111.5 |
| 6 | reactive uptake | MAE | 600 | 65 | 32.4 | 3.06 | 99.1 |
| 7 | reactive uptake | MAE | 900 | 227 | 45.0 | 3.91 | 175.6 |
| 8 | reactive uptake | MAE | 900 | 138 | 24.9 | 3.91 | 97.1 |
| 9 | reactive uptake | MAE | 900 | 236 | 29.0 | 3.90 | 113.1 |
| 10 | reactive uptake | MAE | 1200 | 300 | 47.5 | 4.04 | 191.9 |
| # | Experiment | Epoxide Precursor (ppbv) | | Initial Seed (μg $m^{-3}$) | Final Seed (μg $m^{-3}$) | Sampling Volume ($m^3$) | Mass Collected (μg) |
| 11 | control | -- | -- | 77 | 42 | 3.06 | 182.1 |
| 12 | control | -- | -- | 328 | 143 | 3.06 | 721.4 |

**Table 4.2.** List of genes identified with significant expression fold-changes (p<0.05) upon exposure to IEPOX or MAE-derived SOA constituents. False Discovery Rate (FDR) adjusted p-value: 0.05/84=0.0005. Full names of gene symbols can be found in Table 3.1.

| SOA Precursor | Gene Name | Fold Change | p-value | NRF2-associated Genes | <FDR |
|---|---|---|---|---|---|
| IEPOX | *ALOX12* | 1.75 | 0.019612 | | |
| | *CYGB* | 1.55 | 0.000313 | | * |
| | *DUOX2* | 1.80 | 0.012251 | | |
| | *LHPP* | 1.63 | 0.004871 | | |
| | *NQO1* | 1.59 | 0.002976 | + | |
| | *PTGS2* | 2.85 | 0.000080 | | * |
| MAE | *AKR1C2* | 13.61 | 0.002067 | | |
| | *ALB* | 1.60 | 0.008062 | | |
| | *ALOX12* | 1.97 | 0.024048 | | |
| | *APOE* | 2.07 | 0.004920 | | |
| | *ATOX1* | 2.08 | 0.000666 | | * |
| | *B2M* | 1.93 | 0.005968 | | |
| | *BNIP3* | 2.68 | 0.000278 | | * |
| | *CCL5* | 23.64 | 0.000160 | | * |
| | *CYGB* | 1.91 | 0.000004 | | * |
| | *FTH1* | 2.56 | 0.000144 | + | * |
| | *GCLC* | 1.84 | 0.006009 | + | |
| | *GCLM* | 1.64 | 0.009746 | + | |
| | *GLA* | 2.10 | 0.002010 | | |
| | *GPX2* | 3.47 | 0.019059 | + | |
| | *GSTP1* | 1.71 | 0.001398 | + | |
| | *HMOX1* | 6.03 | 0.001071 | + | |
| | *HSPA1A* | 1.69 | 0.015415 | | |
| | *MB* | 1.70 | 0.039873 | | |
| | *NCF1* | 1.64 | 0.005790 | | |
| | *NCF2* | 9.94 | 0.000523 | | |
| | *NCOA7* | 2.36 | 0.000064 | | * |
| | *NOX5* | 1.56 | 0.002049 | | |

| | | | | |
|---|---|---|---|---|
| *NQO1* | 2.36 | 0.001263 | + | |
| *PRDX1* | 1.67 | 0.001969 | + | |
| *PRDX4* | 1.59 | 0.000644 | | * |
| *PRDX5* | 1.57 | 0.007514 | | |
| *PRNP* | 2.35 | 0.003207 | | |
| *PTGR1* | 1.99 | 0.001422 | + | |
| *PTGS2* | 5.04 | 0.000355 | | * |
| *SEPP1* | 1.50 | 0.000177 | | * |
| *SOD2* | 5.98 | 0.000230 | + | * |
| *SPINK1* | 1.87 | 0.038476 | | |
| *SQSTM1* | 4.57 | 0.000017 | + | * |
| *TXN* | 2.11 | 0.000451 | + | * |
| *TXNRD1* | 2.98 | 0.000169 | + | * |
| *VIMP* | 2.04 | 0.000516 | | |

## CHAPTER V: ROS GENERATION POTENTIAL OF ISOPOOH-DERIVED SOA AND ITS EFFECTS ON OXIDATIVE STRESS-RELATED GENES

### *5.1 Overview*

We determined that IEPOX- and MAE-derived SOA alter the expression of oxidative stress-related genes in Chapter 4 but did not account for all the genes altered by the total isoprene SOA mixture nor did they account for the high fold change seen in *HMOX1* following isoprene-derived SOA exposure. Therefore, the objective of this study was to evaluate the potential contributions of ISOPOOH-derived SOA (through a non-IEPOX route) to oxidative stress-related gene expression changes seen in cells exposed to the total mixture of isoprene-derived SOA in Chapter 2. To be comparable to the PCR array data for the isoprene-derived SOA in Chapter 2 and the IEPOX- and MAE-derived SOA exposures in Chapter 4, we chose a 24-hr exposure time and a dose of 0.1 mg $mL^{-1}$ for the ISOPOOH-derived SOA exposure.

Until recently, we were limited to reactive uptake experiments to form MAE- and IEPOX-derived SOA. Following the study presented in Chapter 4, our laboratory successfully generated ISOPOOH-derived SOA (through a non-IEPOX route) in an indoor chamber through the oxidation of authentic ISOPOOH (Riva et al. 2016a). Although ISOPOOH-derived SOA constituents only account for a small fraction of the isoprene SOA generated in Chapter 2 (<5% based on identified SOA tracers shown in Figure 2.3) they may be the major reactive components responsible for the increased expression of oxidative stress-related genes. Although ISOPOOH + OH mostly yields IEPOX (Berndt et al. 2016), recent work has shown that the low-volatility multifunctional hydroperoxides resulting from ISOPOOH + OH may yield substantial amounts of SOA (Liu et al. 2016; Riva et al. 2016a) even though this only represents 10% of the branching of the ISOPOOH + OH reaction (Berndt et al., 2016).

Additionally, we measured the oxidative potential of ISOPOOH-derived SOA using the DTT assay. In Chapter 4 we showed that MAE-derived SOA altered more oxidative stress-related genes as hypothesized based on its higher oxidative potential compared to IEPOX-derived SOA. Kramer et.al (2016) has shown that, of the known precursors of isoprene-derived SOA, ISOPOOH has the greatest oxidizing potential which may indicate a high oxidative potential for ISOPOOH-derived SOA.

### *5.2 Experimental Section*

#### *5.2.1 Generation and Chemical Characterization of ISOPOOH-derived SOA*

ISOPOOH-derived SOA were generated in a 10-$m^3$ flexible Teflon indoor chamber at the University of North Carolina as described by Riva et al. (2016a). Experiments were performed at room temperature (25°C) under dark and low relative humidity (RH) (<5%) conditions. Prior to each experiment, the chamber was flushed for at least 24 hrs to replace at least five volumes of chamber air to ensure particle-free conditions and $O_3$ and VOC concentrations were below detection limits. Aerosol size distributions were measured continuously using a differential mobility analyzer (DMA; BMI model 2002) coupled to a mixing condensation particle counter (MCPC; BMI model 1710). The $O_3$ concentration was monitored over the course of the experiment using a UV photometric analyzer (Model 49P. Thermo-Environmental). Temperature and RH inside the chamber were continuously monitored using an OM-62 temperature RH data logger (OMEGA Engineering, Inc.).

A non-acidified ammonium sulfate ($(NH_4)_2SO_4$) seed aerosol solution containing 0.06 M $(NH_4)_2SO_4$ was atomized into the chamber until the total aerosol mass concentration in the chamber was ~ 80 $\mu g\ m^{-3}$. Because 90% of ISOPOOH + OH yields IEPOX, non-acidified $(NH_4)_2SO_4$ seed was used to prevent the reactive uptake of IEPOX and allow the 10% of hydroperoxides to condense onto pre-existing aerosol (Berndt et al. 2016). Following aerosol injection, 300 ppb of 1,2-ISOPOOH, synthesized in house as described by Riva et al. (2016a), was injected into the chamber by passing high-purity $N_2$ gas

through a manifold heated to ~70°C at 2 L $min^{-1}$ for 10 mins then at 5 L $min^{-1}$ for 80 mins. $O_3$ was introduced into the chamber using an $O_3$ generator (model L21, Pacific ozone) followed by a continuous injection of tetramethylethylene (TME). The ozonolysyis of TME formed the OH radicals needed for the oxidation of ISOPOOH. A summary of the experimental conditions is given in Table 5.1. Non-acidified $(NH_4)_2SO_4$ seed aerosol only experiments served as controls. Following the 1.5-hr injection of TME, aerosol samples were collected onto Teflon membrane filters (47 mm diameter, 1.0 µm pore size; Pall Life Science). Exact mass loadings on the filters were calculated from total air volume sampled and average mass concentrations of aerosol during the sampling period. A density correction of 1.6 g $cm^{-3}$ (Riedel et al. 2016) and 1.25 g $cm^{-3}$ (Kroll et al. 2006) was applied to convert the measured volume concentrations to mass concentrations for the $(NH_4)_2SO_4$ seed and SOA growth.

Following aerosol sample collection, filter samples were stored in 20 mL scintillation vials at -20°C until cell exposure or chemical analysis. ISOPOOH-derived SOA formed during indoor oxidation experiments have been previously characterized in Riva et al. (2016) by GC/EI-MS, UPLC/ESI-HR-QTOFMS, and total aerosol peroxide analysis. The composition of filter samples collected in this study was validated by UPLC/ESI-HR-QTOFMS operated in the positive (+) ion mode. Detailed filter extraction procedures have been previously described by Lin et al. (2012). Detailed sample preparation, column conditions, operating parameters for GC/EI-MS and UPLC/ESI-HR-QTOFMS have been published elsewhere (Zhang et al. 2011).

### *5.2.2 DTT Assay*

The DTT assay is a commonly used method to quantify redox activity of $PM_{2.5}$ and its potential to generate ROS (Q Li et al. 2009). The rate of DTT consumed with $PM_{2.5}$ extract as a catalyst, is proportional to the concentration of the catalytically active redox-active species present in the sample (Rattanavaraha et al. 2011). Description of the DTT assay has been previously described in detail (Kramer et al. 2016; Rattanavaraha et al. 2011), but briefly, DTT and DTNB stock solutions were made by

adding DTT standard (powder form) (Sigma-Aldrich) or DTNB standard (Sigma-Aldrich) to an aqueous buffer solution containing 0.05 mol $L^{-1}$ potassium phosphate monobasic-sodium hydroxide ($KH_2PO_4$, pH 7.4, Fisher Scientific) and 1 mM ethylenediaminetetraacetic acid (EDTA, Sigma Aldrich). A stock solution of 1,4-naphthoquinone (1,4-NQ) was made by dissolving 0.5 mg of 1,4-NQ in 0.5 mL dimethyl sulfoxide (DMSO). Volumes of stock solutions were added to additional aqueous buffer to make working solutions.

ISOPOOH-derived SOA extracts were prepared by sonicating chamber filters in high-purity methanol (LC/MS CHROMASOLV, Sigma-Aldrich). Three separate filters were used (n=3) and extracts were concentrated by drying under a gentle stream of nitrogen. Each ISOPOOH-derived SOA extract was combined with buffer and 0.05 mM DTT working solution and incubated at 37°C for 30 min. Reactions were quenched with the addition of a 1 mM DTNB working solution. A DTT calibration curve was generated by varying DTT volumes with buffer solution. A calibration curve of 1,4-NQ was generated by varying volumes of 1,4-NQ with a set amount of DTT. The consumption of DTT was measured by the absorbance of 5-thio-2-nitrobenzoic acid (TNB), formed by the oxidation of residual DTT with DTNB, at 412 nm using a UV–Visible Spectrophotometer (Hitachi U-3300 dual beam spectrophotometer) (Q Li et al. 2009; Rattanavaraha et al. 2011). Dilution effects were taken into account by correcting the absorbance measurements for sample volume.

ROS generation potential was expressed as DTT activity (nmol of DTT consumed/min/μg sample) and the normalized index of oxidant generation (NIOG) for comparison with previously published studies (Rattanavaraha et al. 2011). As demonstrated by Rattanavaraha et al. (2011), an index of oxidant generation (IOG) was calculated according to the following equation (Rattanavaraha et al. 2011):

$$IOG = \frac{Abs_0 - Abs'}{Abs_0} \times \frac{100}{T \times M}$$

where T is reaction time (min), M is sample mass (μg), $Abs_0$ and Abs' are initial absorbance and absorbance at time T, respectively. The NIOG calculation normalizes activity with respect to a 1,4-NQ standard as follows:

$$NIOG_{sample} = \frac{IOG_{sample}}{IOG_{1,4-NQ}}$$

### *5.2.3 Cell Exposure*

BEAS-2B were maintained in keratinocyte growth medium (KGM BulletKit; Lonza), a serum-free keratinocyte basal medium (KBM) supplemented with 0.004% of bovine pituitary extract and 0.001% of human epidermal growth factor, insulin, hydrocortisone, and GA-1000 (gentamicin, amphotericin B). The cells were kept at 37°C and 5% $CO_2$ in a humidified incubator and passaged weekly.

The Teflon filter membranes were extracted by sonication in high-purity methanol (LC/MS CHROMASOLV, Sigma-Aldrich). Filter extracts from multiple filter samples were combined to achieve the desired dose of ISOPOOH-derived SOA and were dried under a gentle stream of nitrogen. Growth factor-deprived KBM medium was then added to the extraction vials to re-dissolve ISOPOOH-derived SOA constituents for cell exposure. Control filters collected from non-acidified $(NH_4)_2SO_4$ aerosol-only experiments were extracted and reconstituted in the same manner.

In preparation for exposures, cells were seeded in 24-well plates at a density of $2.5\times10^4$ cells/well in 250 μL of KGM 2 days prior to exposure. At the time of exposure, cells were washed twice with phosphate buffered saline (PBS) buffer, and then exposed to KBM containing 0.1 mg $mL^{-1}$ ISOPOOH-derived SOA or non-acidified $(NH_4)_2SO_4$ aerosol as a negative control. Cells were exposed for 24 hrs for oxidative stress-related gene expression analysis. Additionally, cells were exposed for 9 hrs and 24 hrs for single gene analysis. Extracellular medium was collected and total RNA was isolated using Trizol (Life Technologies) post-exposure. Extracellular medium and the extracted RNA samples were stored at -20°C and -80°C, respectively, until further analysis

### *5.2.4 Assessment of Cytotoxicity*

Cytotoxicity was assessed through measurement of lactate dehydrogenase (LDH) released into the extracellular medium from damaged cells using the LDH cytotoxicity detection kit (Takara). LDH release was assessed and compared to LDH released by positive control cells exposed to 1% Triton X-100 to ensure that cell death would not affect gene expression results.

### *5.2.5 Oxidative Stress-Associated Gene Expression Analysis*

Isolated RNA samples were further purified using the spin column-based Direct-zol RNA MiniPrep (Zymo Research). RNA quality and concentrations were determined using a NanoDrop 2000 spectrophotometer (Thermo Fisher Scientific). The absorbance ratios 260/280 nm of all samples were determined to be > 1.8. An aliquot of RNA (100 ng) was copied into cDNA using a $RT^2$ First Strand Kit (Qiagen). Gene expression analysis was performed using the pathway-focused Human Oxidative Stress Plus $RT^2$ Profiler PCR Array (Qiagen, 96-well format, catalog #: PAHS-065Y) with 84 oxidative stress-associated genes with a Stratagene Mx3005P real time qPCR System (Agilent Technologies). A list of all 84 oxidative stress-associated gens and housekeeping genes included in the array can be found in Table 3.1. Changes in the oxidative stress-related genes from ISOPOOH-derived SOA exposed cells were compared to cells exposed to non-acidified $(NH_4)_2SO_4$ seed aerosol (negative control) at the same concentration (0.1 mg $mL^{-1}$) for the same exposure time (24 hr).

### *5.2.6 Single Gene Expression Analysis for Time Course Analysis*

Additionally, qRT-PCR assays (QuantiTect SYBR® Green RT-PCR Kit, Qiagen) of selected individual genes, including *PTGS2*, *HMOX1* and ACTB (housekeeping gene) were conducted for a quality control check. Changes in *PTGS2* and *HMOX1* mRNA levels were measured using QuantiTect SYBR Green RT-PCR Kit (Qiagen) and QuantiTect Primer Assays for Hs_ACTB_1_SG (Catalog #QT00095431), Hs_*PTGS2*_1_SG (Catalog #QT00040586), and Hs_*HMOX1*_1_SG (Catalog #QT00092645) for one-step RT-PCR analysis. All

mRNA levels were normalized against β-actin mRNA, which was used as a housekeeping gene. The relative expression levels (i.e., fold change) were calculated using the comparative cycle threshold ($2^{-\Delta\Delta CT}$) method (Livak and Schmittgen 2001). Changes in *PTGS2* and *HMOX1* from ISOPOOH-derived SOA exposed cells were compared to cells exposed to non-acidified $(NH_4)_2SO_4$ seed aerosol (negative control) at the same concentration (0.1 mg $mL^{-1}$) for the same exposure time (9-hr or 24-hr).

### *5.2.7 Statistical Analysis*

The software package GraphPad Prism 4 (GraphPad) was used for all statistical analyses. All data were expressed as mean ± SEM (standard error of means). Comparisons between data sets for gene expression analysis were made using unpaired *t*-test with Welch's correction. Significance was defined as $p < 0.05$.

## *5.3 Results and Discussion*

### *5.3.1 Physical and Chemical Characterization of Exposure*

Figure 5.1 shows the change in particle mass concentration over time during an ISOPOOH oxidation experiment. There is no SOA growth observed during ISOPOOH injection into the chamber but as soon as TME is introduced after the $O_3$ injection, OH radicals are formed and proceed to oxidize ISOPOOH leading to SOA formation. Unlike the formation of IEPOX- and MAE-derived SOA in our previous chamber experiments presented in Chapter 4, ISOPOOH-derived SOA formation is via oxidation and not acid-catalyzed reactive uptake.

To verify the composition of our ISOPOOH-derived SOA to the ISOPOOH-derived SOA previously characterized (Riva et al. 2016a), we used UPLC/(+)ESI-HR-QTOFMS to detect SOA products due to its soft ionization and the availability of isoprene-derived hydroxyhydroperoxide standards in house. Based on the accurate mass fitting and retention time presented by Riva et al. (2016a), the UPLC/(+)ESI-HR-QTOFMS EIC shown in Figure 5.2 shows the strong presence of $C_5H_{12}O_5$ and $C_5H_{12}O_6$, which are

tentatively assigned to isoprene trihydroxyhydroperoxide (ISOPTHP) and isoprene dihydroxydihydroperoxide ($ISOP(OOH)_2$) both of which were found in high abundance in ISOPOOH-derived SOA formed under non-acidic conditions characterized by Riva et al. (2016a). More importantly, ISOPTHP and ($ISOP(OOH)_2$) have both been observed in a field study conducted in Centerville, AL (Lee et al. 2016) which highlights its atmospheric significance. Strong correlations have been observed between the mass spectra of laboratory-generated ISOPOOH-derived SOA and a positive matrix factorization (PMF) factor referred to as 91Fac from a field study conducted in Look Rock, TN (Budisulistiorini et al. 2016).

Total aerosol peroxide measurements of ISOPOOH-derived SOA formed under non-acidic conditions show that approximately 40% of the organic mass is attributable to organic peroxides (Riva et al. 2016a), which are strong oxidants and may heavily influence the ROS generation potential of ISOPOOH-derived SOA.

### *5.3.2 ROS Generation Potential of ISOPOOH-Derived SOA*

The NIOG of ISOPOOH-derived SOA generated in the indoor chamber is shown in Figure 5.3 as a comparison to the NIOGs previously measured by Kramer et al. (2016) for other types of isoprene SOA, including the isoprene SOA, IEPOX-derived SOA, and MAE-derived SOA used for exposure in Chapter 2-4, and NIOGs of different types of diesel exhaust measured by Rattanavaraha et al. (2011). As demonstrated in Figure 5.3, ISOPOOH-derived SOA has a much higher oxidative potential than all other types of isoprene SOA, including the total mixture of isoprene SOA generated in the outdoor chamber. Notably, the NIOG for ISOPOOH-derived SOA was also higher than aged diesel exhaust containing oxygenated PAH species as reported by Rattanavaraha et al. (2011).

### *5.3.3 Oxidative Stress Associated Gene Expression*

Cytotoxicity due to 9 and 24-hr exposures is presented in Figure 5.4 as the percentage cell death based on the LDH release for cells exposed to ISOPOOH-derived SOA and control non-acidified $(NH_4)_2SO_4$ seed aerosol compared to positive control cells exposed to 1% Triton X-100. Low cytotoxicity ensured gene expression results were not affected by cell death.

The volcano plot of differential gene expression in BEAS-2B cells upon exposure to ISOPOOH-derived SOA for 24 hrs is shown in Figure 5.5. A complete list of significantly altered genes and p-values is provided in Table 5.2. With a fold change cutoff value of 1.5, 32 oxidative stress-related genes were significantly ($p<0.05$) altered. When FDR is considered, fold changes in 4 oxidative stress-associated genes remain significant.

Compared to MAE-derived SOA, ISOPOOH-derived SOA affects a smaller number of oxidative stress-related genes despite its higher oxidative potential as measured by the DTT assay. This may be a result of the 24 hr exposure time chosen for the exposures and is explored in the single gene time course analysis of *PTGS2* and *HMOX1*. Of the 41 genes ($p<0.05$) altered by the total isoprene-derived SOA mixture, 26 genes are altered by ISOPOOH-derived SOA exposure while 23 are altered by MAE-derived SOA exposures.

Exposure to ISOPOOH-derived SOA accounted for 10 gene alterations observed in the total isoprene SOA mixture exposure that were unaccounted for in the MAE- or IEPOX-derived exposures. However, even after accounting for the ISOPOOH-derived SOA exposure, there were 7 altered genes observed in the total isoprene SOA mixture exposure that were unaffected by MAE-, IEPOX-, or ISOPOOH-derived SOA. This may mean that there is a synergistic effect of different SOA component on gene expression. Alternatively, the components of SOA responsible for the fold regulation may be the uncharacterized portion of the isoprene SOA not yet accounted for in the isoprene SOA formation mechanism shown in Figure 1.

### *5.3.4 Pathway Enrichment Analyses*

The 32 differentially expressed genes from the ISOPOOH-derived SOA exposure were analyzed for enrichment within biological pathways. Similar to the isoprene SOA exposure and the MAE- and IEPOX-derived SOA, the top canonical pathway for the ISOPOOH-derived SOA exposure was the nuclear factor erythroid 2-like 2 (Nrf2)-mediated oxidative stress response ($p=6.12x10^{-19}$) with 13 genes associated with the pathway. When adjusted for the FDR, only one gene remained associated with the pathway. As discussed previously, Nrf2 serves as a key transcription factor protecting against proinflammatory effects of particulate pollutants through its regulation of antioxidant defense (Li et al. 2004). ISOPOOH-derived SOA, like the other component types of isoprene SOA, may contribute to inflammatory effects in human lung cells which elicit an antioxidant response from the Nrf2 pathway.

### *5.3.5 Single Gene Analysis of PTGS2 and HMOX1*

Single gene analysis of PTGS2 and *HMOX1* was conducted for quality control. Additionally, single gene analysis was conducted for a 9 hr and 24 hr exposure to explore the effects of exposure time on gene expression changes. This was done as a result of ISOPOOH-derived SOA altering fewer genes than MAE-derived SOA for a 24 hr exposure despite its higher oxidative potential measured by DTT.

Figure 5.6 shows the changes in mRNA levels of *PTGS2* and *HMOX1* for cells exposed to ISOPOOH-derived SOA for 9- or 24-hr exposure. Fold changes are relative to the non-acidified $(NH_4)_2SO_4$ aerosol seed (negative control) exposure. There is no change in the expression of *PTGS2* at 9 or 24-hrs, but *HMOX1* is significantly altered at both exposure time points. The time course for the expression of *HMOX1* with a higher fold change following a 9-hr exposure compared to the 24-hr exposure is consistent with the differences in expression between 9 and 24-hr for the isoprene-derived SOA exposure in Chapter 2.

Table 5.3 compiles the fold change data for *PTGS2* and *HMOX1* expression in cells exposed to each type of isoprene SOA, previously discussed in Chapters 2-5, for 24-hr exposures. Despite ISOPOOH-

derived SOA having the highest ROS generating potential compared to IEPOX- and MAE-derived SOA as measured through the DTT assay, there is little and no effect on *HMOX1* and *PTGS2* expression, respectively, at 24-hrs. This challenges the idea that DTT assay measurements can be correlated with *HMOX1* expression (Li et al. 2003b). Since correlations between ROS formation, as measured by the acellular DTT assay, and gene expression may be exposure type and time specific, the DTT assay may not be an appropriate tool to determine potential effects of exposure on oxidative stress-related genes. For example, the high ROS generating potential of ISOPOOH-derived SOA may have meant that *HMOX1* was elevated at a very early exposure time and was decreasing as seen in the time profile shown in Figure 5.6.

Of the different SOA types generated from different precursors, MAE-derived SOA has the greatest effect on both *PTGS2* and *HMOX1* when compared to IEPOX- and ISOPOOH-derived SOA. However, the fold regulation of *HMOX1* observed for MAE-derived SOA exposure does not account for the magnitude of the fold regulation of *HMOX1* observed for isoprene-derived SOA. Even the *HMOX1* gene expression of all isoprene SOA types taken together is minimal compared to the significant fold change observed after a 24-hr exposure to the total mixture of isoprene-derived SOA. This is additional evidence that the components of SOA responsible for the fold regulation may be the uncharacterized portion of the isoprene SOA not yet accounted for in the isoprene SOA formation mechanism shown in Figure 1.

### *5.4 Conclusion*

The results of this study indicate that ISOPOOH-derived SOA, despite its high ROS generation potential, as measured through the DTT assay, did not alter as many oxidative stress-related genes as MAE-derived SOA nor did it alter the level of *HMOX1* expression as highly as MAE-derived SOA. The DTT assay results were not correlated with *HMOX1* expression for the different types isoprene SOA exposures at 24-hrs as the levels of gene expression changed based on exposure time. Regardless, the

DTT assay may be useful as an initial screening tool for ROS generating potential but cannot replace the need for *in vitro* and *in vivo* studies.

ISOPOOH-derived SOA, like the other components of isoprene SOA, affected the Nrf2-mediated oxidative stress response which was also activated by the total mixture. However, the high fold change of *HMOX1* gene expression and the total number of oxidative stress-related genes altered due to isoprene SOA generated from photooxidation of isoprene, could not be explained by the individual isoprene types or by its sum. This highlights the importance of treating air pollution as a mixture because exposures are rarely isolated to specific compounds and could have synergistic effects.

**Table 5.1**. Summary of experimental condition for ISOPOOH oxidation experiments and control experiments.

| Experiment | Precursor Concentration (ppb) | Target $O_3$ (ppm) | TME | Initial Seed (µg $m^{-3}$) | SOA Growth (µg $m^{-3}$) | sampling volume ($m^3$) | mass collected (µg) |
|---|---|---|---|---|---|---|---|
| ISOPOOH | 300 | 1.5 | yes | 76.45 | 47.76 | 2.80 | 133.71 |
| ISOPOOH | 300 | 1.5 | yes | 76.99 | 52.44 | 2.66 | 139.76 |
| ISOPOOH | 300 | 1.5 | yes | 77.28 | 54.34 | 3.04 | 165.47 |
| Seed only | - | - | no | 587.54 | - | 0.45 | 267 |

**Table 5.2.** List of genes identified with significant expression fold-changes (p<0.05) upon exposure to ISOPOOH-derived SOA constituents. False Discovery Rate (FDR) adjusted p-value: 0.05/84=0.0005. Full names of gene symbols can be found in Table 3.1.

| Gene Name | Fold Regulation | p-value | NRF2-associated Genes | <FDR |
|---|---|---|---|---|
| *AKR1C2* | 2.2038 | 0.013377 | | |
| *ATOX1* | 1.5619 | 0.024189 | | |
| *BAG2* | 2 | 0.00763 | | |
| *CAT* | 1.5801 | 0.006833 | + | |
| *DHCR24* | 1.5837 | 0.001557 | | |
| *FTH1* | 2.2763 | 0.008796 | + | |
| *GCLC* | 2.5907 | 0.003719 | + | |
| *GCLM* | 2.8945 | 0.001271 | + | |
| *GLA* | 1.7371 | 0.034903 | | |
| *GPX1* | 1.544 | 0.014517 | | |
| *GPX2* | 5.9518 | 0.000725 | + | |
| *GPX3* | 1.8747 | 0.000538 | | |
| *GSR* | 1.6857 | 0.027743 | + | |
| *GSTP1* | 1.6283 | 0.041316 | + | |
| *HMOX1* | 2 | 0.016293 | + | |
| *HSP90AA1* | 2.0946 | 0.000988 | | |
| *HSPA1A* | 1.5948 | 0.001239 | | |
| *NQO1* | 4.9588 | 0.003367 | + | |
| *PRDX1* | 2.1886 | 0.007017 | + | |
| *PRDX3* | 1.6133 | 0.047334 | | |
| *PRDX6* | 1.5018 | 0.023451 | | |
| *PTGS1* | 2.0186 | 0.025923 | | |
| *RNF7* | 1.7818 | 0.040105 | | |
| *SIRT2* | 1.6396 | 0.000194 | | * |
| *SLC7A11* | 3.4343 | 0.000005 | | * |
| *SQSTM1* | 2.3565 | 0.000085 | + | * |
| *SRXN1* | 2.7195 | 0.000015 | | * |
| *TXN* | 2.2294 | 0.016836 | + | |
| *TXNRD1* | 4.8793 | 0.003985 | + | |
| *TXNRD2* | 1.7859 | 0.000992 | | |
| *VIMP* | 1.5619 | 0.001192 | | |
| *DUOX1* | -2.0139 | 0.011647 | | |

**Table 5.3.** Comparison of single gene expression for *PTGS2* and *HMOX1* over different types of isoprene SOA for a 24-hr exposure measured through PCR. ns: no significant fold change.

| | *PTGS2* | | *HMOX1* | |
|---|---|---|---|---|
| **Exposure type** | **fold regulation** | **p-value** | **fold regulation** | **p-value** |
| Isoprene SOA | 3.02 | 0.001327 | 123.64 | 0.00002 |
| IEPOX-derived SOA | 2.85 | 0.00008 | ns | ns |
| MAE-derived SOA | 5.04 | 0.000355 | 6.03 | 0.001071 |
| ISOPOOH-derived SOA | ns | ns | 2 | 0.016293 |

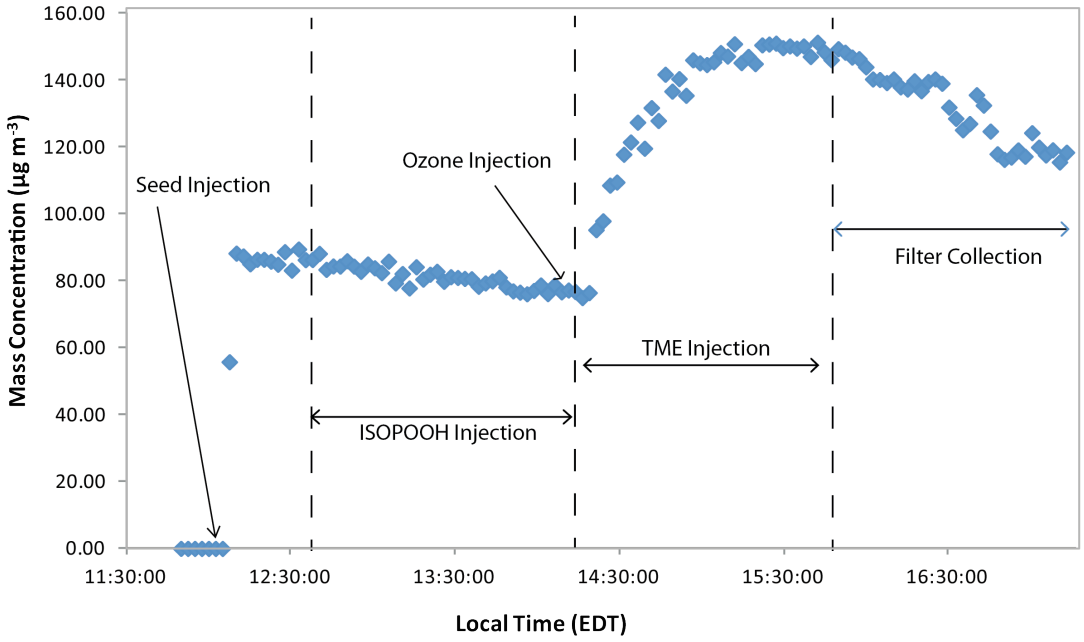


**Figure 5.1**. Time profile of measured aerosol mass concentrations during ISOPOOH oxidation experiments.

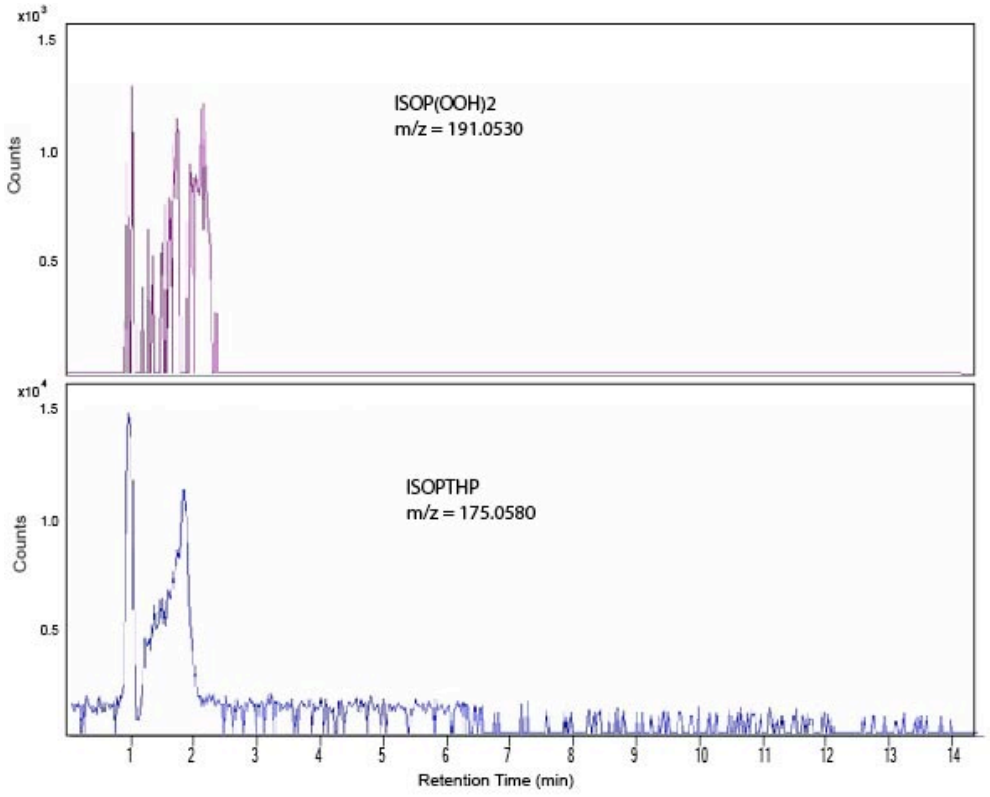


**Figure 5.2.** UPLC/(+)ESI-HR-QTOFMS extracted ion chromatograms (EICs) at *m/z* 191.0530 and 175.0580 corresponding to ISOP(OOH)$_2$ and ISOPTHP SOA constituents, respectively.

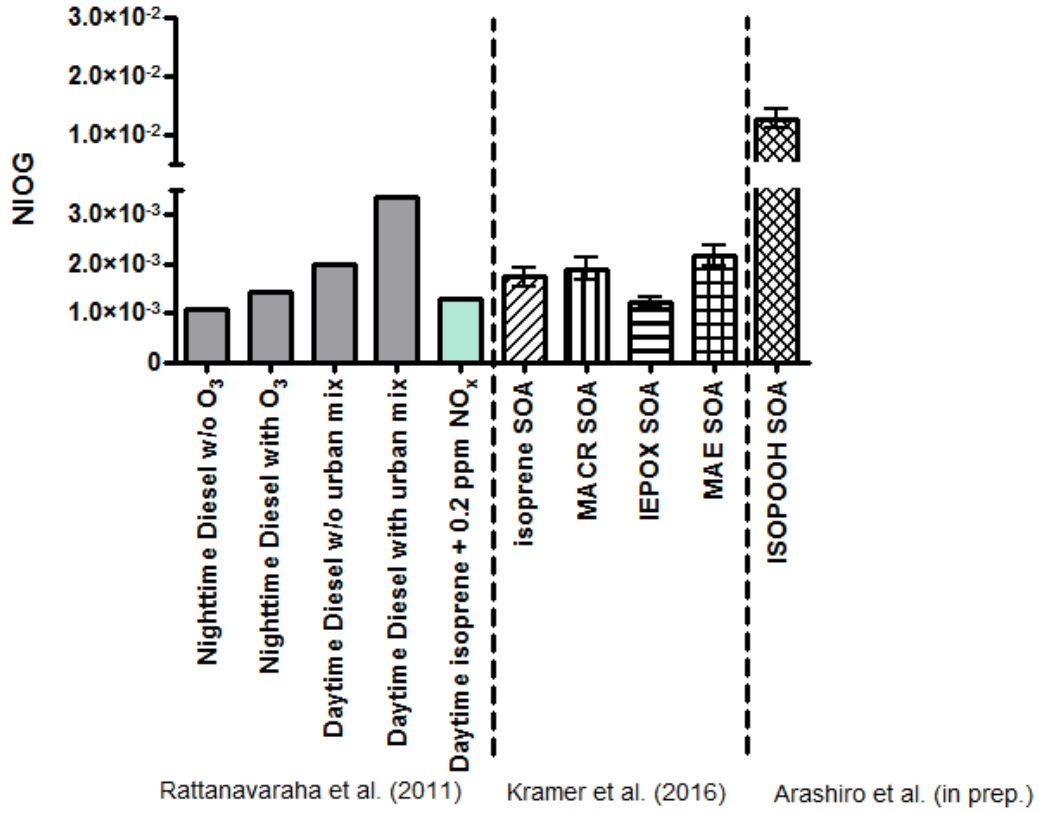


**Figure 5.3.** Comparison of NIOG values of ISOPOOH-derived SOA generated in this study to those of chamber-generated PM samples in Kramer et al. (2016) and Rattanavaraha et al. (2011).

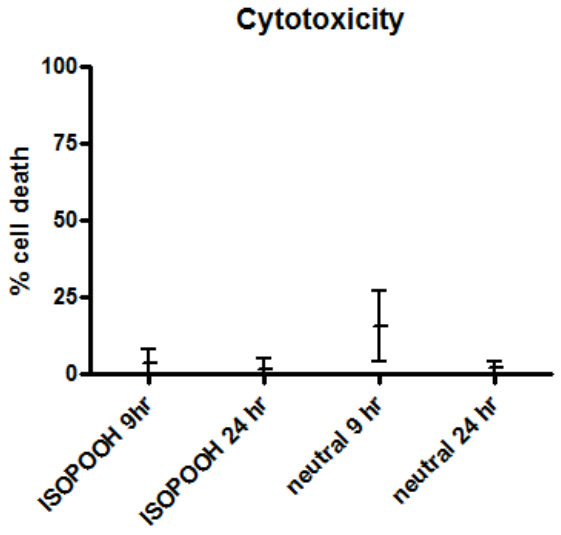


**Figure 5.4.** Cytotoxicity for each exposure type represented as % cell death determined by LDH assay.

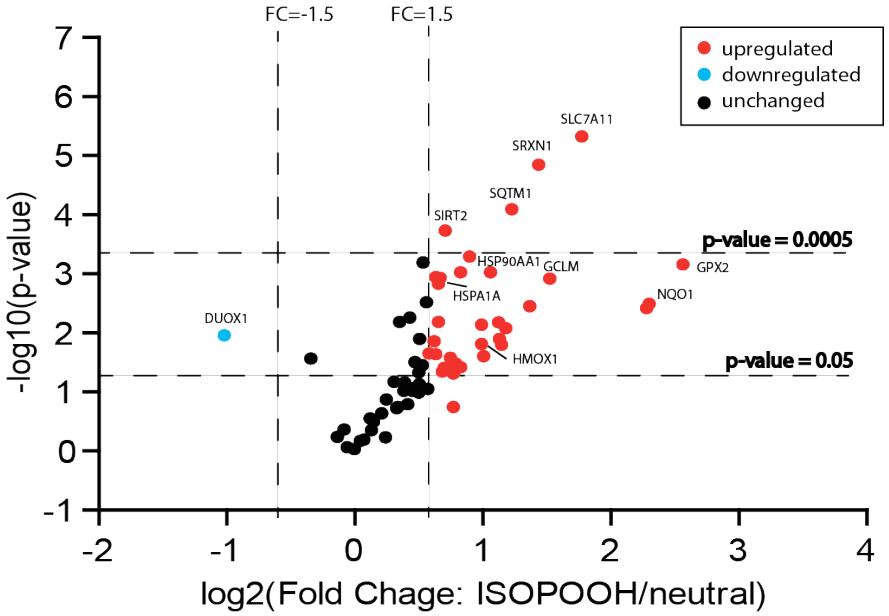


**Figure 5.5.** Volcano plot of differentially expressed genes in BEAS-2B cells upon exposure to ISOPOOH-derived SOA for 24 hours. A full list of differentially expressed genes can be found in Table 3.2.

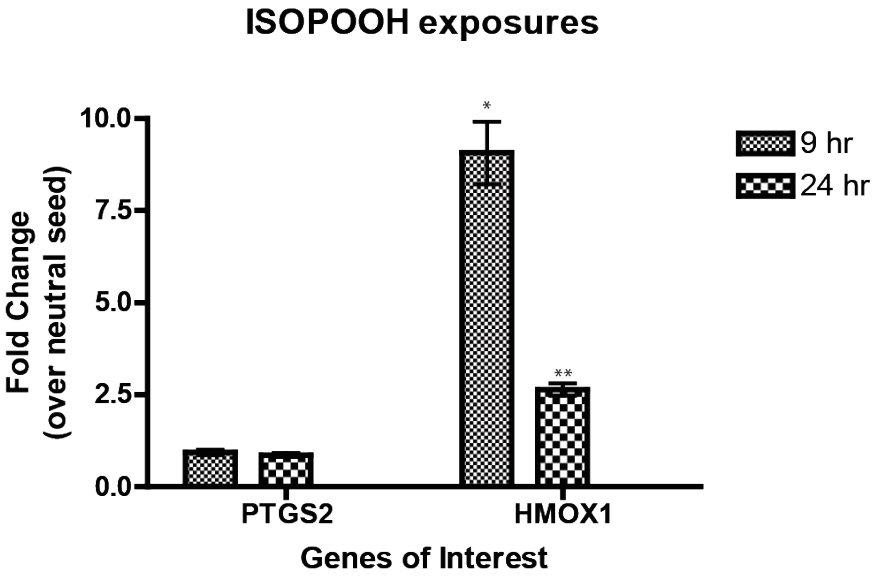


**Figure 5.6.** *PTGS2 and HMOX1* mRNA expression induced by exposure to ISOPOOH-derived SOA all normalized to non-acidified $(NH_4)_2SO_4$ seed and against housekeeping gene, β-actin. *p<0.05 and **p<0.005

## CHAPTER VI: CONCLUSIONS AND RECOMMENDATIONS

### *6.1 Summary of Significant Findings by Study*

The overall objective of this dissertation was to identify any early biological effect associated with isoprene SOA exposures. We chose to focus on oxidative stress-related gene expression and found that isoprene SOA in all its forms significantly alter the expression of oxidative stress-related genes with the Nrf2-mediated stress response being the top canonical pathway triggered by each exposure. Each study had important findings which are highlighted below:

**Study 1:** Effect of isoprene-derived secondary organic aerosol on PTGS2 and IL-*8*

**Notable results:** Atmospherically relevant compositions of isoprene –derived SOA generated in the UNC rooftop chamber elevated the expression of PTGS2 and IL-8 in direct deposition exposures. Gene expression changes for *PTGS2* and IL-8 in BEAS-2B exposed to isoprene SOA filter extracts in resuspension exposures were comparable to expression changes observed in direct deposition exposures justifying the use of resuspension cellular exposures for subsequent studies.

**Study 2:** Effect of isoprene-derived SOA on oxidative stress related genes

**Notable results:** Exposures to atmospherically relevant compositions of isoprene-derived SOA, generated in the UNC rooftop chamber, via resuspension yields an increase in oxidative stress-related genes following a 9-hr and 24-hr exposure with the 24-hr exposure altering a greater number of genes. Nrf2-mediated stress response, which has antioxidant defense properties, was the top canonical pathway triggered by our exposure for both time points and *HMOX1*, a gene transcriptionally regulated by Nrf2, was the most altered gene at both times.

**Study 3:** Effect of MAE- and IEPOX-derived SOA on the expression of oxidative stress related genes

**Notable results:** IEPOX- and MAE-derived SOA, generated in an indoor chamber, both altered the expression of oxidative stress-related genes and the canonical pathway for Nrf2-mediated oxidative stress response was enriched in both sets of exposures similar to the isoprene-SOA exposure presented in Study 2. MAE-derived SOA altered a greater number of oxidative stress-related genes than IEPOX-derived SOA.

**Study 4:** ROS generation potential of ISOPOOH-derived SOA and its effects on the expression of oxidative stress related genes

**Notable results:** ISOPOOH-derived SOA, despite having a higher ROS generation potential than MAE-derived SOA as measured through the DTT assay, did not alter as many oxidative stress-related genes. However, similar to the other types of isoprene-derived SOA, ISOPOOH-derived SOA triggered the Nrf2-mediated oxidative stress response.

### *6.2 Overall Findings and Conclusions*

Taken together, the studies have shown that the individual components of isoprene SOA (MAE-, IEPOX-, and ISOPOOH-derived SOA) all affect the Nrf2-mediated oxidative stress response pathway similar to the total isoprene-derived SOA mixture. However, the three known major component types of isoprene-derived SOA did not account for all gene expression changes observed in the exposure to the total isoprene-derived SOA mixture. Figure 6.1 shows the number of altered genes in common between each exposure in a Venn diagram. There were 41 oxidative stress related genes affected by the total isoprene mixture but the individual components only accounted for 34 out of the 41 altered genes. This may mean that there is a synergistic effect of different SOA components leading to alteration of the 7 genes not altered by individual components. Alternatively, the components of SOA responsible for the fold regulation may be the uncharacterized portion of the isoprene SOA not yet accounted for in the isoprene SOA formation mechanism shown in Figure 1. The large magnitude of *HMOX1* seen in the total isoprene SOA mixture but not in the exposures to the individual components shown in Table 5.3 also

alludes to the possibility of synergism between known components or the presence of uncharacterized components.

Figure 6.1 also highlights gene expression changes unique to each component type of isoprene SOA with MAE-derived SOA having the greatest number of uniquely altered genes in addition to the greatest number of altered genes. Despite all being components of isoprene-derived SOA, the constituents of MAE-, IEPOX-, and ISOPOOH-derived SOA varies, primarily through functional groups specific to the pathway of formation. The functional groups contributing to the differences in MAE-, IEPOX-, and ISOPOOH-derived SOA constituents, which are carboxylic acids, alcohols, and hydroperoxides, respectively likely lead to the differences in genes altered by each component. Our findings suggest that the carboxylic acid functional groups may be the dominant contributor to observed gene expression alterations as MAE-derived SOA altered the greatest number of genes.

The single gene common to all exposure types was NAD(P)H quinone dyhydrogenase 1 (*NQO1*), a cytoprotective protein whose primary function is the detoxification of quinones (Dinkova-Kostova and Talalay 2010). *NQO1* is induced by oxidative stress, dioxin, and polycyclic aromatic hydrocarbons (PAHs) (Dinkova-Kostova and Talalay 2010). Isoprene SOA, despite not being chemically similar to quinones elicit the expression of *NQO1* in all its forms. The expression of *NQO1* is mediated through the KEAP1/Nrf2/ARE pathway (Dinkova-Kostova and Talalay 2010) which is consistent with the enrichment of the Nrf2 pathway in all our exposures. *NQO1* is cited as being protective against the toxic and carcinogenic effects of numerous carcinogens and oxidative stress with polymorphisms in *NQO1* associated with increased risk for disease such as cancer (Dinkova-Kostova and Talalay 2010).

### *6.3 Implications of Findings*

The results presented in this dissertation suggest that exposure to isoprene-derived SOA extracts of all types increase levels of oxidative stress responses in BEAS-2B cells. Oxidative stress can occur as a result of damage to cellular proteins, lipids, membranes, and DNA due to reactive oxygen

species generated by particle uptake in target cells such as airway epithelial cells (Nel 2005). The exact mechanism in which isoprene-derived SOA is capable of generating reactive oxygen species in human lung cells is still unknown, but we can conclude that the isoprene-derived SOA leads to oxidative stress as seen by the activation of the Nrf2 pathway as an antioxidant response. If the Nrf2 pathway cannot restore oxidative balance, continued oxidative stress can lead to the activation and recruitment of cytokines and chemokines which cause localized inflammation of lung tissue and systemic inflammation (Nel 2005).

Oxidative stress is associated with chronic pulmonary inflammation, and contributes to respiratory and cardiovascular health outcomes (Donaldson et al. 2001; Kirkham and Barnes 2013; Rahman and Adcock 2006) and cancer (Reuter et al. 2010). However, the enrichment of the Nrf2 network does not necessarily suggest definite health hazards associated with isoprene-derived SOA as it may just mean increased antioxidant defense capabilities in response to isoprene-derived SOA exposure. For diesel exhaust, Nrf2 serves as a key transcription factor protecting against proinflammatory effects of particulate pollutants through its regulation of antioxidant defense (Li et al. 2004). Study 1, however, showed elevations of *IL-8* gene expression in BEAS-2B exposed to isoprene SOA which is an indication of the proinflammatory effects of isoprene-derived SOA. Further studies exploring additional inflammation-associated genes and proteins may be needed to posit that oxidative stress caused from isoprene-derived SOA exposure can cause localized lung tissue inflammation.

As mentioned previously, although *HMOX1* promoter polymorphisms are rare they leave certain populations at risk of respiratory diseases due to decreased defenses against oxidative stress (Fredenburgh et al. 2007; Yamada et al. 2000). Additionally, polymorphisms in *NQO1*, the gene common to all tested types of isoprene SOA exposure, may increase lung cancer risk (Saldivar et al. 2005). With significant fold changes of *HMOX1* associated with isoprene SOA and fold changes of *NQO1* seen in all

exposures, there may be a subset of the population that could be susceptible to disease resulting from high levels of oxidative stress due to isoprene SOA exposure.

Aside from the biological implications of this work, there are numerous atmospheric implications as well. The results of this dissertation showed that of all the isoprene SOA types formed from various precursors, MAE-derived SOA had the greatest effect on oxidative stress-related gene expression. Although MAE-derived SOA accounts for a smaller fraction of isoprene SOA compared to IEPOX-derived SOA, as it did in our total isoprene SOA mixture, it may be responsible for more biological effects even at its smaller fraction. In areas with high-$NO_x$ concentrations, MAE-derived SOA comprises a greater fraction of isoprene SOA mass; however, recent work has shown that IEPOX- and ISOPOOH-derived SOA account for the largest fraction of isoprene SOA mass (Hu et al. 2015). This has implications on pollution control because $NO_x$ is a controllable pollutant and if controlled can potentially alter the composition of isoprene SOA, which we have shown has differing effects on gene expression.

Because isoprene SOA comprises a large portion of global atmospheric fine particles ($PM_{2.5}$) (Carlton et al. 2009; Hallquist et al. 2009; Henze et al. 2008; Hu et al. 2015), there is a large potential global public health impact of this research. There are direct impacts to areas such as the Southeastern U.S. where particle-phase products found in our photochemical experiments have been measured in significant quantities (accounting on average for 40% of fine organic aerosol mass) in ambient fine organic aerosol particles collected in the Southeastern U.S. (Budisulistiorini et al. 2013; Budisulistiorini et al. 2016; Y-H Lin et al. 2013; Rattanavaraha et al. 2016). Even in areas of the world not directly affected by isoprene-derived SOA this research has major implications as it has demonstrated that the functional group associated with the different isoprene-derived SOA constituents likely affects the alterations of oxidative stress-related gene expression. Specifically, the carboxylic acid functional group may be more influential in altering gene expression than alcohols or hydroperoxides. This may aid in predicting the

gene expression altering capability of SOAs derived from other biogenic (non-isoprene) or anthropogenic VOCs specific to a location.

Finally, we have shown that the total isoprene SOA mixture significantly affects a large number of oxidative stress-related genes, some at very high levels, which could not be explained by the individual isoprene types or by its sum. This highlights the importance of treating air pollution of all types as a mixture because exposures are rarely isolated to specific compounds and could have synergistic effects.

### *6.4 Research Limitations*

Because this was an initial exploration into the biological effects of isoprene SOA, we chose to conduct *in vitro* exposures using BEAS-2B. Because BEAS-2B are an immortalized line of human bronchial epithelium, there are limitations with its use such as it being genetically homogeneous, being a single cell type, and being SV-40 transformed (Reddel et al. 1988). However, BEAS-2B is a stable, proliferative cell line shown to be useful in airway inflammation studies such as ours (Devlin et al. 1994). The choice to conduct *in vitro* exposure also prevented us from extrapolating results found *in vitro* to effects found *in vivo* because *in vivo* systems are much more complex. For example, *in vitro* air pollution exposures may not be directly comparable to *in vivo* exposures, since the lung fluid contains proteins and antioxidants that would mitigate the effects of inhaled chemicals (Cross et al. 1994). Cells isolated from their local environment for use during *in vitro* studies may be more susceptible to damage and alteration (Devlin et al. 2005).

Although we began our studies using a direct deposition device to conduct our *in vitro* exposures in order to mimic a more biologically relevant exposure, we shifted to using resuspension exposure methods. We recognize that the resuspension exposure model which potentially alters shape, size, and composition of a particulate exposure may not be as sensitive to particulate exposure. However, we decided resuspension exposures were better for controlled exposures at various time

points and exposures to isoprene SOA generated by uptake experiments which were done under very dry conditions not conducive to cell viability.

As an initial exploration, the biological endpoint explored in this work was pathway focused gene expression which is a single end point and does not necessarily translate to cellular functions which are regulated at the protein level nor does it indicate health outcomes measured at the tissue or organ system level. However, we can use the gene expression data to hypothesize likely outcomes to design future studies on the downstream effects of gene alteration including protein production and physiological effects. Because gene expression is continuous, even two time points at 9-hr and 24-hrs is not enough to analyze changes over time. We may be missing the expression of genes that are altered much earlier or much later than the chosen time points. With its strong ROS generating potential, ISOPOOH-derived SOA may induce a significant change in *HMOX1* after a 1 hr exposure that could decrease by 9 or 24 hrs. This may explain why we see fewer oxidative stress related genes affected by a 24 hr exposure to ISOPOOH-derived SOA than MAE-derived SOA despite ISOPOOH-derived SOA having greater oxidative potential as measured by the DTT assay.

Additionally, measures of oxidative potential through the DTT assay may not be directly relatable to all oxidative stress response observed in a biological system. As a chemical assay, the DTT assay is a measure of the ability of a compound to oxidize DTT. In relation to oxidative stress, the DTT assay aims to measure the compounds ability to modify the cysteine residues of KEAP1 leading to Nrf2 activation through a measure of its electrophilicity. As expected, we demonstrated that the Nrf2 pathway was activated by all types of isoprene-derived SOA which we determined had ROS generating potential through the DTT assay. We are limited to drawing any further conclusions about oxidative stress, including relative gene expression levels, in a biological system aside from the potential to activate the Nrf2 pathway. The DTT assay can serve as an initial screening for the potential of a

compound to affect oxidative stress response in cells but biological assays are needed to verify actual biological response in a cellular model.

Finally, even though we measured significant gene expression changes due to isoprene-derived SOA exposure, a limitation of the present research is the lack of direct comparison to known toxic compounds. There are no existing studies conducted in a similar manner using the same exposure conditions and biological endpoint with a known toxicant. Our findings could have been strengthened by conducting tandem resuspension exposures with a known air toxicant, such as diesel exhaust, at the same dose and exposure time to serve as a positive control.

### *6.5 Future Work*

Despite the limitations described, the series of studies presented in this dissertation accomplished its objective by identifying an initial biological response associated with isoprene SOA exposure. Our gene expression profiling showed that exposures to isoprene-derived SOA may elicit an oxidative stress response primarily through the Nrf2 pathway in BEAS-2B cells. Studies that can be conducted to support our gene expression findings include confirmation of the translocation of Nrf2 into the nucleus by using fluorescent staining (C-Q Li et al. 2009) and measurements of proteins regulated by the Nrf2 pathway (Moran et al. 1999).

Many other types of studies can follow this initial exploration of biological effect of isoprene SOA. First, other pathway-focused gene expression analysis complementing oxidative stress, particularly inflammation-associated genes, can be conducted to see if the antioxidant defense elevated by isoprene SOA exposure prevents potential pulmonary inflammation. We have already shown that *PTGS2* and *IL-8* are altered through isoprene-derived SOA exposure. Following measurements for inflammation-associated genes, direct measurements for chemokines and cytokines can confirm inflammatory effects of isoprene-derived SOA exposure. An exploration of genes related to lung cancer development may also be interesting because of the links between oxidative stress and cancer (Reuter et al. 2010) and

more specifically the link between *NQO1*, the single gene common to all isoprene-SOA exposures, and lung cancer (Saldivar et al. 2005). A genome-wide analysis can then be conducted to explore more pathways that may be more crucial to isoprene SOA than the one determined through our pathway focused analysis.

Other *in vitro* studies that can be conducted include the exploration of the potential synergistic effect of different isoprene SOA types potentially with measurements of metabolites which may differ in the total isoprene SOA mixture and in the individual components. Directly measuring the ROS in lung cells exposed to different types of isoprene-SOA not only ensure that our observed gene expression alterations lead to actual physiological alterations but also may also help elucidate the difference in biological response observed from the exposures to the total mixture and individual components. More importantly, highlighting the importance of treating air pollution as a mixture, *in vitro* exposures can be conducted using extracts of ambient particles which have been analyzed for the presence of isoprene SOA tracer and compared to the isoprene SOA generated in the outdoor chamber.

Cell exposures are not enough to predict health outcomes so future studies should include *in vitro* exposure using tissue models and *in vivo* exposures. Regarding *in vivo* exposures, previous studies showed airway irritation in mice due to exposure to isoprene+$O_3$ mixtures (Rohr et al. 2003; Rohr 2013; Wilkins et al. 2001; Wilkins et al. 2003). The complete source of the sensory irritation was unaccounted for in those studies and may be due to the newly discovered types of reactive products. Our results could motivate future *in vivo* work that has not been performed previously for IEPOX- MAE-, and ISOPOOH-derived SOA. Animal studies can lead way to human exposure studies as well. Similar to human exposure studies for ozone (Devlin et al. 1991), participants can be exposed to low levels of isoprene-derived SOA and bronchoalveolar lavage (BAL) can be performed to analyze the cells and fluid for indicators of inflammation.

Finally, exploration of the protective effect of Nrf2-mediated oxidative stress response can be done using knock out mice or even BEAS-2B cell models. Using knock out mice or cell lines can identify populations who may be susceptible to specific types of exposure. Nrf2 knockout mice have shown accelerated DNA adduct formation in the lung after exposure to diesel exhaust (Aoki et al. 2001). There may be similar susceptibilities to isoprene SOA and other SOA types with carboxylic acid functional groups. As further *in vitro* and *in vivo* studies confirm or identify negative effects associated with isoprene SOA exposure, identifying susceptible populations will become a greater public health concern and necessary to implement policies preventing exposures.

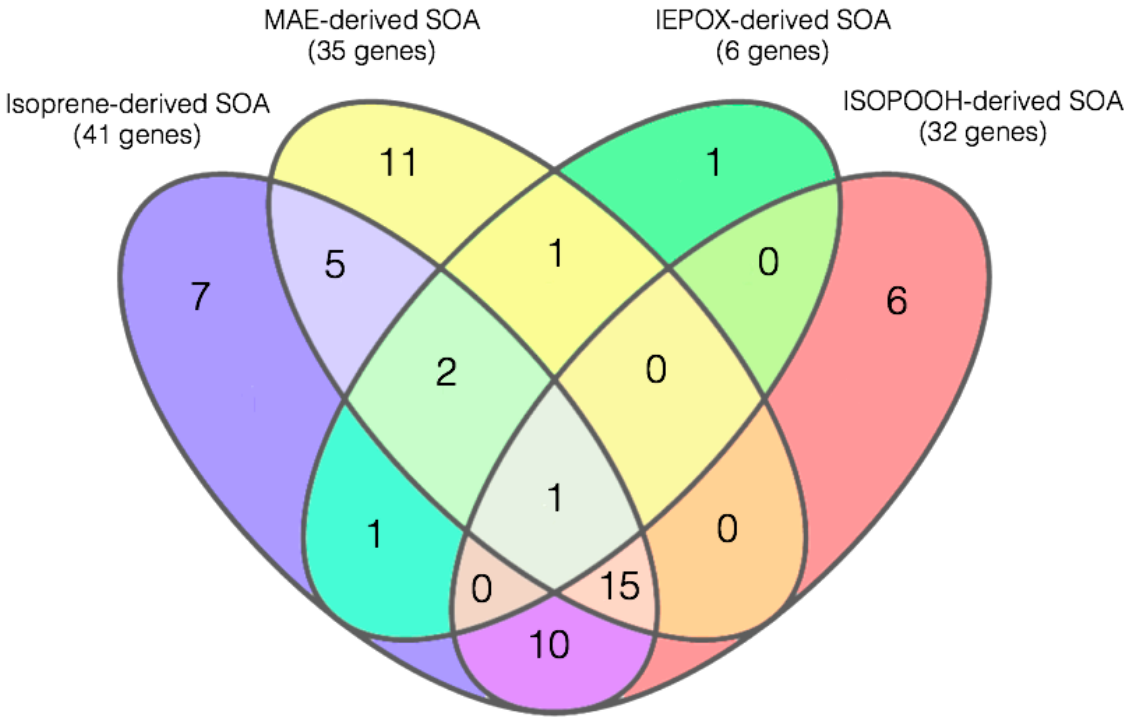


**Figure 6.1.** Venn diagram of gene expression changes ($p<0.05$) common between isoprene-derived SOA, MAE-derived SOA, IEPOX-derived SOA, and ISOPOOH-derived SOA exposure.

**Table 6.1.** Papers relating to the dissertation that have been published or are in preparation.

| Paper citation | Related Chapter | My contributions to paper |
|---|---|---|
| Arashiro, Maiko, Ying-Hsuan Lin, Kenneth G. Sexton, Zhenfa Zhang, Ilona Jaspers, Rebecca C. Fry, William G. Vizuete, Avram Gold, and Jason D. Surratt. In vitro exposure to isoprene-derived secondary organic aerosol by direct deposition and its effects on COX-2 and *IL-8* gene expression. Atmospheric Chemistry and Physics 16, no. 22 (2016): 14079-14090 | Chapter 2 | ➢ Conducted outdoor chamber experiments and exposures<br>➢ Chemical analysis<br>➢ Biological analysis<br>➢ Data analysis<br>➢ Lead on writing |
| Lin Ying-Hsuan, Maiko Arashiro, Kenneth G. Sexton, William G. Vizuete, Avram Gold, Ilona Jaspers, Rebecca C. Fry, and Jason D. Surratt. Gene Expression Profiling in Human Lung Cells to Assess the Early Biological Responses upon Exposure to Isoprene-Derived Secondary Organic Aerosol. In prep. | Similar to Chapter 3 but using the EAVES exposure device instead of resuspension exposure and including inflammation gene panel in addition to oxidative stress | ➢ Conducted outdoor chamber experiments and exposures<br>➢ Chemical analysis<br>➢ Prepared sample for biological analysis<br>➢ Paper editing |
| Lin, Y.-H., Arashiro, M., Martin, E., Chen, Y., Zhang, Z., Sexton, K. G., Gold, A., Jaspers, I., Fry, R. C., and Surratt, J. D.: Isoprene-Derived Secondary Organic Aerosol Induces the Expression of Oxidative Stress Response Genes in Human Lung Cells, Environmental Science & Technology Letters, 3, 250-254, 10.1021/acs.estlett.6b00151, 2016. | Chapter 4 | ➢ Conducted indoor chamber experiments<br>➢ Chemical analysis<br>➢ Paper editing |
| Arashiro, M., Lin, Y.-H., Zhang, Z., Gold, A., Jaspers, I., Fry, R. C., and Surratt, J. D. Reactive oxidative potential of ISOPOOH-derived SOA and its effect on oxidative stress response genes in human lung cells. In prep. | Chapter 5 | ➢ Conducted indoor chamber experiments and exposures<br>➢ Biological analysis<br>➢ Chemical analysis preparation<br>➢ Data analysis<br>➢ Lead on writing |

## REFERENCES


Aoki Y, Sato H, Nishimura N, Takahashi S, Itoh K, Yamamoto M. 2001. Accelerated dna adduct formation in the lung of the nrf2 knockout mouse exposed to diesel exhaust. Toxicology and Applied Pharmacology 173:154-160.

Barnes PJ, Adcock IM. 1997. Nf-kb: A pivotal role in asthma and a new target for therapy. Am J Physiol 265:C577-506.

Baulig A, Garlatti M, Bonvallot V, Marchand A, Barouki R, Marano F, et al. 2003. Involvement of reactive oxygen species in the metabolic pathways triggered by diesel exhaust particles in human airway epithelial cells. American Journal of Physiology - Lung Cellular and Molecular Physiology 285:L671.

Berndt T, Herrmann H, Sipilä M, Kulmala M. 2016. Highly oxidized second-generation products from the gas-phase reaction of oh radicals with isoprene. The Journal of Physical Chemistry A.

Bowler RP, Crapo JD. 2002. Oxidative stress in allergic respiratory diseases. Journal of Allergy and Clinical Immunology 110:349-356.

Budisulistiorini SH, Canagaratna MR, Croteau PL, Marth WJ, Baumann K, Edgerton ES, et al. 2013. Real-time continuous characterization of secondary organic aerosol derived from isoprene epoxydiols in downtown atlanta, georgia, using the aerodyne aerosol chemical speciation monitor. Environmental science & technology 47:5686-5694.

Budisulistiorini SH, Li X, Bairai ST, Renfro J, Liu Y, Liu YJ, et al. 2015. Examining the effects of anthropogenic emissions on isoprene-derived secondary organic aerosol formation during the 2013 southern oxidant and aerosol study (soas) at the look rock, tennessee ground site. Atmos Chem Phys 15:8871-8888.

Budisulistiorini SH, Baumann K, Edgerton ES, Bairai ST, Mueller S, Shaw SL, et al. 2016. Seasonal characterization of submicron aerosol chemical composition and organic aerosol sources in the southeastern united states: Atlanta, georgia,and look rock, tennessee. Atmos Chem Phys 16:5171-5189.

Carlton AG, Wiedinmyer C, Kroll JH. 2009. A review of secondary organic aerosol (soa) formation from isoprene. Atmospheric Chemistry and Physics 9:4987-5005.

Cho AK, Sioutas C, Miguel AH, Kumagai Y, Schmitz DA, Singh M, et al. 2005. Redox activity of airborne particulate matter at different sites in the los angeles basin. Environ Res 99:40-47.

Choi AM, Alam J. 1996. Heme oxygenase-1: Function, regulation, and implication of a novel stress-inducible protein in oxidant-induced lung injury. American Journal of Respiratory Cell and Molecular Biology 15:9-19.

Cross CE, van der Vliet A, O'Neill CA, Louie S, Halliwell B. 1994. Oxidants, antioxidants, and respiratory tract lining fluids. Environmental Health Perspectives 102:185-191.

de Bruijne K, Ebersviller S, Sexton KG, Lake S, Leith D, Goodman R, et al. 2009. Design and testing of electrostatic aerosol in vitro exposure system (eaves): An alternative exposure system for particles. Inhalation toxicology 21:91-101.

Delfino RJ, Staimer N, Vaziri ND. 2011. Air pollution and circulating biomarkers of oxidative stress. Air Quality, Atmosphere & Health 4:37-52.

Devlin RB, McDonnell WF, Mann R, Becker S, House DE, Schreinemachers D, et al. 1991. Exposure of humans to ambient levels of ozone for 6.6 hours causes cellular and biochemical changes in the lung. American Journal of Respiratory Cell and Molecular Biology 4:72-81.

Devlin RB, McKinnon KP, Noah T, Becker S, Koren HS. 1994. Ozone-induced release of cytokines and fibronectin by alveolar macrophages and airway epithelial cells. American Journal of Physiology - Lung Cellular and Molecular Physiology 266:L612-L619.

Devlin RB, Frampton ML, Ghio AJ. 2005. In vitro studies: What is their role in toxicology? Experimental and Toxicologic Pathology 57, Supplement 1:183-188.

Dinkova-Kostova AT, Talalay P. 2010. Nad(p)h:Quinone acceptor oxidoreductase 1 (nqo1), a multifunctional antioxidant enzyme and exceptionally versatile cytoprotector. Archives of biochemistry and biophysics 501:116-123.

Dockery DW, Pope CA, Xu XP, Spengler JD, Ware JH, Fay ME, et al. 1993. An association between air-pollution and mortality in 6 united-states cities. New England Journal of Medicine 329:1753-1759.

Donaldson K, Stone V, Seaton A, MacNee W. 2001. Ambient particle inhalation and the cardiovascular system: Potential mechanisms. Environ Health Perspect 109:523–527.

Doyle M, Sexton KG, Jeffries H, Bridge K, Jaspers I. 2004. Effects of 1,3-butadiene, isoprene, and their photochemical degradation products on human lung cells. Environmental health perspectives 112:1488-1495.

Doyle M, Sexton KG, Jeffries H, Jaspers I. 2007. Atmospheric photochemical transformations enhance 1,3-butadiene-induced inflammatory responses in human epithelial cells: The role of ozone and other photochemical degradation products. Chemico-Biological Interactions 166:163-169.

Ebersviller S, Lichtveld K, Sexton KG, Zavala J, Lin YH, Jaspers I, et al. 2012a. Gaseous vocs rapidly modify particulate matter and its biological effects – part 2: Complex urban vocs and model pm. Atmos Chem Phys 12:12293-12312.

Ebersviller S, Lichtveld K, Sexton KG, Zavala J, Lin YH, Jaspers I, et al. 2012b. Gaseous vocs rapidly modify particulate matter and its biological effects – part 1: Simple vocs and model pm. Atmos Chem Phys 12:12277-12292.

Edney EO, Kleindienst TE, Jaoui M, Lewandowski M, Offenberg JH, Wang W, et al. 2005. Formation of 2-methyl tetrols and 2-methylglyceric acid in secondary organic aerosol from laboratory irradiated isoprene/nox/so2/air mixtures and their detection in ambient pm2.5 samples collected in the eastern united states. Atmospheric Environment 39:5281-5289.

FitzGerald GA. 2003. Cox-2 and beyond: Approaches to prostaglandin inhibition in human disease. Nat Rev Drug Discov 2:879-890.

Fong CY, Pang L, Holland E, Knox AJ. 2000. Tgf-β1 stimulates il-8 release, cox-2 expression, and pge2release in human airway smooth muscle cells. American Journal of Physiology - Lung Cellular and Molecular Physiology 279:L201-L207.

Fredenburgh LE, Perrella MA, Mitsialis SA. 2007. The role of heme oxygenase-1 in pulmonary disease. American Journal of Respiratory Cell and Molecular Biology 36:158-165.

Gangwal S, Brown JS, Wang A, Houck KA, Dix DJ, Kavlock RJ, et al. 2011. Informing selection of nanomaterial concentrations for toxcast in vitro testing based on occupational exposure potential. Environmental Health Perspectives 119:1539-1546.

Gaschen A, Lang D, Kalberer M, Savi M, Geiser T, Gazdhar A, et al. 2010. Cellular responses after exposure of lung cell cultures to secondary organic aerosol particles. Environmental science & technology 44:1424-1430.

Gaston CJ, Riedel TP, Zhang ZF, Gold A, Surratt JD, Thornton JA. 2014. Reactive uptake of an isoprene-derived epoxydiol to submicron aerosol particles. Environmental Science & Technology 48:11178-11186.

Gong KW, Zhao W, Li N, Barajas B, Kleinman M, Sioutas C, et al. 2007. Air-pollutant chemicals and oxidized lipids exhibit genome-wide synergistic effects on endothelial cells. Genome Biology 8:R149-R149.

Hallquist M, Wenger JC, Baltensperger U, Rudich Y, Simpson D, Claeys M, et al. 2009. The formation, properties and impact of secondary organic aerosol: Current and emerging issues. Atmos Chem Phys 9:5155-5236.

Hatch GE, Duncan KE, Diaz-Sanchez D, Schmitt MT, Ghio AJ, Carraway MS, et al. 2014. Progress in assessing air pollutant risks from in vitro exposures: Matching ozone dose and effect in human airway cells. Toxicological Sciences.

Hawley B, Volckens J. 2013. Proinflammatory effects of cookstove emissions on human bronchial epithelial cells. Indoor air 23:4-13.

Hawley B, L'Orange C, Olsen DB, Marchese AJ, Volckens J. 2014a. Oxidative stress and aromatic hydrocarbon response of human bronchial epithelial cells exposed to petro- or biodiesel exhaust treated with a diesel particulate filter. Toxicological Sciences 141:505-514.

Hawley B, McKenna D, Marchese A, Volckens J. 2014b. Time course of bronchial cell inflammation following exposure to diesel particulate matter using a modified eaves. Toxicology in Vitro 28:829-837.

Hayashi Y. 2005. Designing in vitro assay systems for hazard characterization. Basic strategies and related technical issues. Experimental and Toxicologic Pathology 57, Supplement 1:227-232.

Henze DK, Seinfeld JH, Ng NL, Kroll JH, Fu TM, Jacob DJ, et al. 2008. Global modeling of secondary organic aerosol formation from aromatic hydrocarbons: High- vs. Low-yield pathways. Atmospheric Chemistry and Physics 8:2405-2420.

Hu WW, Campuzano-Jost P, Palm BB, Day DA, Ortega AM, Hayes PL, et al. 2015. Characterization of a real-time tracer for isoprene epoxydiols-derived secondary organic aerosol (iepox-soa) from aerosol mass spectrometer measurements. Atmos Chem Phys 15:11807-11833.

Huang Y-CT, Karoly ED, Dailey LA, Schmitt MT, Silbajoris R, Graff DW, et al. 2011. Comparison of gene expression profiles induced by coarse, fine, and ultrafine particulate matter. Journal of Toxicology and Environmental Health, Part A 74:296-312.

Jang M, Ghio AJ, Cao G. 2006. Exposure of beas-2b cells to secondary organic aerosol coated on magnetic nanoparticles. Chemical Research in Toxicology 19:1044-1050.

Kelly FJ, Fussell JC. 2012. Size, source and chemical composition as determinants of toxicity attributable to ambient particulate matter. Atmospheric Environment 60:504-526.

Kirkham PA, Barnes PJ. 2013. Oxidative stress in copd. Chest 144:266-273.

Kjaergaard HG, Knap HC, Ørnsø KB, Jørgensen S, Crounse JD, Paulot F, et al. 2012. Atmospheric fate of methacrolein. 2. Formation of lactone and implications for organic aerosol production. The Journal of Physical Chemistry A 116:5763-5768.

Kramer AJ, Rattanavaraha W, Zhang Z, Gold A, Surratt JD, Lin Y-H. 2016. Assessing the oxidative potential of isoprene-derived epoxides and secondary organic aerosol. Atmospheric Environment 130:211-218.

Krechmer JE, Coggon MM, Massoli P, Nguyen TB, Crounse JD, Hu W, et al. 2015. Formation of low volatility organic compounds and secondary organic aerosol from isoprene hydroxyhydroperoxide low-no oxidation. Environmental Science & Technology 49:10330-10339.

Kroll JH, Ng NL, Murphy SM, Flagan RC, Seinfeld JH. 2006. Secondary organic aerosol formation from isoprene photooxidation. Environ Sci Technol 40:1869-1877.

Kunkel SL, Standiford T, Kasahara K, Strieter RM. 1991. Interleukin-8 (il-8) - the major neutrophil chemotactic factor in the lung. Experimental lung research 17:17-23.

Lee BH, Mohr C, Lopez-Hilfiker FD, Lutz A, Hallquist M, Lee L, et al. 2016. Highly functionalized organic nitrates in the southeast united states: Contribution to secondary organic aerosol and reactive nitrogen budgets. Proceedings of the National Academy of Sciences 113:1516-1521.

Li C-Q, Kim MY, Godoy LC, Thiantanawat A, Trudel LJ, Wogan GN. 2009. Nitric oxide activation of keap1/nrf2 signaling in human colon carcinoma cells. Proceedings of the National Academy of Sciences 106:14547-14551.

Li H, Edin ML, Bradbury JA, Graves JP, DeGraff LM, Gruzdev A, et al. 2013. Cyclooxygenase-2 inhibits t helper cell type 9 differentiation during allergic lung inflammation via down-regulation of il-17rb. American Journal of Respiratory and Critical Care Medicine 187:812-822.

Li N, Hao M, Phalen RF, Hinds WC, Nel AE. 2003a. Particulate air pollutants and asthma: A paradigm for the role of oxidative stress in pm-induced adverse health effects. Clinical Immunology 109:250-265.

Li N, Sioutas C, Cho A, Schmitz D, Misra C, Sempf J, et al. 2003b. Ultrafine particulate pollutants induce oxidative stress and mitochondrial damage. Environmental Health Perspectives 111:455-460.

Li N, Alam J, Venkatesan MI, Eiguren-Fernandez A, Schmitz D, Di Stefano E, et al. 2004. Nrf2 is a key transcription factor that regulates antioxidant defense in macrophages and epithelial cells: Protecting

against the proinflammatory and oxidizing effects of diesel exhaust chemicals. The Journal of Immunology 173:3467-3481.

Li Q, Wyatt A, Kamens RM. 2009. Oxidant generation and toxicity enhancement of aged-diesel exhaust. Atmospheric Environment 43:1037-1042.

Lichtveld KM, Ebersviller SM, Sexton KG, Vizuete W, Jaspers I, Jeffries HE. 2012. In vitro exposures in diesel exhaust atmospheres: Resuspension of pm from filters versus direct deposition of pm from air. Environmental science & technology 46:9062-9070.

Lim SS, Vos T, Flaxman AD, Danaei G, Shibuya K, Adair-Rohani H, et al. 2012. A comparative risk assessment of burden of disease and injury attributable to 67 risk factors and risk factor clusters in 21 regions, 1990–2010: A systematic analysis for the global burden of disease study 2010. The Lancet 380:2224-2260.

Lin Y-H, Zhang Z, Docherty KS, Zhang H, Budisulistiorini SH, Rubitschun CL, et al. 2012. Isoprene epoxydiols as precursors to secondary organic aerosol formation: Acid-catalyzed reactive uptake studies with authentic compounds. Environmental science & technology 46:250-258.

Lin Y-H, Zhang H, Pye HOT, Zhang Z, Marth WJ, Park S, et al. 2013. Epoxide as a precursor to secondary organic aerosol formation from isoprene photooxidation in the presence of nitrogen oxides. Proceedings of the National Academy of Sciences of the United States of America 110:6718-6723.

Lin Y-H, Budisulistiorini SH, Chu K, Siejack RA, Zhang H, Riva M, et al. 2014. Light-absorbing oligomer formation in secondary organic aerosol from reactive uptake of isoprene epoxydiols. Environmental Science & Technology 48:12012-12021.

Lin Y-H, Arashiro M, Martin E, Chen Y, Zhang Z, Sexton KG, et al. 2016. Isoprene-derived secondary organic aerosol induces the expression of oxidative stress response genes in human lung cells. Environmental Science & Technology Letters 3:250-254.

Lin YH, Knipping EM, Edgerton ES, Shaw SL, Surratt JD. 2013. Investigating the influences of so2 and nh3 levels on isoprene-derived secondary organic aerosol formation using conditional sampling approaches. Atmos Chem Phys 13:8457-8470.

Liu J, D'Ambro EL, Lee BH, Lopez-Hilfiker FD, Zaveri RA, Rivera-Rios JC, et al. 2016. Efficient isoprene secondary organic aerosol formation from a non-iepox pathway. Environmental Science & Technology 50:9872-9880.

Livak KJ, Schmittgen TD. 2001. Analysis of relative gene expression data using real-time quantitative pcr and the 2−δδct method. Methods 25:402-408.

Moran JL, Siegel D, Ross D. 1999. A potential mechanism underlying the increased susceptibility of individuals with a polymorphism in nad(p)h:Quinone oxidoreductase 1 (nqo1) to benzene toxicity. Proceedings of the National Academy of Sciences of the United States of America 96:8150-8155.

Morse D, Choi AMK. 2002. Heme oxygenase-1. American Journal of Respiratory Cell and Molecular Biology 27:8-16.

Nel A. 2005. Air pollution-related illness: Effects of particles. Science 308:804.

Nguyen TB, Coggon MM, Bates KH, Zhang X, Schwantes RH, Schilling KA, et al. 2014. Organic aerosol formation from the reactive uptake of isoprene epoxydiols (iepox) onto non-acidified inorganic seeds. Atmospheric Chemistry and Physics 14:3497-3510.

Nguyen TB, Bates KH, Crounse JD, Schwantes RH, Zhang X, Kjaergaard HG, et al. 2015. Mechanism of the hydroxyl radical oxidation of methacryloyl peroxynitrate (mpan) and its pathway toward secondary organic aerosol formation in the atmosphere. Physical Chemistry Chemical Physics 17:17914-17926.

Nocker RET, Schoonbrood DFM, vandeGraaf EA, Hack CE, Lutter R, Jansen HM, et al. 1996. Interleukin-8 in airway inflammation in patients with asthma and chronic obstructive pulmonary disease. Int Arch Allergy Immunol 109:183-191.

Paulot F, Crounse JD, Kjaergaard HG, Kuerten A, St Clair JM, Seinfeld JH, et al. 2009. Unexpected epoxide formation in the gas-phase photooxidation of isoprene. Science 325:730-733.

Paur H-R, Cassee FR, Teeguarden J, Fissan H, Diabate S, Aufderheide M, et al. 2011. In-vitro cell exposure studies for the assessment of nanoparticle toxicity in the lung—a dialog between aerosol science and biology. Journal of Aerosol Science 42:668-692.

Peng H, Chen P, Cai Y, Chen Y, Wu Q-h, Li Y, et al. 2008. Endothelin-1 increases expression of cyclooxygenase-2 and production of interlukin-8 in hunan pulmonary epithelial cells. Peptides 29:419-424.

Peretz A, Peck EC, Bammler TK, Beyer RP, Sullivan JH, Trenga CA, et al. 2007. Diesel exhaust inhalation and assessment of peripheral blood mononuclear cell gene transcription effects: An exploratory study of healthy human volunteers. Inhalation Toxicology 19:1107-1119.

Pye HOT, Pinder RW, Piletic IR, Xie Y, Capps SL, Lin Y-H, et al. 2013. Epoxide pathways improve model predictions of isoprene markers and reveal key role of acidity in aerosol formation. Environmental science & technology 47:11056-11064.

Rager JE, Lichtveld K, Ebersviller S, Smeester L, Jaspers I, Sexton KG, et al. 2011. A toxicogenomic comparison of primary and photochemically altered air pollutant mixtures. Environmental health perspectives 119:1583-1589.

Rager JE, Bauer RN, Müller LL, Smeester L, Carson JL, Brighton LE, et al. 2013. Dna methylation in nasal epithelial cells from smokers: Identification of ulbp3-related effects. American Journal of Physiology - Lung Cellular and Molecular Physiology 305:L432-L438.

Rahman I, Adcock IM. 2006. Oxidative stress and redox regulation of lung inflammation in copd. Eur Respir J 28:219-242.

Rattanavaraha W, Rosen E, Zhang H, Li Q, Pantong K, Kamens RM. 2011. The reactive oxidant potential of different types of aged atmospheric particles: An outdoor chamber study. Atmospheric Environment 45:3848-3855.

Rattanavaraha W, Chu K, Budisulistiorini SH, Riva M, Lin YH, Edgerton ES, et al. 2016. Assessing the impact of anthropogenic pollution on isoprene-derived secondary organic aerosol formation in pm2.5 collected from the birmingham, alabama, ground site during the 2013 southern oxidant and aerosol study. Atmos Chem Phys 16:4897-4914.

Reddel RR, Ke Y, Gerwin BI, McMenamin MG, Lechner JF, Su RT, et al. 1988. Transformation of human bronchial epithelial cells by infection with sv40 or adenovirus-12 sv40 hybrid virus, or transfection via strontium phosphate coprecipitation with a plasmid containing sv40 early region genes. Cancer Research 48:1904-1909.

Reuter S, Gupta SC, Chaturvedi MM, Aggarwal BB. 2010. Oxidative stress, inflammation, and cancer: How are they linked? Free Radical Biology and Medicine 49:1603-1616.

Riedel TP, Lin Y-H, Budisulistiorini SH, Gaston CJ, Thornton JA, Zhang Z, et al. 2015. Heterogeneous reactions of isoprene-derived epoxides: Reaction probabilities and molar secondary organic aerosol yield estimates. Environmental Science & Technology Letters.

Riedel TP, Lin YH, Zhang Z, Chu K, Thornton JA, Vizuete W, et al. 2016. Constraining condensed-phase formation kinetics of secondary organic aerosol components from isoprene epoxydiols. Atmos Chem Phys 16:1245-1254.

Riva M, Budisulistiorini SH, Chen Y, Zhang Z, D'Ambro EL, Zhang X, et al. 2016a. Chemical characterization of secondary organic aerosol from oxidation of isoprene hydroxyhydroperoxides. Environmental Science & Technology 50:9889-9899.

Riva M, Budisulistiorini SH, Zhang Z, Gold A, Surratt JD. 2016b. Chemical characterization of secondary organic aerosol constituents from isoprene ozonolysis in the presence of acidic aerosol. Atmospheric Environment 130:5-13.

Rohr AC, Shore SA, Spengler JD. 2003. Repeated exposure to isoprene oxidation products causes enhanced respiratory tract effects in multiple murine strains. Inhal Toxicol 15:1191-1207.

Rohr AC. 2013. The health significance of gas- and particle-phase terpene oxidation products: A review. Environment International 60:145-162.

Saldivar SJ, Wang Y, Zhao H, Shao L, Lin J, Spitz MR, et al. 2005. An association between a nqo1 genetic polymorphism and risk of lung cancer. Mutation Research/Genetic Toxicology and Environmental Mutagenesis 582:71-78.

Samet JM, Dominici F, Curriero FC, Coursac I, Zeger SL. 2000. Fine particulate air pollution and mortality in 20 us cities, 1987-1994. New England Journal of Medicine 343:1742-1749.

Schreck R, Albermann K, Baeuerle PA. 1992. Nuclear factor kb: An oxidative stress-responsive transcription factor of eukaryotic cells (a review). Free Radical Research Communications 17:221-237.

Schwartz J, Slater D, Larson TV, Pierson WE, Koenig JQ. 1993. Particulate air-pollution and hospital emergency room visits for asthma in seattle. American Review of Respiratory Disease 147:826-831.

Seagrave J. 2008. Mechanisms and implications of air pollution particle associations with chemokines. Toxicology and Applied Pharmacology 232:469-477.

Sies H. 1991. Oxidants and antioxidants: Pathophysiologic determinants and therapeutic agentsoxidative stress: From basic research to clinical application. The American Journal of Medicine 91:S31-S38.

Surratt JD, Murphy SM, Kroll JH, Ng NL, Hildebrandt L, Sorooshian A, et al. 2006. Chemical composition of secondary organic aerosol formed from the photooxidation of isoprene. The Journal of Physical Chemistry A 110:9665-9690.

Surratt JD, Kroll JH, Kleindienst TE, Edney EO, Claeys M, Sorooshian A, et al. 2007. Evidence for organosulfates in secondary organic aerosol. Environmental science & technology 41:517-527.

Surratt JD, Chan AWH, Eddingsaas NC, Chan M, Loza CL, Kwan AJ, et al. 2010. Reactive intermediates revealed in secondary organic aerosol formation from isoprene. Proceedings of the National Academy of Sciences of the United States of America 107:6640-6645.

Tao F, Gonzalez-Flecha B, Kobzik L. 2003. Reactive oxygen species in pulmonary inflammation by ambient particulates. Free Radical Biology and Medicine 35:327-340.

Uchida K. 2008. A lipid-derived endogenous inducer of cox-2: A bridge between inflammation and oxidative stress. Mol Cells 25:347-351.

Volckens J, Dailey L, Walters G, Devlin RB. 2009. Direct particle-to-cell deposition of coarse ambient particulate matter increases the production of inflammatory mediators from cultured human airway epithelial cells. Environmental science & technology 43:4595-4599.

Wilkins CK, Clausen PA, Wolkoff P, Larsen ST, Hammer M, Larsen K, et al. 2001. Formation of strong airway irritants in mixtures of isoprene/ozone and isoprene/ozone/nitrogen dioxide. Environmental Health Perspectives 109:937-941.

Wilkins CK, Wolkoff P, Clausen PA, Hammer M, Nielsen GD. 2003. Upper airway irritation of terpene/ozone oxidation products (tops). Dependence on reaction time, relative humidity and initial ozone concentration. Toxicol Lett 143:109-114.

Wittkopp S, Staimer N, Tjoa T, Stinchcombe T, Daher N, Schauer JJ, et al. 2016. Nrf2-related gene expression and exposure to traffic-related air pollution in elderly subjects with cardiovascular disease: An exploratory panel study. Journal of exposure science & environmental epidemiology 26:141-149.

Xu L, Guo HY, Boyd CM, Klein M, Bougiatioti A, Cerully KM, et al. 2015. Effects of anthropogenic emissions on aerosol formation from isoprene and monoterpenes in the southeastern united states. Proceedings of the National Academy of Sciences of the United States of America 112:37-42.

Yamada N, Yamaya M, Okinaga S, Nakayama K, Sekizawa K, Shibahara S, et al. 2000. Microsatellite polymorphism in the heme oxygenase-1 gene promoter is associated with susceptibility to emphysema. American Journal of Human Genetics 66:187-195.

Yan Z, Wang J, Li J, Jiang N, Zhang R, Yang W, et al. 2015. Oxidative stress and endocytosis are involved in upregulation of interleukin-8 expression in airway cells exposed to pm2.5. Environmental Toxicology:n/a-n/a.

Zavala J, Lichtveld K, Ebersviller S, Carson JL, Walters GW, Jaspers I, et al. 2014. The gillings sampler – an electrostatic air sampler as an alternative method for aerosol in vitro exposure studies. Chemico-Biological Interactions 220:158-168.

Zhang H, Surratt JD, Lin Y-H, Bapat J, Kamens RM. 2011. Effect of relative humidity on soa formation from isoprene/no photooxidation: Enhancement of 2-methylglyceric acid and its corresponding oligoesters under dry conditions. Atmos Chem Phys 11:6411-6424.

Zhang Z, Lin Y-H, Zhang H, Surratt JD, Ball LM, Gold A. 2012. Technical note: Synthesis of isoprene atmospheric oxidation products: Isomeric epoxydiols and the rearrangement products *cis*- and *trans*-3-methyl-3,4-dihydroxytetrahydrofuran. Atmos Chem Phys 12:8529-8535.